UNIVERSITÀ DEGLI STUDI DI PADOVA

DIPARTIMENTO DI INGEGNERIA CIVILE, EDILE E AMBIENTALE

Department Of Civil, Environmental and Architectural Engineering

Corso di Laurea Magistrale in Environmental Engineering

"Soil Protection and Water Management"

TESI DI LAUREA

Integration of GNSS and InSAR multi-temporal data for land subsidence monitoring in the Po River Delta area (Italy)

Relatore:

Chiar.mo PROF. Massimo Fabris

Laureando:

Mattia Battaglia

Matricola:

2016748

ANNO ACCADEMICO 2021-2022

INDEX

Pag.

ABSTRACT I

INTRODUCTION II

CHAPTER 1: THE PO RIVER DELTA STUDY AREA

1.1. Geography 1

1.2. Geology 4

CHAPTER 2: PROBLEMS OF INTEREST

2.1. Land subsidence 7

2.1.1. Natural land subsidence 8

2.1.2. Anthropic land subsidence 11

2.1.3. Effects of land subsidence 13

2.2. Salt wedge intrusion 15

2.2.1. Cause of salt wedge intrusion 17

2.2.2. Effects of salt wedge intrusion 18

2.3. Reduction of solid transport 19

2.4. Eustatism 22

CHAPTER 3: TYPE OF SURVEY

3.1. Survey with GNSS stations 27

3.1.1. Equation of pseudo-range 28

3.1.2. Global Navigation Satellite Systems 29

3.1.2.1. GPS system 29

3.1.2.2. GLONASS system 31

3.1.2.3. GALILEO system 31
3.1.2.4. BeiDou-3 system 31
3.1.3. PODELNET network 32
3.2. Satellite survey 37
3.2.1. Synthetic Aperture Radar 38
3.2.1.1. Interferometric techniques (PSInSAR) 38
3.2.2. Advantages & Disadvantages of PSInSAR 43
3.2.3. Applicability of PSInSAR 44
3.2.4. Sentinel satellites 45
3.2.5. Cosmo-SkyMed satellites 46
3.3. Survey of coastline 48
3.3.1. Survey with total station 48
3.3.1.1. Total station Leica TCR1201 48
3.3.2. Survey with LiDAR 49
3.3.2.1. Advantages and disadvantages of LiDAR 50
3.3.3. Survey with UAV instruments 51
3.3.3.1. Drone Parrot 51

CHAPTER 4: DATA VISUALIZATION

4.1. Software GIS 53
4.1.1. Geodatabase 54
4.1.2. WebGIS 55

CHAPTER 5: DATA ANALYSIS

5.1. GNSS data analysis 59
5.2. SAR data analysis 63
5.3. Comparison between GNSS data and Sentinel data 69
5.4. Comparison between GNSS data and Cosmo data 73

CHAPTER 6: ANALYSIS OF RESULTS

6.1. Analyses of points with high errors 83
6.1.1. Uses of artificial reflectors 90
6.2. Analyses of area with high lowering velocity 91
6.2.1. Analyses of critical levees detected with Sentinel-1 95
6.2.2. Analyses of critical levees detected with Cosmo 98
6.2.3. Analyses of critical inlet area detected with Cosmo 109

CHAPTER 7. FINAL CONSIDERATIONS

7.1. Geological aspect of Po River Delta 112
7.2. Expansion of Po River Delta 115

CHAPTER 8. CONCLUSION

BIBLIOGRAPHY

SITOGRAPHY

GRATITUDE

INDEX FIGURE

Figure 1. Physical map of the Po River Delta 1
Figure 2. Altimetry in the PRD 2
Figure 3. Cutting of Porto Viro 3
Figure 4. Evolution of the PRD 5
Figure 5. Geological survey in the PRD 6
Figure 6. Effects of land subsidence on the urbanization 7
Figure 7. Tectonic processes 8
Figure 8. Embankment of Po di Goro and water pump of Goro 9
Figure 9. Calcium ions 10
Figure 10. Sodium ions 10
Figure 11. Compression stations in concrete 11
Figure 12. Reconstruction of new build on the “Canale Veneto” 13
Figure 13. Isolines of land subsidence from 1947 to 1970 13
Figure 14. Phenomenon of high water in Venice 14
Figure 15. Extension of salt wedge intrusion 15
Figure 16. Location of measured point 16
Figure 17. Example of artificial lake 17
Figure 18. Halophilic vegetation 18
Figure 19. Flood event 19
Figure 20. Check dams 20
Figure 21. Longshore current 21
Figure 22. Melting of the ice 22
Figure 23. Groins 23
Figure 24. Mean sea level along the years (ISPRA) 24
Figure 25. LiDAR survey 25
Figure 26. Relative positioning 27
Figure 27. Multipath error 29
Figure 28. GNSS orbits 30
Figure 29. GPS satellite 31
Figure 30. PODELNET network 34
Figure 31. Principle of radar system 39

Figure 32. PSInSAR techniques 40
Figure 33. Effects of temporal decorrelation on a forest 41
Figure 34. PS data 42
Figure 35. Difference in point density between Sentinel's and Cosmo's sensor 43
Figure 36. Example of attribute table 44
Figure 37. Temporal evolution of deformation 45
Figure 38. Sentinel Satellites 47
Figure 39. Cosmo satellite 49
Figure 40. Total Station 51
Figure 41. DSM and DTM 53
Figure 42. Drone parrot ANAFI 54
Figure 43. Logo QGIS 55
Figure 44. Overlap of layer 55
Figure 45. Lizmap interface 57
Figure 46. WebGIS interface 58
Figure 47. Extension of SAR data and PODELNET 59
Figure 48. LOS of satellites 61
Figure 49. Example of SAR image 63
Figure 50. Electric poles 65
Figure 51. Cavane 66
Figure 52. High lowering velocity 67
Figure 53. Old roof 68
Figure 54. ScanSAR mode 73
Figure 55. Point 077801 83
Figure 56. Point 077704 84
Figure 57. Point 077703 84
Figure 58. Point 077721 85
Figure 59. Point 077911 85
Figure 60. Point 077707 86
Figure 61. Point 077912 86
Figure 62. Point 077718 87
Figure 63. Point 077717 87
Figure 64. Point 077708 88

Figure 65. Point 077713 88
Figure 66. Point 077915 89
Figure 67. Point 077917 89
Figure 68. Example of an artificial reflectors 90
Figure 69. Section of the sea coastal defence embankment 91
Figure 70. Original points 92
Figure 71. Points cleared 92
Figure 72. Effects of flood events during 1951 in Polesine 94
Figure 73. SAR points in north area of Boccasette 95
Figure 74. SAR points in central oil of Porto Tolle 96
Figure 75. SAR points in south area of Boccasette 97
Figure 76. SAR points in south area of Boccasette 97
Figure 77. SAR points in area of Goro and Gorino 98
Figure 78. SAR points in “Sacca degli Scardovari” 99
Figure 79. SAR points in area of Bonelli 100
Figure 80. SAR points in area of Polesine Camerini 101
Figure 81. SAR points in central oil of Porto Tolle 102
Figure 82. SAR points in north area of Pila 103
Figure 83. SAR points in Boccasette area 104
Figure 84. SAR points in north area of Boccasette 105
Figure 85. SAR points in porto Levante area 106
Figure 86. SAR points in Albarella area 107
Figure 87. SAR points in south area of Boccasette 108
Figure 88. SAR points in the area south of the Po di Venezia 109
Figure 89. SAR points in the area north of the Po di Venezia 110
Figure 90. Geological survey of Po River Delta 112
Figure 91. SAR data in PRD over the Geological survey 113
Figure 92. Degree of Consolidation over time 115
Figure 93. Expansion of the PRD over the centuries 116
Figure 94.SAR data over expansion of the PRD 117
Figure 95. Lowering velocity of the soil measured with GNSS data 119
Figure 96. Lowering velocity of the critical embankments 121
Figure 97. Po River Delta 124

INDEX TABLE

Table 1. Velocity along vertical of PODELNET network 37
Table 2. Precision of Sentinel..... 44
Table 3. Velocity along vertical 62
Table 4. Sentinel-1, permanent stations..... 70
Table 5. Sentinel-1, rover station with buffer 200m..... 71
Table 6. Sentinel-1, rover station with buffer 100m..... 72
Table 7. Sentinel-1, rover station with buffer 250m..... 72
Table 8. Cosmo-SkyMed, permanent stations..... 74
Table 9. Research of translation 76
Table 10. Cosmo-SkyMed, permanent stations..... 78
Table 11. Cosmo-SkyMed, rover station with buffer 200m..... 79
Table 12. Cosmo-SkyMed, rover station with buffer 100m..... 80
Table 13. Cosmo-SkyMed, rover station with buffer 250m..... 80
Table 14. Cosmo-SkyMed, threshold.3, rover station with buffer 200m..... 81
Table 15. Cosmo-SkyMed, WEST zone, rover station with buffer 200m 82
Table 16. Velocity of Sentinel-1 and Cosmo-SkyMed of urban centres..... 94
Table 17. Analyses of lowering Velocity according to the age of the soil..... 117

ABSTRACT

The purpose of the thesis is to monitor the rate of land subsidence in the Po Delta area due to the phenomenon of soil subsidence. The study is carried out through the processing of data from multi-time detection campaigns carried out with GNSS instrumentation on the PODELNET (PO DELta NETwork) and with satellite surveys thanks to the use of Sentinel-1 and Cosmo-SkyMed images. The collected data were then visualized and processed together on GIS software. In this way it was possible to identify the evolution of the phenomenon and through an integration with the literature it was possible to identify the most sensitive areas.

The goal of the work is to analyze the different types of surveys used in the monitoring of the Po Delta area and select the best methodology (or a combination of them) that can identify quickly, precision and cost-effectiveness future useful works that will need to be designed to limit or reduce damage resulting from natural events. A second objective is to raise public awareness of the issue of land subsidence using a WebGIS, thus trying to increase the financial funds needed to safeguard the territory.

INTRODUCTION

Italy is a high-risk country, mainly due to natural hydrogeological disasters such as floods and landslides, natural geological disasters such as earthquakes and volcanic eruptions and the risks associated with human activities. To cope with these natural risks, the environment must be prevented and protected. Having an excellent knowledge of natural phenomena and the interactions between human activity and the environment is essential to develop optimal emergency response strategies, acting mainly through prevention activities consisting of structural interventions to reduce risks. An area particularly at risk is the Po Delta, a vast and constantly evolving territory with active geomorphological processes linked to river dynamics and subsidence factors of the territory due to natural and anthropogenic factors, without forgetting external factors that affect the environment such as tidal regimes and wave movement (*M. Coppola, 2009*). All these processes take place slowly, lowering the ground by a few centimeters per year and lifting the sea by several millimeters. In this way the effect is almost imperceptible considering a short time scale, but in the long run the consequences will be catastrophic. Studies say that without the necessary precautions due to rising sea levels, by 2100 more than most of the Veneto and Friuli coast will end up under water, including the city of Venice (*L. Jonathan, 2019*).

It is therefore necessary to take immediate action to monitor the intensity of each individual aspect and to assess the future consequences, in order to begin to intervene already now on a vast territory protected by hundreds of kilometers of banks that in the current conditions at the end of the century may not be enough. Limiting itself to the Delta area, a careful analysis today could thus allow to safeguard a territory that has territorial and ecological characteristics that make it unique in its kind. In facts the Delta covers a total area of over 52,000 hectares of areas considered among the most productive and rich in biodiversity despite being one of the most man-made and economically developed protected areas of the country. The Po Delta Park in fact preserves the largest Italian extension of protected wetlands, inside which there is an incredible biodiversity of plants (Halophilic, reeds, etc.) and fauna (in particular, the park has more than 280 species of birds).

These are the reasons that led me to undertake this study, the possibility of making a small contribution to the preservation of the national territory, trying to draw the attention of the population and politicians on issues that in decades will have irreversible consequences and on which it will no longer be possible to act as it has already happened for the climate changes that currently are destroying the planet.

Several techniques have been used to study these phenomena, in the case under consideration the investigations have concerned the emerged areas, have been used GNSS techniques, satellite surveys with SAR instrument, aerial surveys with LiDAR technology, photogrammetric measurements using UAV devices and surveys with classical instrumentation such as the total station. The data were then expanded with research and studies focused on different fields such as geological studies or studies on the effectiveness of the works of defense at sea that over the years have been carried out by researchers. All these data were then collected on a GIS software able to visualize and process them, thus deriving the areas most at risk and allowing us in this way to have a future estimate of the decreases to already foresee a planning of the interventions, starting from the areas most at risk. In this way we try to avoid catastrophes such as that of the flood of the Delta of 1957 that led to the breakup of the bank of the Po in Cà Vendramin causing the flooding of the territory of the island of Ariano (leading 30000 people to abandon their homes) and the breakdown of a system of dunes in Porto Tolle flooding 6000 hectares of land (*La Voce di Rovigo, 1951*).

The following thesis includes a brief description of the phenomena that affect the area under consideration and the methodologies used to estimate the scope of the latter. The analysis of the data will therefore aim to find the best methodology to monitor the intensity of the phenomena, going to indicate the areas most at risk. The last phase considered perhaps the most important in order not to make the study useless, is to go and share such results with the population through a WebGIS, in this way through an easy but truthful representation of the phenomenon, it will be easier to get to people, shifting the interest of politics and people on these issues.

CHAPTER 1. THE PO RIVER DELTA STUDY AREA

1.1. Geography

The Po is the largest river in Italy, originating at the foot of Monviso. It opens in the northern sector of the Adriatic Sea with a large delta of about 400 Km^2 that extends towards the sea for about 25 km (*N. Cenni, 2021*). In the Delta, the main river (Po di Venezia) divides into seven branches: Po of Volano, Po of Goro, Po of Gnocca or of Donzella, Po of Tolle, Po of Pila, Po of Maistra and Po of Levante (*Figure 1*).

Figure 1. Physical map of the Po River Delta

It is a complex territory from a morphological and hydrographical point of view. There are 42,000 hectares of agricultural land resulting from land reclamation works carried out over the past centuries, while 18,000 hectares are wetlands, consisting of fishing valleys and lagoons (*F. Ferro, 2009*). A large part of the territory are below mean sea level and the rivers that flow through it (*Figure 2*), for this reason the area is protected by 400 km of embankments and is hydraulically regulated by a dense network of canals that are connected to numerous drainage systems, in addition there are a complex of wide sandy beach ridges that stretch from south to north can be considered as the natural western boundary of the reclaimed territories and play an important role in protecting the area.

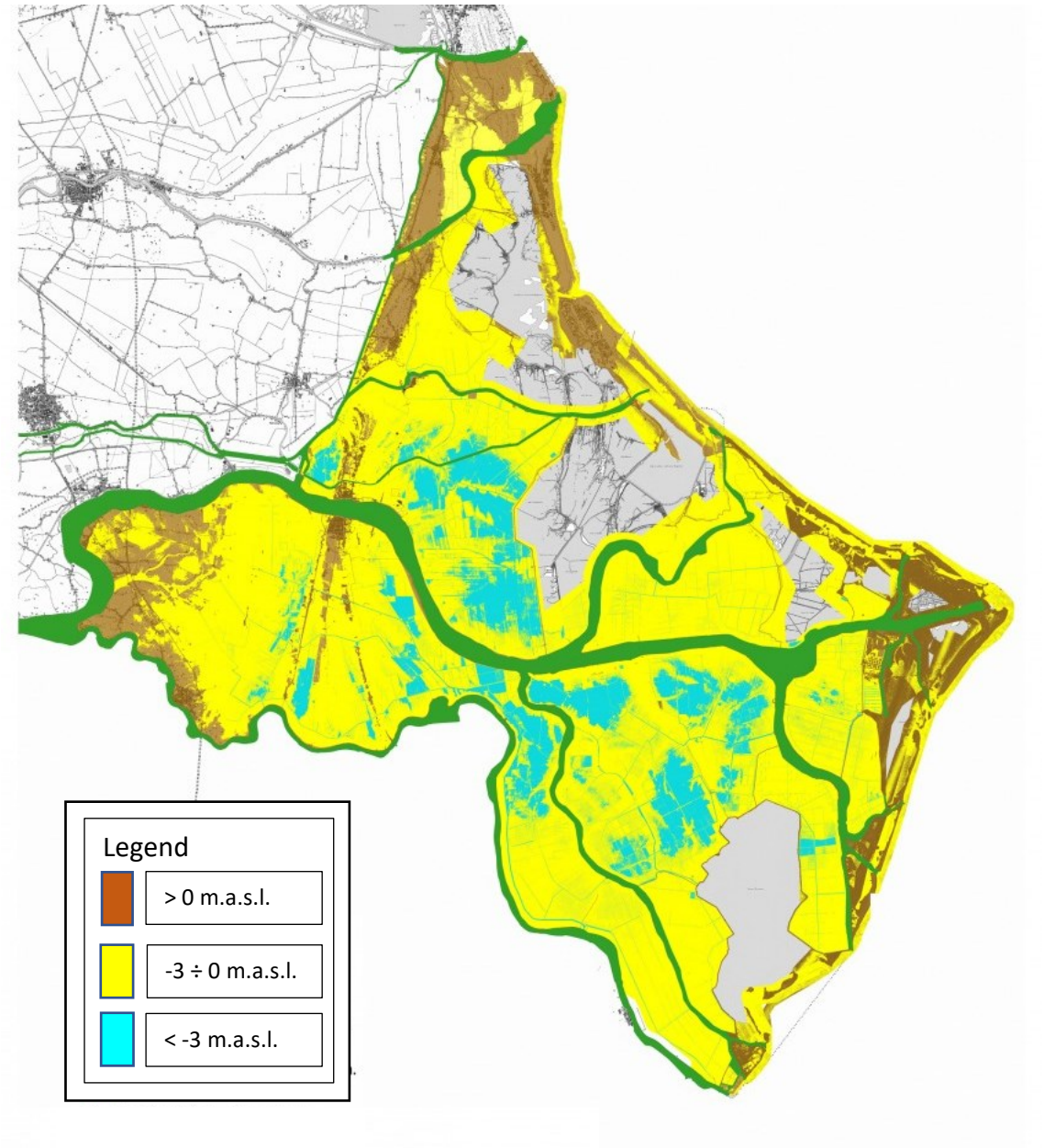

Figure 2. Altimetry in the PRD

The formation of the modern delta is the result of natural processes and human interactions. As far as natural processes are concerned, the formation of the Delta originates from the progressive deposition of the considerable solid transport of the two main Italian rivers (Po and Adige) on the shallow waters of the Adriatic, which determines their ascent and thus the constant extension of the seabed of the various branches.

As far as human processes are concerned, the land reclamation works carried out in the area are notable, such as the Ficarolo route and the Taglio of Porto Viro (*Figure 3*), a major hydraulic engineering work carried out by the Serenissima Republic of Venice in the 1600s mainly to avoid any danger of silting up the inlets (*P. Colombo, 2009*). The events that have heavily influenced the evolution of this area since 1950 include the very serious phenomenon of land subsidence (1940-1960) caused by the extraction of methane and water from the subsoil and the flooding caused by the breaking of the banks of the Po in 1951, which only saved the hydrographic delta between the Po of Goro and the Po of Venezia. In addition, the presence of containment dams in the mountains have caused a large decrease in solid transport, often leading to a negative sediment balance in the PRD.

Figure 3. Cutting of Porto Viro

1.2. Geology

The plains represent the most fragile physical environments. Most of the sediments that emerge on the surface of the plain of Emilia-Romagna are recent (less than 10000 years), many of which have been deposited in the last 2000 years. They derive from the complex relationship between the Po River in the north, the Apennine rivers in the south and the Adriatic Sea in the east. The entire Po Valley has undergone great changes over the geological eras that have led to repeated advances and retreats of the coastline. As a result, the Delta has moved hundreds of kilometers and changed its shape and extension countless times. Among the factors that have caused these phenomena we can mention the collision between the Eurasian and African plates (which for millions of years has caused a slow rise of the Alps and the Apennines related to land subsidence phenomena of the surrounding plains) variously compensated by alluvial deposits (*Kent, 2002*), the variation of the sea level (related to the glaciation phases), the erosion of the mountain ranges (with consequent deposit on the bottom of the material removed) and in general the phenomenon of solid transport generated by the rivers (*M. Bondesan, 1980*).

During the advancing phases of the plain, accelerations in the land subsidence of sediments have often occurred that are not sufficiently compensated by solid river intake. The consequence has been the formation of large swampy areas (valleys), now largely reclaimed, where the emerging soils have marked clayey characteristics with high compressibility often associated with a more difficult vertical drainage. The sand cords instead represent the various extensions of the Delta area of the Po in the centuries, these cords are deductible from the lithologies in surfacing and sub-surfacing, from the altimetric structures and from the country reliefs (penetrometer tests).

The extension of the Po Delta shows many variations over the years (*Figure 4*).

Between 1200 and 1600 there was an advancement of the coastline in the upper part east of Adria following the course of the Po at Ficarolo which caused the main course of the river to move northwards. With the cutting of Porto Viro, the formation of today's Po Delta began. Between 1800 and 1930 the coastline underwent a general advancement linked to the river inputs. After 1930 the extraction of gas and water from the subsoil began, which led to a negative evolutionary trend for the coast and the seabed. Since 1964 there has also been a strong reduction in the solid transport of rivers due to the presence of dams and the cleaning of riverbeds.

Land subsidence from gas extraction reached its highest levels in the period between 1947 and 1960 and after the closure of the wells in 1963, this land subsidence caused a major redesign of the banks (with rises) to overcome the land subsidence problem (*P. Colombo, 2009*). This study on the evolution of the area is important to determine the degree of soil compaction, a factor that, as described below, will be decisive for understanding land subsidence.

Figure 4. Evolution of the PRD

To determine the type of soil present, a geological survey *(Figure 5*) was carried out at the end of the 1990s which showed the general compressibility (green area) with a tongue of sand that identify the presence of ancient beach and brown area with lower compressibility than clay (*N. Cenni, 2021*). Unfortunately, we do not know how the survey was carried out and we do not know the sampling depths, or the precision used. The map of the present lithology is taken into consideration by the Emilia-Romagna and Veneto region, and this is deduced from the location of the Romea state road and from the houses and towns that are concentrated in the areas above the sandy areas. Therefore, such study will be taken in great consideration to give a logic to the results obtained in the following thesis.

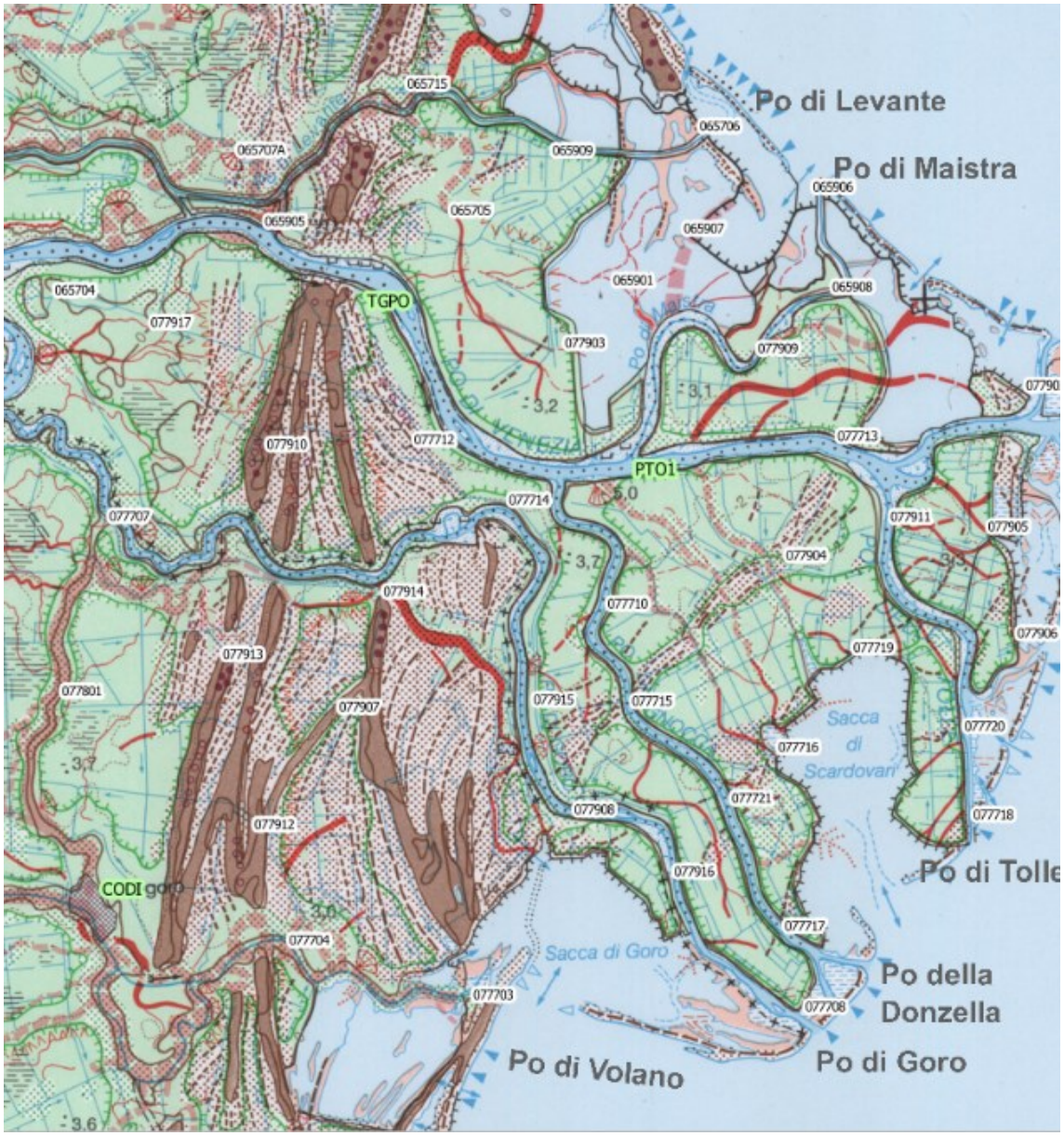

Figure 5. Geological survey in the PRD

CHAPTER 2. PROBLEMS OF INTEREST

2.1. Land subsidence

Land subsidence is defined as any vertical lowering movement of the Earth's surface, regardless of the cause that produced it, the size of the area, the temporal evolution of the phenomenon, the speed of soil movement and the consequent environmental changes (*R. Schumann, 2016*). Soil land subsidence may be related to natural causes, such as tectonic processes, isostatic movements, chemical-physical transformations (diagenesis) of sediments due to lithostatic load or fluctuations in groundwater level.

In addition, some aspects of human activity can significantly influence or even trigger the phenomenon. Human induced land subsidence generally occurs in a relatively short period of time (at most a few decades), with effects that can seriously impair human works and activities if preventive action is not taken with control and management measures. The most common causes are mainly the overexploitation of aquifers, the extraction of hydrocarbons and the hydraulic reclamation (L. *Carbognin, 1977*). The degree of urbanization and industrialization of an area "sensitive" to land subsidence can therefore influence and be influenced by this phenomenon (*Figure 6*).

Figure 6. Effects of land subsidence on the urbanization

2.1.1. Natural land subsidence

Lowering due to natural aspects is particularly evident in areas where active sedimentation produces massive series of debris with thicknesses that can be thousands of meters. This process can only be explained by allowing a slow descent of the basin connected simultaneously with deposition and sediment accumulation. Usually land subsidence phenomena can occur, both in the epicontinental areas (shallow marine sedimentation environment located on vast inland areas of a continent) or delta and lagoon (the cities of Ravenna and Venice are two characteristic examples). Natural land subsidence results from four types of causes:

- tectonic processes
- crushing and landscaping
- change in the chemical characteristics of clayey soil
- deterioration of surface organic matter

Speaking of tectonic processes, suppose that the Po Basin is a sedimentary basin subsisting between the Alps and the Apennines, we have tectonic forces between the two mountain ranges, over the centuries, created and fed a natural failure called structural failure, which accompanied the geological history of the plain.

In this geological context a phenomenon is created that, with the rise of the Apennines, the plain is lowered (*Figure 7*). In the plain, structural land subsidence is not homogeneous, but is strongly influenced by deep tectonic structures, which identify areas where land subsidence is accentuated (*A.W. Bally, 1985*).

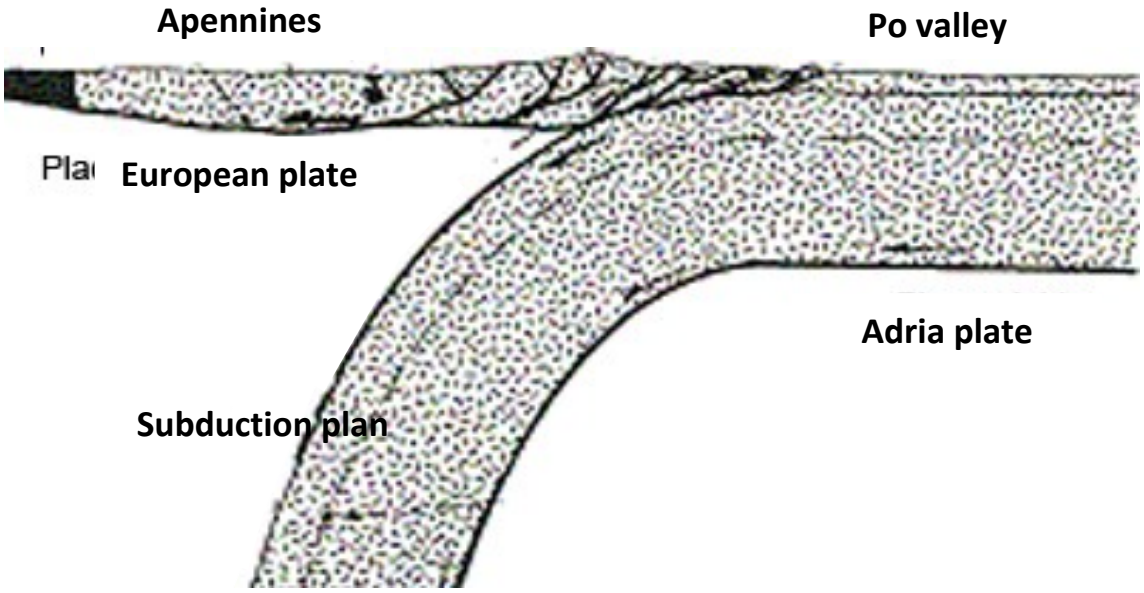

Figure 7. Tectonic processes

These phenomena occur in very long times (even millennia), while if we consider instead shorter time intervals, we have that land subsidence is mainly given by phenomena such as constipation and consolidation of materials that characterize the quaternary, whose base in the Po Delta near the sea reaches 3000m and the surface layers.

In floodplains, such as the Po Valley, sedimentation usually occurs during floods, an event that tends to affect lower areas by filling the previously depressed soil and thus levelling the surface.

This phenomenon makes it possible to compensate for the lowering caused by land subsidence even if the supply of material will subject the lower layers to a greater weight, thus increasing the compaction and therefore the lowering (*G. Gambolati, 1998*).

However, this natural phenomenon is no longer feasible, considering the great works of reclamation and embankment (*Figure 8*) aimed at avoiding harmful phenomena for the population and allowing to drain and keep the soil dry.

Figure 8. Embankment of Po di Goro and water pump of Goro

About the coastal zone of the Po Delta, the natural phenomenon of land subsidence is no longer compensated even by solid transport, which has gradually decreased over time, with a consequent lower contribution of sandy sediments and an increasingly marked reduction of the beaches and the surrounding areas.

Numerous investigations have been carried out on the natural causes of failure by the CNR which, detecting an abnormal lowering, looked for further causes, finding the greatest suspicion in the chemical composition of the clays. The Delta area is in fact partly composed of a particular clay, the montmorillonite, a clay rich in calcium. With the advancement of the saline wedge due to the lowering of the earth and the rising of the middle sea, were added huge amounts of sodium ions (Na) and chlorine ions (Cl). Sodium ions (*Figure 10*) have replaced the calcium ions (*Figure 9*) of clay, but since the ionic radius of the sodium ion is smaller than the ionic radius of the calcium ion, it occupies a smaller volume, causing a lowering of the area (*G. Zambon, 2020*).

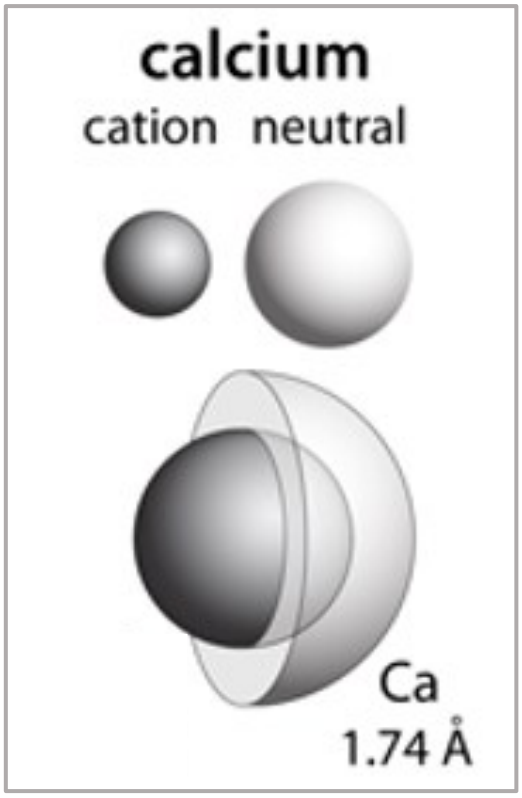

Figure 9. Calcium ions

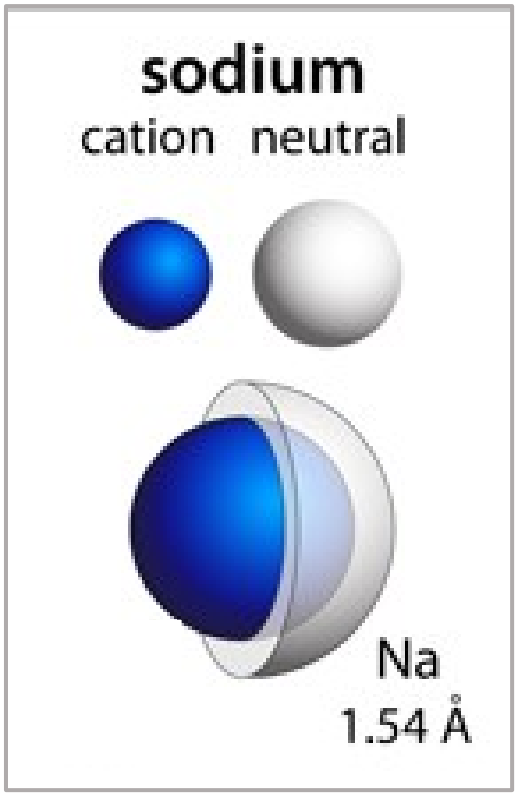

Figure 10. Sodium ions

A final contribution of natural lowering is linked to drying and modification of the surface layers of the soil. The reclamation, with the advent of mechanical means of water lifting affected lagoons, valleys and marshy areas submerged by water whose soil level has been lowered for various causes such as the passage from partially saturated submerged soils to dry soils by putting the organic matter present on the surface in contact with the air. The organic matter in this way will undergo a rapid degradation action, with a consequent reduction in the volume of the soil.

2.1.2. Anthropic land subsidence

Soil lowering can also be linked to certain aspects of human activity that can significantly affect the phenomenon, or even determine the trigger. Human-induced land subsidence generally occurs in a relatively short time (even a few decades), with irreversible effects that can seriously compromise works and activities. The most common causes are mainly over-exploitation of aquifers, hydrogeological remediation or hydrocarbon extraction, as in this case.

The report of the "*Consorzio per la bonifica del Delta del Po Adige of 2011*" provides some useful data to better understand the extent of the extraction of hydrocarbons in a territory that, by its nature, it was alluvial and therefore already subject to phenomena of natural land subsidence previously described.

From the 1930s, and especially in the 1940s and 1950s, until the government decided to suspend in 1961, billions of cubic meters of methane water and natural gas were mined in the Po Delta area. The extraction took place from hundreds of wells that reached a depth of 1000 meters. The gas was sent to the compression stations by means of concrete structures, some of which are still visible in the area *(Figure 11*), while the saltwater present in the amount of 1 m^3 of water per m^3 of gas extracted was discharged into ditches and drains (*Sessant'anni di bonifica nel delta del Po*).

Figure 11. Compression stations in concrete

From 1954 to 1958, 230 million m^3 of gas were extracted per year with a maximum of 300 million in 1959. From 1951 to 1960 an average drop of about one meter was measured, with peaks of up to two meters and, despite the suspension of extraction from 1961, the territory continued to decrease progressively in the following years with effects felt even now.

From the beginning of the '50s to the middle of the '70s the territory has fallen by an average of over 2 meters, up to localized peaks of 3.5 meters. The investigations conducted in 2008 by the *LRG Laboratory (Laboratory of Survey and Geomatics)* of the Faculty of Engineering of the University of Padua have established that the territories of the Veneto Delta east of Taglio of Po have further decreased by about 0,35 meters, which are added to the 2 - 3 meters that occurred between the '50s and '70s.

During the late 1990s and the early years of this century, the studies of institutions and technicians particularly addressed the danger of gas extraction in the Upper Adriatic. The decision to activate extractions from the deposits of the Upper Adriatic can determine the start of a sequence of very serious phenomena for the coastal areas and for the sea defences of the Venice lagoon and the Po delta. The mechanism seems to be that of the formation of depressions in the submerged coast, which capture the solid contributions indispensable for the stability of the beaches and the defences to sea, which could soon enter crisis. The monitoring systems set up to respond promptly to the first signs of land subsidence are inadequate to cope with the phenomenon, because this is always delayed in time compared to the causes that have caused it, resulting in a late response to an irreversible phenomenon.

2.1.3. Effects of land subsidence

The consequences of lowering, also from the economic point of view, are easily imaginable:

- **Higher cost for remediation**: It is necessary to carry out extraordinary maintenance work on the entire drainage system with recalibration of the hydrographic network, demolition and reconstruction of buildings, sewers, bridges on the canals (*Figure 12*) and drainage networks by reconstructing or adapting water pumps to new water levels.

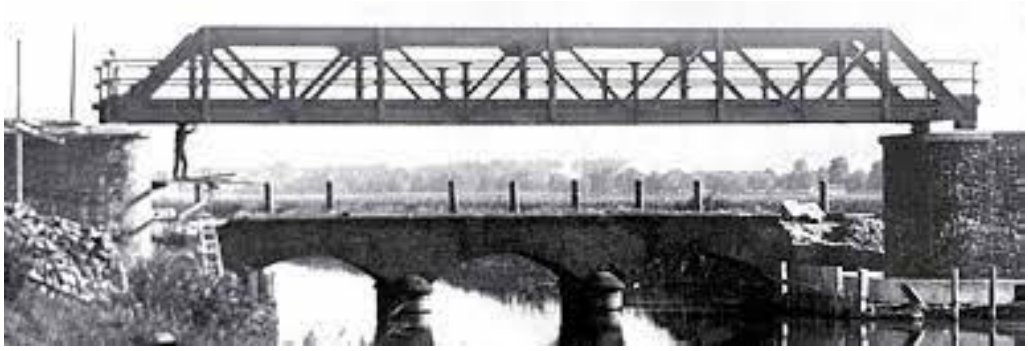

Figure 12. Reconstruction of new build on the "Canale Veneto"

- **Effects on the levees**: the lowering of the ground also drags the embankments (*Figure 13*), this causes a reduction in the safety franc, greater water pressure, greater possibility of formation of fountains and overflows and greater possibility of collapse of the levee.

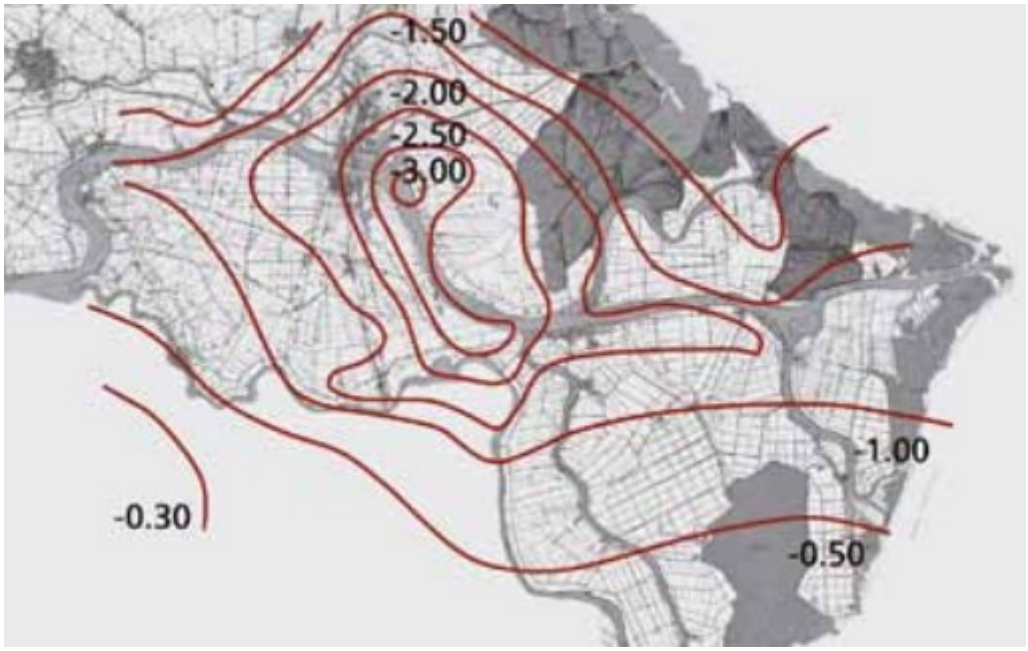

Figure 13. Isolines of land subsidence from 1947 to 1970

- **Risks arising from the collection or spillage of water**: if the phenomenon affects an area equipped with drinking water supply services (aqueduct) or water disposal or drainage services (sewerage), it is necessary to restore these works against enormous costs. In the first case there is the risk of polluting the groundwater supply with marine water, causing the non-use of these sources, and a possible change in the natural characteristics of the soil itself.

- **Hygienic-sanitary discomfort**: In the case of surface marine entrances the phenomenon of high water occurs with enormous inconvenience to the population and commercial activities. A well-known case is that of the high water in Venice (Figure 14), a phenomenon indicating particularly pronounced tidal peaks occurring with periodicity in the northern Adriatic Sea. The phenomenon is more and more pronounced because of the combined action of land subsidence that causes a lowering of the soil and the phenomenon of eustatism that increases the average sea level.

Figure 14. Phenomenon of high water in Venice

2.2. Salt wedge intrusion

The typical feature of a Delta is to represent the transition between river and sea, which involves unique hydraulic, morphological, and biological characteristics, and not comparable to those of other water bodies. This peculiarity involves a negative aspect that consists in transporting the salt present in the water to the mouth of the river: this event is known as the propagation of the salt wedge. From a theoretical point of view, this phenomenon is hydraulically framed within the so-called density currents in which there are two distinct layers of different densities are created within a basin of water where saltwater remains on the bottom compared to freshwater lighter (*P. Peruzzo, 2020*). This phenomenon occurs when the flow of the river falls below the critical speed, the limit above which the salt wedge is completely rejected. In recent decades, however, the saline wedge has assumed increasingly worrying proportions, with a progressive intrusion of water bodies to the hinterland. The phenomenon, which from the 1930s to the 1960s was only felt for two or three kilometres from the mouth, subsequently spread, with damaging consequences both on the ecosystem and on economic activities. In the '70s and '80s, the gravity of the situation began to be felt, because the saline wedge had pushed about 10 km from the mouth. More recently, the presence of the salt wedge has been detected up to 30 km from the sea, a distance such that the effects are alarming (*Sessant'anni di bonifica nel delta del Po*). The data mentioned can be summarised and briefly represented with a sequence of clear and representative images in which we can see in the left the extension of salt wedge intrusion in 1970, while in the right the extension in recent years (*Figure 15*).

Figure 15. Extension of salt wedge intrusion

A technique called “moving boat” has been applied to monitor the lifting of the saline wedge, where a multiparametric probe is used that, moving at the speed of the tidal wave, performs salinity measurements at the same time of high tide. In this way, during a day, saline intrusion can be monitored at high and low tide, depending on the distance of wedge intrusion. Campaigns for the distribution of the flow and the intrusion of salt wedges have been recently used to calibrate a simulation model of wedge increase that Arpa-Sim keeps operating within the modelling to support the management of water resources. The model allows to simulate the salt concentration in the branches of the Po, assuming as a limit condition the temperature and salinity in selected points of each branch (F*igure 16*).

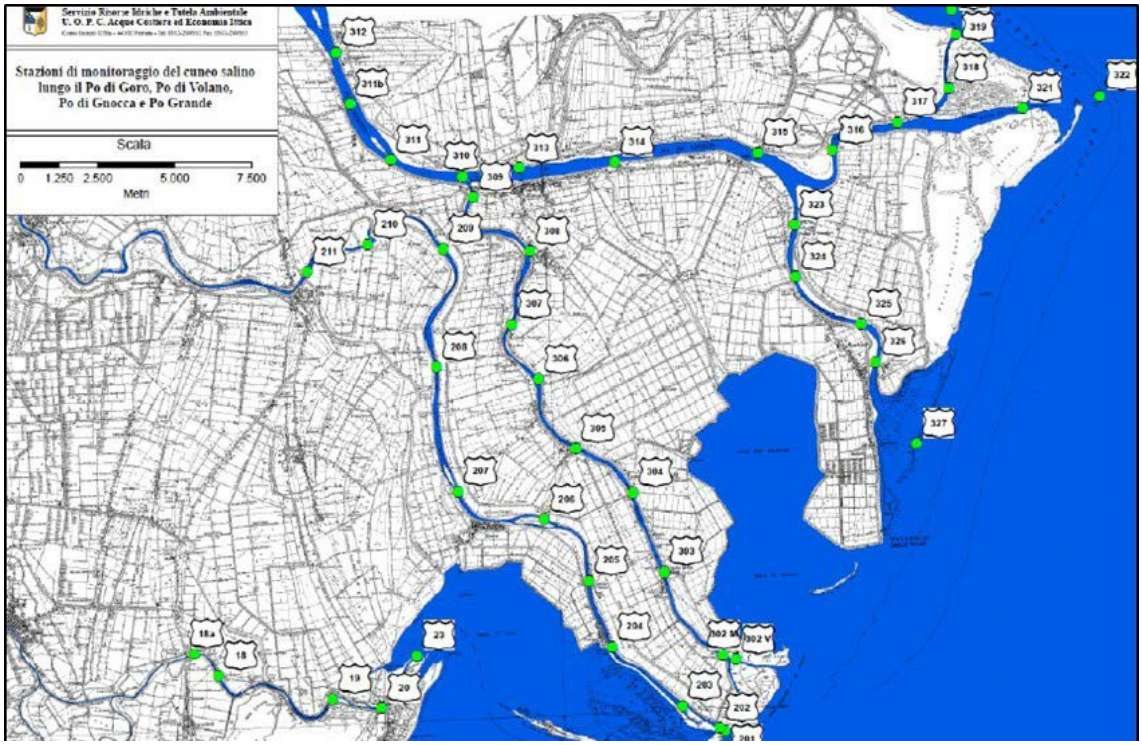

Figure 16. Location of measured point

To prevent this problem, a series of measures must be taken to ensure that Pontelagoscuro has a flow rate of not less than 330 m3/s by building mountain reservoirs and increasing the outgoing flow (*Sessant’anni di bonifica nel delta del Po*). In addition, to prevent the problem, it is possible to move the irrigation leads further upstream or use the anti-sale barriers. In particular, the latter were built on the Po of Gnocca, on the Taglio canal, at the mouth of the Po of Tolle and at the mouth of the Adige.

Such structures have demonstrated the effectiveness in allowing the outflow from upstream to downstream but blocking the salt water from the valley to upstream. However, account must be taken of the many problems associated with the river's lean periods, navigation and maintenance costs.

2.2.1. Causes of salt wedge intrusion

The increase in the entry of the saline wedge of the Po Delta, detected in the surveys mentioned above, is attributable to several factors, including:

- Descent of delta soils due to natural and artificial failure.
- Sea level rise, as even a few centimetres may be particularly influential given the altitude of the Delta.
- Change in precipitation regime with concentrated precipitation resulting in rapid flooding and prolonged periods of low flow rates.
- Increase of the derivations for different uses along the Po.
- Lowering of the riverbed due to a lower contribution of sediment from the tributaries and for the withdrawal of aggregates.
- Less release from artificial lakes (*Figure 17*) to avoid lack of availability in dry periods.

Figure 17. Example of artificial lake

2.2.2. Effects of salt wedge intrusion

The saline wedge therefore has various negative effects in the Po Delta area, such as:

- Modification of the biological characteristics of the terminal sections with changes in the trophic chain and consequent effects on fish fauna.
- Interruption of irrigated branches.
- Interruption of supplies of aqueduct in the eastern part of the Polesine.
- Salinisation of groundwater.
- Drainage of coastal areas and micro-desertification in which sterilization phenomena may occur with habitat change. It has been recorded that in the areas of interest, the halophilic vegetation (Figure 18) is expanding in typical brackish environments that end up losing their typicality and assume typical aspects of desert areas, such as coastal sandy areas.

Figure 18. Halophilic vegetation

2.3. Reduction of solid transport

Solid transport is a natural phenomenon induced by the current of a stream that, by virtue of the speed and availability of sediments, moves solid granular material (gravel, sand and silt) both in suspension and on the bed of the riverbed. The transported sediment mainly derives from the erosion of slopes caused by atmospheric agents (*J. M. Fox, 2004*).

The material that is transported in suspension is very fine (its presence is generally indicated by the dark colour (*Figure 19*) that the water of a river assumes during a flood). On the contrary, the material transported to the bottom has coarser dimensions and crosses the stream from mountain to valley with jumps and rolls.

Figure 19. Flood event

Due to the reduced slope of the watercourse bed, the flow rate and the speed of the current, the deposition phenomenon affects elements of ever finer grain size. In fact, the greater the strength of the current, the greater the part of the solid transport that remains suspended in the water, to the detriment of what is deposited. As the velocity of the current decreases, the particle size of the deposited materials also decreases, to the point of considering materials such as sand and silt which are particle sizes common to areas near the outlet to the sea. The solid transport process is not constant but varies with the flow rate of the watercourse.

On the events of drought and flooding of watercourses, there is a general remodelling of these phenomena with the mobilization of already sedimented aggregates and a consequent faster translation towards the valley of the deposits that make up the seabed.

From these considerations, a balance can be established between sedimentation and erosion, which in turn determines the state of erosion or sedimentation of the delta. This territory is fundamentally affected by what is termed "solid flow" which is the amount of solid substance transported by a stream through a given hydraulic section. Today the reduction of solid transports is one of the main causes of erosion of the Venetian beaches ("*C. Del Grande, 2000*"). The main causes of this reduction in solid transport are due to the presence of mountain basins that retain part of the water reducing the flow of the river especially for the long periods of drought and remediation works carried out along the river that can lead to bed cleaning or slope reduction (which leads to an increase in sedimentation) thanks to the use of the check dams (*Figure 20*).

Figure 20. Check dams

Recent studies have shown that in the late 1970s there was a 3 to 4 times decrease in solid transport compared with the situation in the 1940s.

This situation, already precarious, is aggravated by the fact that in Veneto beaches and marine sediments have a strong sandy component with percentages ranging from 100% in the emerged beaches, up to about 80% in the depths closest to the coastline, with a coast orientation such that the sediment movement takes place in a particular way. In facts the energy of the sea that is discharged to the coast and the consequent capacity of transport along the coast (*Figure 21*) is higher than the contribution of sediments from rivers that reach the sea through their mouths, thus causing a shortage of material that leads to a reduction in beaches (*L. Martinelli, 2021*).

Figure 21. Longshore current

2.4. Eustatism

One of the most hazardous consequences of ongoing climate change is sea level rise. Rising sea levels are a problem which has serious consequences in many parts of the world and is bound to have more and more. About two-thirds of the world's population lives within 60 kilometres of the coast, and nearly half of the world's cities with more than a million people are located near river estuaries (*G. McGranahan, 2007*). This phenomenon is due to the thermal expansion of seawater and the melting of continental ice. When we speak of thermal expansion of sea water, we refer to a normal physical phenomenon according to which a fluid, subjected to gradually higher temperatures, expands, increasing its volume.

The oceans absorb most of the excess heat emitted into the atmosphere by human activity (about 90%), and for this reason the most superficial layers have seen their temperature increase by about 0.11 ºC for decades during the last decades. This, together with the overheating of the deeper layers, leads to an inevitable expansion of the water and therefore the increase of the average sea level (*T. Frederikse, 2020*).

Another phenomenon behind sea level rise is the melting of continental ice (*Figure 22*). The melting of the ice, in fact, once reached the Oceans, induces an additional supply of water, with a consequent rise in sea level. Not all ice, however, contributes to the rise. Sea ice, being a floating body composed of solid sea water due to low temperatures, would not add any additional water mass to the oceans if it melted.

Figure 22. Melting of the ice

To protect the coasts, it is necessary to build massive barriers to reduce the effects of high tides as in Venice with the "MOSE", provide with interventions to raise the banks and plan future strategies to reduce the inconvenience to citizens. The defence of the beaches instead will need a system of dunes and works of defence to sea as groins (*Figure 23*) and detached breakwaters useful to bring and retain sand along the coast, thus managing to reduce the effects of the advance of the sea (*P. Ruol, 2020*).

Figure 23. Groins

According to "*Estimating global mean sea-level rise and its uncertainties by 2100 and 2300*" from an expert survey also respecting the 2 degrees of the Paris Agreement, which at the moment seems unlikely since the projections lead us to an increase in temperature of at least 3.5 degrees by the end of the century, the sea level could rise by about two meters. A different forecast from that made by the IPCC (Intergovernmental Panel on Climate Change), which over time underestimated the extent of this phenomenon.

This statement has been recalled by the author of the study Stefan Rahmstorf, of the Postdam Climate Impact Research Institute: "*In its studies the IPCC tends to be very cautious and conservative, which is why it has had to correct itself upwards already several times*". There are three reliable forecasts for the Po Delta:

- IPCC: increase in sea level of 594 mm in case of significant reduction of pollutants
- IPCC: increase in sea level of 999 mm in case of continuous emission of pollutants
- Rahmstorf predicting an increase in sea level of 1395 mm

Most coastal regions in Europe have experienced an increase in absolute sea level and sea level relative to land and according to a study by ENEA and its projections within the 2100 thousand square kilometres of Italian coastal areas risk to be submerged by the sea. The monitoring of sea level in Italy is entrusted to several departments, there is the "Rete Mareografica Nazionale" managed by "Servizio mareografico nazionale (SMN)" that consist of 36 observation stations in real time of level (*Figure 24*), atmospheric pressure, wind speed and direction and temperature (*L. Carbognin, 2009*).

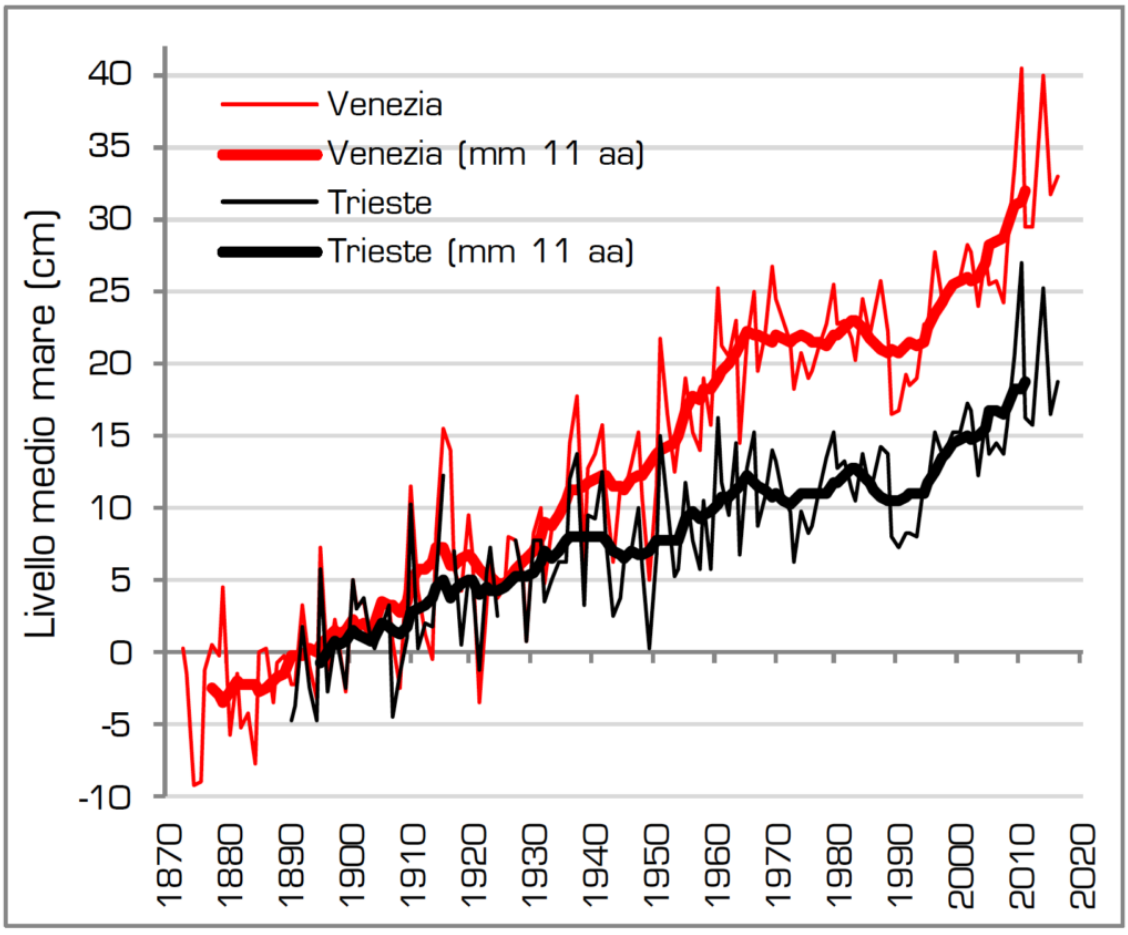

Figure 24. Mean sea level along the years (ISPRA)

Another contribution is given by various universities or research institutes that through the study of the shoreline via relief LiDAR (*Figure 25*), GNSS, photogrammetric flight or classical topography techniques (with the use of total station) can reconstruct and then monitor the trend of the wet front studying the effects of eustatism on the wet front.

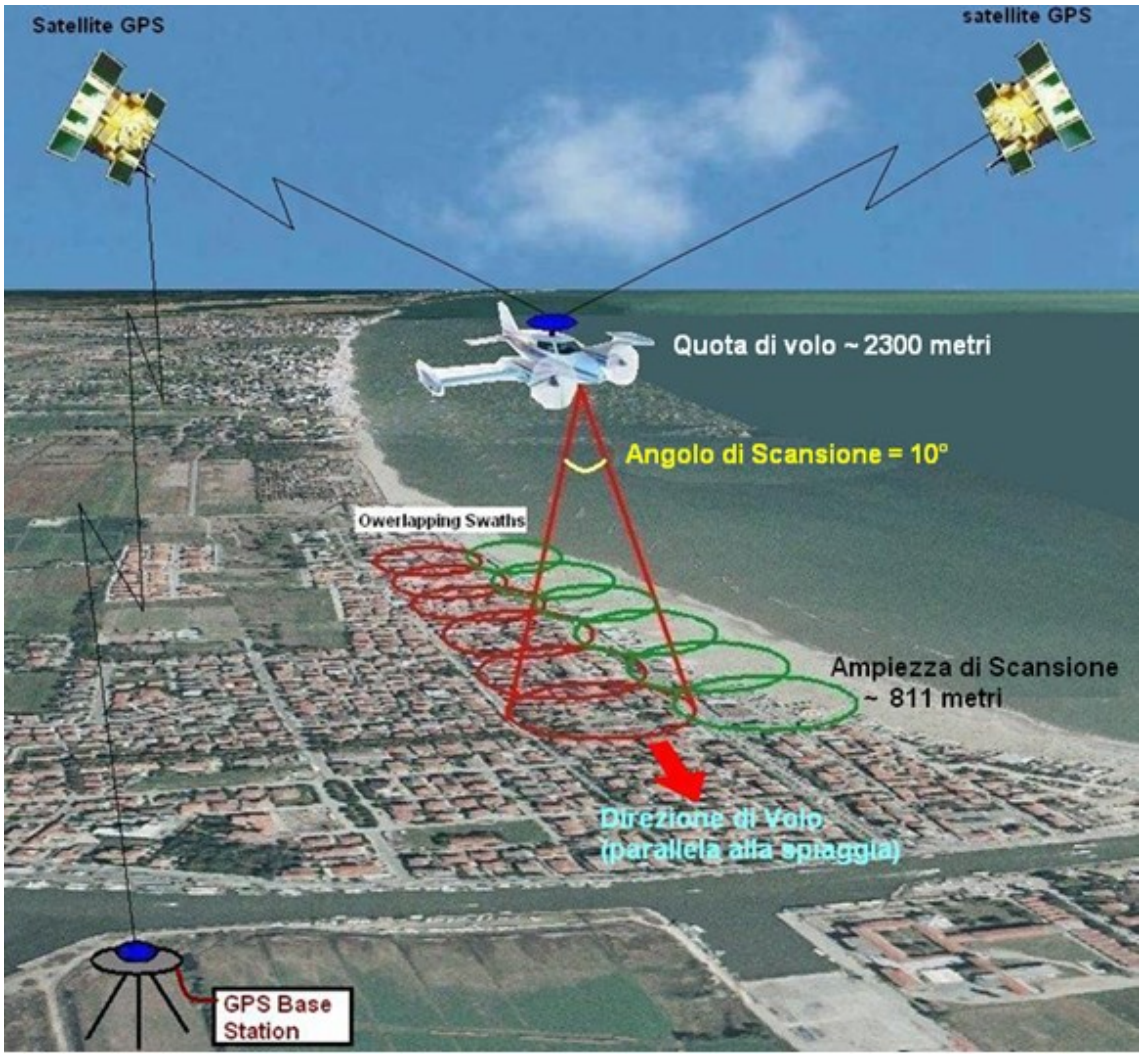

Figure 25. LiDAR survey

The comparison between these methods is much complicated since all methods guarantee pro and contro. For example, the GNSS relief, the photogrammetric relief with UAV instruments and the classical topography allow us a centimetric precision and a good representation of the wet front with no tide, but unfortunately, they offer a limited representation at the territorial level being methods applicable in short periods of time (to get the tide zero) and for short stretches of beach.

The LiDAR relief to the contrary offer's minor precisions, but tolerable considering the precisions of the representation of the coastline, moreover it is optimal for having a representation of vast areas, but unfortunately without the possibility to operate in the moments of tide zero.

The results then show the wet front at different times and with different tidal altitudes, making it difficult to interpret the analysis and comparison between them.
It was decided to divide the LiDAR relief from the others, in particular the multitemporal LiDAR relief was useful to understand the variation of the areas emerged over the years (although there will always be a big mistake due to the different tides present at the time of the survey) and thus verify the influence of land subsidence but especially of eustatism on coastal areas.

Results from multitemporal LiDAR surveys have shown a reduction in areas emerged since 1950, showing peaks between the years 1955 and 1977. In recent years thanks to use of defence works such as groins, detached breakwaters and sandbanks, and thanks to the reduction of the effects of land subsidence, there has been an inversion in the delta area, with an increase in areas emerged. This is a demonstration of how it is possible to limit the effects of irreversible phenomena such as land subsidence and eustatism.

CHAPTER 3. TYPE OF SURVEY

Now it is necessary to understand the various techniques used for the study of phenomena affecting the Po River Delta.

3.1. Survey with GNSS stations

It's a real-time 3D positioning system on the globe, based on a constellation of artificial satellites, this method provides the three-dimensional position of a point on the Earth's surface with a maximum accuracy of 1 cm (*M. Fabris, 2022*). The signal emitted by the satellite is received by the antenna of the receiver on the ground, which saves it in the form of an observation file. The instrument simultaneously receives multiple signals that are captured through different reception channels. Through the components "code" and "phase" it is possible to calculate the position of the instrument, normally the information provided by the code are used for real-time positioning with low precisions, while the data provided by the phase offers greater precision and are used in post-processing. The choice of the acquisition technique to be used depends on the type of survey and the type of data processing. A first technique is the absolute positioning that consists in the use of a single receiver and involves high errors. Another technique is the differential positioning in which I have the use of two receivers: a master positioned on a known point and a rover positioned on the point to be calculated, in this case the accuracy increases because I can make additional adjustments. The technique that allows maximum precision is relative positioning (*Figure 26*).

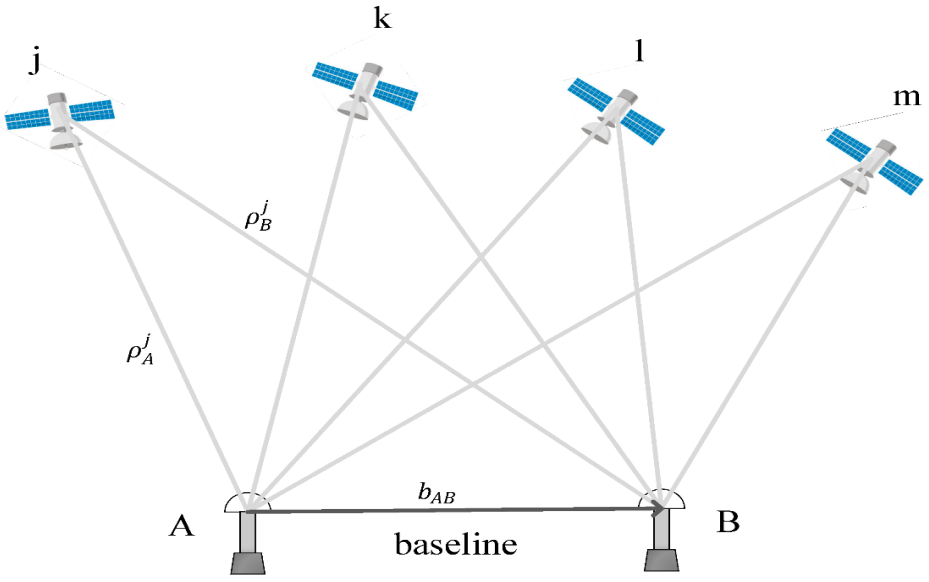

Figure 26. Relative positioning

In this technique, the vector that connects the two stations (baselines) is measured. The position calculation is made in post-processing through the data acquired by the rover and master stations. Being known in fact a point M (position of the master station) and the vector union (baseline) with a second point R it is possible to obtain the position of the rover (point R).

3.1.1. Equation of pseudo-range

The signal produced by the satellite and received by the receiver antenna takes a certain interval to reach the destination and this is the concept behind the GNSS survey. Assuming perfect synchronization between code sending and signal reception, the signal takes a time from t_0 (signal sending) to t_1 (signal receiving) to reach the receiver. However, this does not happen because an offset is always generated due to the difference in accuracy between the hydrogen clocks of the satellites and the quartz clocks of the ground receivers and this offset produces a big error.
In algebraic analysis you will then have 4 variables (3 coordinates and the offset due to non-synchronization clocks). It will then take 4 pseudo-distance equations to derive the position of the unknown point. The pseudo-range equation is:

$$\boldsymbol{\rho}_{ij=}c * \mathbf{\Delta t} = \sqrt{\left(\boldsymbol{x_j} - \boldsymbol{x_i}\right)^2 + \left(\boldsymbol{y_j} - \boldsymbol{y_i}\right)^2 + \left(\boldsymbol{z_j} - \boldsymbol{z_i}\right)^2} \pm \mathbf{c} * \boldsymbol{\delta_{tij}}$$

c : light speed in the space;
$\mathbf{\Delta t}$: time of flight of the GPS signal;
$\boldsymbol{x_j}, \boldsymbol{y_j}, \boldsymbol{z_j}$: Satellite ephemerides;
$\boldsymbol{x_i}, \boldsymbol{y_i}, \boldsymbol{z_i}$: coordinates of the point on the Earth's surface;
$\boldsymbol{\delta_{tij}}$: error of non-synchronization clocks.

The non-synchronization error of the clocks is not the only source of error, there are in fact other errors such as the error of ionospheric and tropospheric refraction, the error due to multiple reflections, cycle jumps, operator errors and satellite orbit errors.

3.1.2. Advantages and Disadvantages of GNSS methods

The GNSS survey is an ideal survey method for areas such as the Po Delta, which has isolated but often easily accessible areas and the area is free of obstacles. In particular, the GNSS survey is more useful in areas where the SAR survey does not detect a good density of points. The main advantages of GNSS surveying are precision, the ability to make multitemporal acquisitions over the years and then evaluate the trend over time. Moreover, it is not excluded the possibility of detecting points in any area, in agricultural or wooded areas (thanks to the reception of four constellations) areas that with the SAR would not be possible to detect except with the construction of artificial reflectors. Moreover, to hold in consideration is the cost of the relief that removed the cost of the instrumentation turns out to be economic being the duration of survey inferior to the week.

Unfortunately, the limits of this technique are many, first the GNSS precision even if good is not suitable to detect the drops due to subsidence in the Delta area, in fact the average lowering of the area settles on 5/6 mm/yr, while the GNSS accuracy is equal to one centimetre, this means that to appreciate the lowering it is necessary to run a major GNSS campaign every two years (*M. Fabris, 2022*). In addition, the GNSS technique has many errors, but the error to which we must pay more attention in this case is the multipath due to the reflection of the signal by the many bodies of water present in the area.

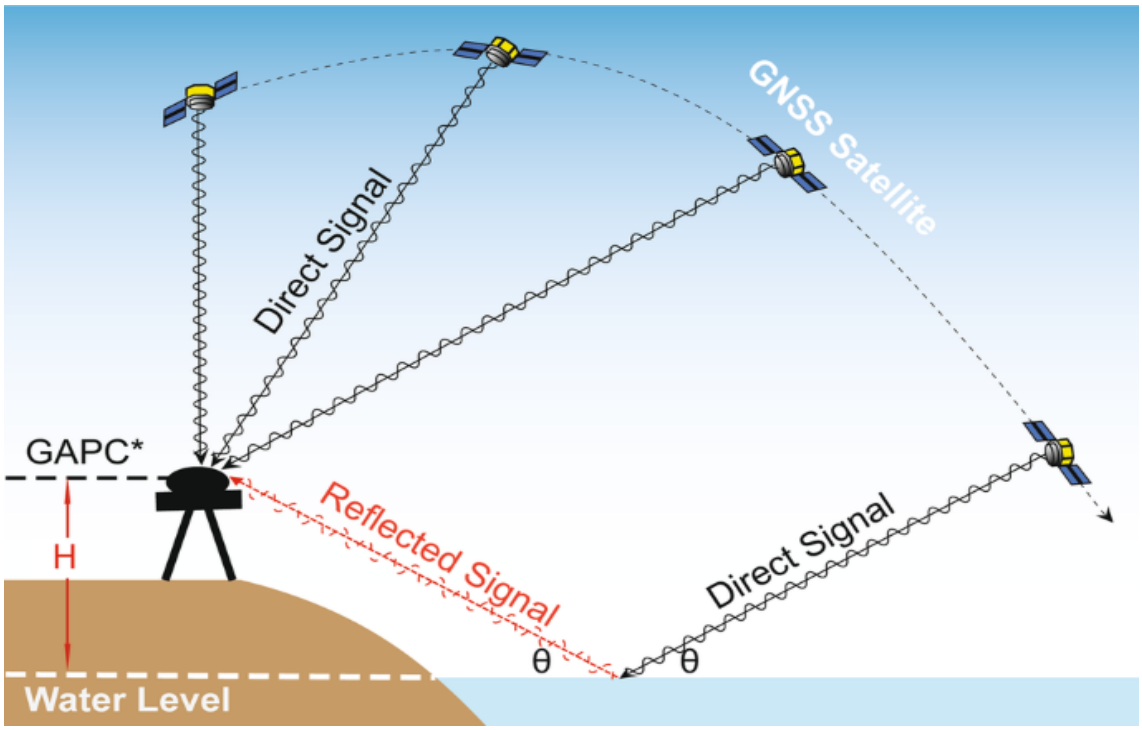

Figure 27. Multipath error

Another disadvantage is the cost of equipment which could be reduced thanks to the use of RTX services or correction networks on the Italian territory and the cost of operators being the method of static survey with parking equal to three hours.

3.1.3. Global Navigation Satellite Systems (GNSS)

The Global Navigation Satellites System (*Figure 27*) is composed by different constellation, there are GPS (American system), GLONASS (Russian system), GALILEO (European system) and BEIDOU3 (Chinese system). These systems can be separated into three segments: space, control and users.

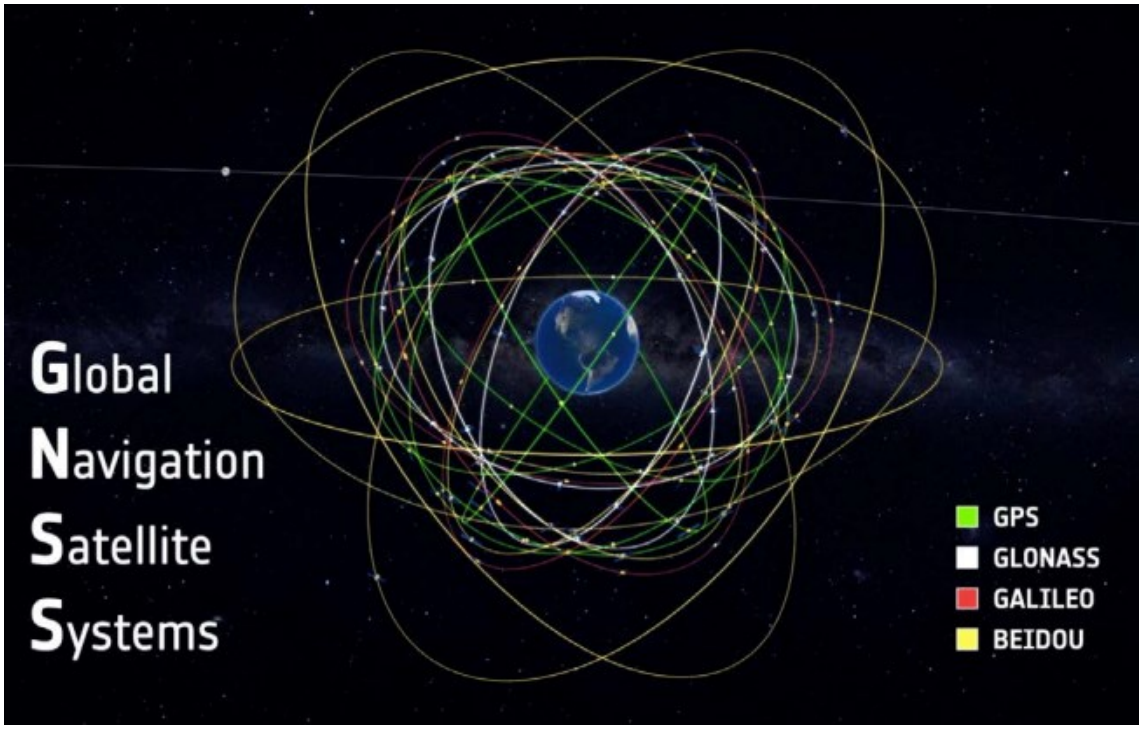

Figure 28. GNSS orbits

3.1.3.1. GPS system

The GPS system is an American military satellite navigation and positioning system operating since 1994. the GPS system consists of three different segments: the space segment, the control segment and the user segment. The space segment is composed of the constellation of satellites in orbit that rotate around the earth on almost circular orbits. There are 30 satellites on 6 orbital planes. These satellites are 20200 km from the surface and need 11 hours and 58 minutes to perform an entire revolution around the planet. This arrangement allows at any time and at any point to receive at the same time

the necessary information from a minimum number of 4 satellites present within a cone with elevation from the horizontal of at least 15 degrees (*M. Fabris, 2022*).

Each satellite presents a certain type of apparatus to accomplish its work such as atomic oscillators composed of high precision clocks, transmission and reception apparatus, calculation unit to define the orbits to be followed and memory.

Moreover, there are a self-powering system consisting of photovoltaic panels and a navigation apparatus consisting of small thrusters to adjust the orbit. For the communication of information each satellite (*Figure 28*) transmits navigation signals in phase modulation on two carrier waves called L1 and L2 both multiple of the fundamental frequency fo equal to 10,23 Mhz. In addition, I can have a code C/A which is a square wave built by sine wave L1, code P is a square wave built using both the code L1 and L2 and code D which is a navigation code of the messages useful to send information on the survey in RINEX to users and to send ephemeris and predictive status of the signal thanks to use of different parameters called GDOP, HDOP, VDOP and PDOP.

Figure 29. GPS satellite

The control segment is composed of five main stations (Ascension, Diego Garcia, Kwajakiin, Hawaii and Colorado Springs) on the Earth's surface, these main stations are located along the equatorial plane and are used to monitor the ephemeris, to predict the next orbit and to correct the orbit. I have three types of ephemerides: reference ephemeris which are a first estimate of ephemeris considering the trajectory in the last week, in this case the precision is of the order of 50m; predicted ephemerides that provide an estimate of the trajectory considering the trajectory in the last 12-24 hours, in this case the precision is about ten meters.

In the end I have precise ephemeris, this type of data is available with a delay in the order of 10-15 days and provide the exact trajectory of the satellites.
The user segment consists of users equipped with GPS receiver consisting of antenna, controller (with microprocessor), data recording system and power supply system.

3.1.3.2. GLONASS system

The GLONASS system is a Russian military and civilian satellite navigation and positioning system operating since 1995. the GLONASS system is indicated to improve the signal in high latitudes where the GPS signal can be problematic. Even in this case is composed by three different segments: the space segment, the control segment and the user segment. The space segment is composed of the constellation of satellites in orbit that rotate around the earth on almost circular orbits. There are 24 satellites on 3 orbital planes. These satellites are 19100 km from the surface and need 11 hours and 15 minutes to perform an entire revolution around the planet. GLONASS satellites transmit two types of signals: open standard-precision signal L1OF/L2OF, and obfuscated high precision signal L1SF/L2SF.
As for the GPS system even with GLONASS I have ground monitoring stations that receive the information sent by satellites and transmit them to the master station where they are processed and corrected.

3.1.3.3. GALILEO system

The GALILEO system is a European civilian navigation and positioning system operating since 2016. Is composed by three different segments: the space segment, the control segment and the user segment.
The space segment is composed of the constellation of satellites in orbit that rotate around the earth on almost circular orbits. There are 27 satellites on 3 orbital planes. These satellites are 23222 km from the surface and need 14 hours and 4 minutes to perform an entire revolution around the planet. Each satellite can work in dual frequency by default with two carrier waves modulated on the code sequence Pseudo-Random Noise (PRN); in this way, the accuracy obtained will be of the order of cm. The control segment is instead composed of two main control stations (Fucino and Oberpfaffenhodef) and five additional control stations.

3.1.3.4. BeiDou-3 system

BeiDou-3 is a new global navigation satellite system being developed by China National Space Administration (CNSA) as an alternative to the global positioning system (GPS) of the USA, Russia's GLONASS, and Europe's Galileo. The BeiDou-3 is part of the BeiDou navigation satellite system (BDS), which aims to develop space infrastructure for round-the-clock, all-weather, accurate navigational, positioning, and timing services. The BeiDou-3 constellation includes 35 satellites which has been offering a full range of services since 2020. Five of the 35 satellites are placed in geostationary orbit (GEO), three are placed in inclined geostationary orbit (IGSO), and the remaining 27 in the medium Earth orbit (MEO).

3.1.4. PODELNET network

The PO Delta Network (PODELNET) is a low-cost network of non-permanent stations and continuous GNSS stations (*Figure 29*) located in the Po River Delta (PRD). The network was developed to improve 3D remediation information in the PRD area, monitored until 2016 with only two CGNSS sites located within the study area (TGPO-Taglio di Po and PTO1-Porto Tolle) and three in the surrounding areas (CGIA-Chioggia, CODI-Codigoro and GARI-Porto Garibaldi).

PODELNET was developed in 2016 in agreement with the IGMI (Istituto Geografico Militare Italiano) and the Veneto Region by the Territorial Information System and Cartography Project Unit and the Rovigo Civil Engineering Organizational Unit): consists of 46 non-permanent stations monitored with the GNSS technique. This low-cost and low-impact network is the first application of the 7 km density of the IGM95 network in the Veneto Region and, for this reason, the points are named according to the IGM procedures (*N. Cenni, 2021*).

PODELNET is also used as a reference framework for the activities carried out by the public authorities of the territory, both Veneto Region and of the Po Delta Reclamation Consortium. The PODELNET summits were chosen to consider both the existing points belonging to the IGMI levelling network (*line 19 and line 174*) and other points belonging to local authorities and institutions. In addition, 16 new sites have been identified to achieve a uniform distribution of the network and avoid gaps. Of the 46 non-permanent GNSS sites in the PODELNET network, 24 concerned the nearest levelling parameter, which provided an orthometric elevation of the points related to the

last IGMI geometric levelling measures, carried out in 2005. The other 22 NPSs are the reference points of the IGMI levelling network.

Each point of the PODELNET refers to the nearest point using a baseline between 5 km and 7 km.

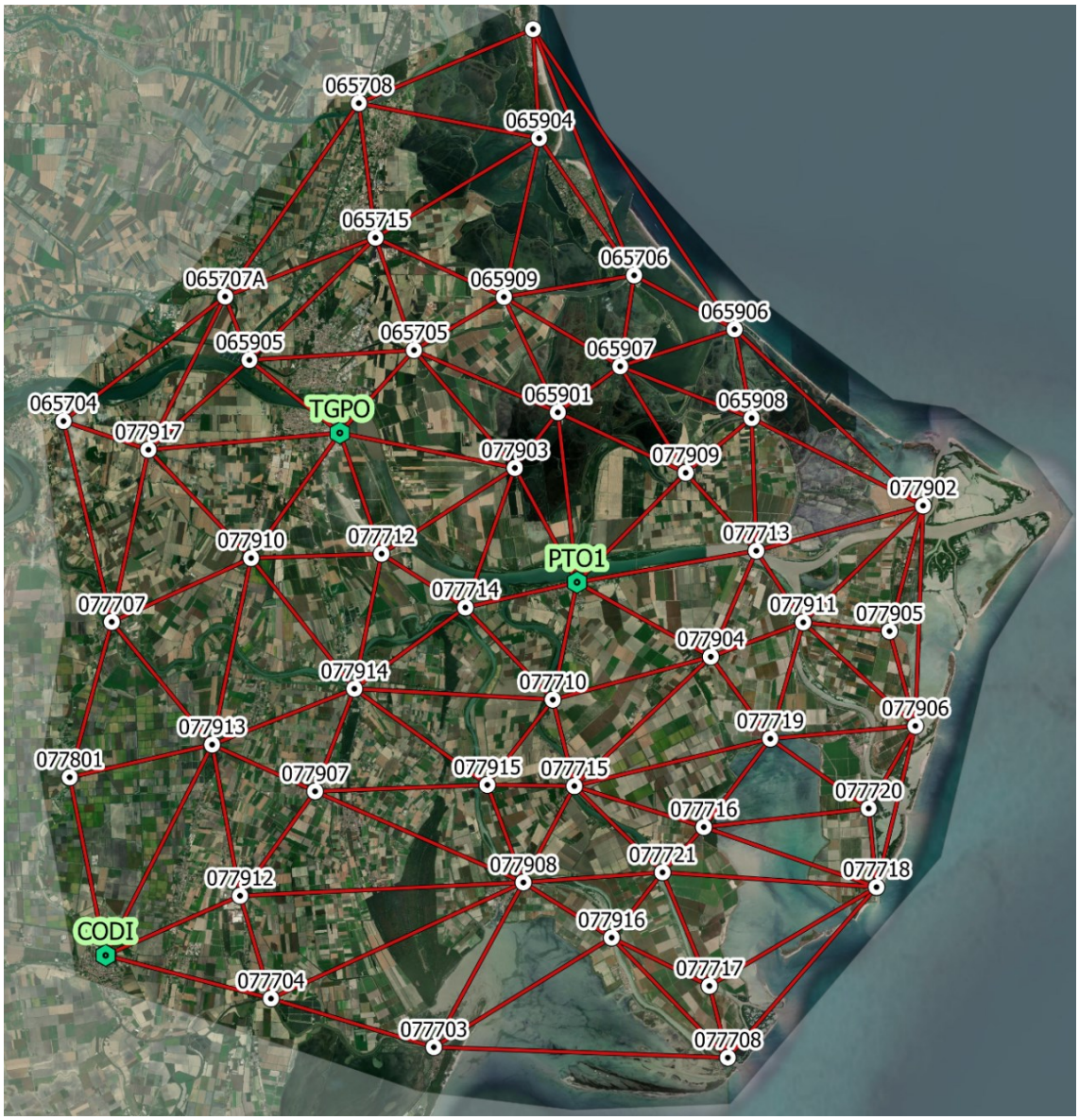

Figure 30. PODELNET network

The first measurement was carried out in June/July 2016 and the second survey was two years later, but in the same months to reduce the potential influence of seasonal signals in measured speeds.

The amplitudes of these seasonal signals are not usually negligible and may introduce distortions in the estimation of speed (*N. Cenni, 2021*). The two surveys were also designed to reduce the impact of the measurement conditions on the estimate of 46 NPS stations. In particular, the two campaigns were conducted by probing the same reference bases, where possible, with the same percentages of sampling, time of stationing and instruments.

The instruments that are used are Leica GPS system 1200, Leica Viva GNSS GS14 and Leica Viva GNSS GS16. The minimum observation time at each site was 3 h, with a sampling rate of 15 s. The data obtained from the permanent station are processed in the office with the "Bernese" software, while the data from the non-permanent station are processed with the software "Leica Infinity".

The point of non-permanent stations is called with six numbers in which the first three numbers are based on cartography: with 065 points are located above Po's Venice, while with 077 points are located below Po's Venice. Instead, the second number three are related to the type of IGM network level (first, second or third order).

3.1.4.1. Results of survey campaigns

The results of the two measurements are shown in the table (*Table 1*), the measurements represent the velocity in mm/yr along the vertical direction between 2016 and 2020.

ID	E [m]	N [m]	Vel GNSS [vert]
077703	757825,256	4966209,149	-16,2
077912	750825,087	4971669,295	-12,6
077704	751940,974	4967960,692	-16,0
077902	775501,151	4985737,955	-11,9
065906	768690,503	4992097,303	-10,8
065704	744443,14	4988787,557	-8,8
065908	769308,307	4988892,977	-8,3
077911	771170,294	4981529,522	-14,9
077710	762125,124	4978742,982	-11,0
077914	754954,745	4979134,403	-7,1
065907	764558,913	4990762,553	-8,3
077714	758966,315	4982066,132	-6,8

077801	744670,489	4975941,71	-14,7
065904	761631,296	4998989,19	-8,2
077708	768445,765	4965830,68	-17,3
077707	746188,739	4981545,757	-10,1
CODI	745967,869	4969519,825	-2,8
TGPO	754427,755	4988361,841	-5,1
PTO1	762996,544	4982974,015	-5,1
077909	766925,645	4986922,727	-4,8
065706	765062,79	4994042,661	-6,9
077721	766087,388	4972512,072	-14,0
065903	761407,718	5002922,314	-8,8
065905	751160,271	4990990,377	-5,4
077910	751223,757	4983847,229	-4,7
065901	762304,224	4989103,169	-5,7
077719	769980,197	4977334,481	-10,4
077715	762902,394	4975624,273	-9,2
077917	747512,15	4987754,104	-7,2
077713	769475,861	4984110,782	-7,3
065909	760358,32	4993264,166	-4,0
065705	757109,453	4991346,546	-5,1
077718	773819,108	4971981,29	-15,5
077905	774288,277	4981212,813	-8,0
065715	755717,585	4995403,759	-4,1
077907	753535,649	4975435,115	-4,6
077712	755936,765	4984002,507	-4,5
077915	759756,954	4975668,396	NULL
077913	749816,246	4977120,667	-4,4
077908	761059,962	4972149,939	-11,0
065707A	750286,76	4993280,113	-4,6
077904	767831,251	4980289,859	-5,8
077903	760753,491	4987098,085	-3,4

065708	755113,675	5000253,036	-3,0
077716	767579,113	4974146,538	-9,6
077916	764249,412	4970158,938	-10,2
077906	775224,129	4977794,295	-12,3
077717	767781,618	4968418,334	-9,3
077720	773535,229	4974818,483	-12,2

Table 1. Velocity along vertical of PODELNET network

There are some considerations to make on the points:

- Point 077915 was destroyed during mowing operations. Nearby, a new vertex called 077918 was materialized. The point has already been detected with 1 hour of stationing while from 2022 the point will begin to be detected with a static method with 3 hours of stationing.

- Point 077907 is at risk because a roundabout will be built there, and the point will be destroyed. For this reason, a new vertex was materialized in a shoulder of a bridge 500 meters from the previous position. The two vertices were connected simultaneously with geometric levelling from the centre. The new summit will be measured by a static method from 2022.

- The location of point 077905 is not favourable to satellite reception due to the presence of obstacles and, moreover, was difficult to occupy. The consequence of a bad reception was found in the results of the network compensation which determined the worst precision for this vertex with double values of root mean square compared to the other vertices (*A. Menin, 2020*). For this, a new vertex has been materialized, already connected in real time with levelling from the medium and that will be measured with the static method from 2022.

- Point 077721 is on a stable foundation plate, shows high lowering values, the point must be kept under control.

- Point 077801 is located on a small pillar on a channel which is often submerged, the point must be kept under control.

- point 077911 is on an unstable pillar near the shoulder of a bridge, the point has high inclination values, and the point will certainly need to be changed.

- Points 077708 and 077713 are extremely important because being in isolated areas, they have no SAR points nearby. This is an advantage of GNSS vertices because they allow me to get results in areas that would otherwise not be possible with SAR data alone. One might think in the future of refining the delta area in less urbanized areas, then using the GNSS vertices present in urban areas as a verification on SAR data.

To determine other GNSS vertices that have problems it is necessary to compare them with the SAR data, to find a substantial difference between the two measures. To evaluate the results just obtained, it is necessary to first make a note on the tolerances allowed between GNSS speed and SAR speed.
For permanent stations a tolerance of 2 mm/yr is set which is equivalent to a maximum difference of 0,8 cm in four years, while for non-permanent stations the tolerance is set to 5 mm/yr which is equivalent to a maximum difference of 2 cm in four years.

3.2. Satellites survey

Radar systems (radio detection and range) are active satellite sensors, meaning they send a signal that is reflected from the Earth's surface and received by the sensor. Compared to the most popular optical systems operate continuously, being able to acquire data in the presence of cloud cover and both during the day and night (*M. G. Ciminelli, 2009*).
The principle of operation is the same for all radar systems (*Figure 30*): a transmission device illuminates the surrounding space with an electromagnetic wave (with a certain wavelength and frequency) which affects any object subjected to a phenomenon of disordered reflection (diffusion, dispersion). A part of the diffuse field returns to the transmitting station, also equipped for reception, where its characteristics are measured. The device can detect the electromagnetic target (detection) and by measuring the phase shift between the emitted signal and the received one, evaluate the distance (range) in which the target is located, accurately locating it along the pointing direction antenna (direction of the range).

The directivity of the antenna used to transmit and receive the radar signal (i.e. the selectivity in the illumination of the surrounding space) also allows the object to be positioned along the other dimension that are the direction parallel to the satellite's orbit (called azimuth). The direction of the sensor-target junction (perpendicular to the orbit and tilted from an angle θ (off-nadir) relative to the vertical) is called LOS (Line of Sigh).

The larger the antenna, the narrower its footprint and, as a result, the definition of the target grows, to the detriment, however, of the extension of the illuminated area.

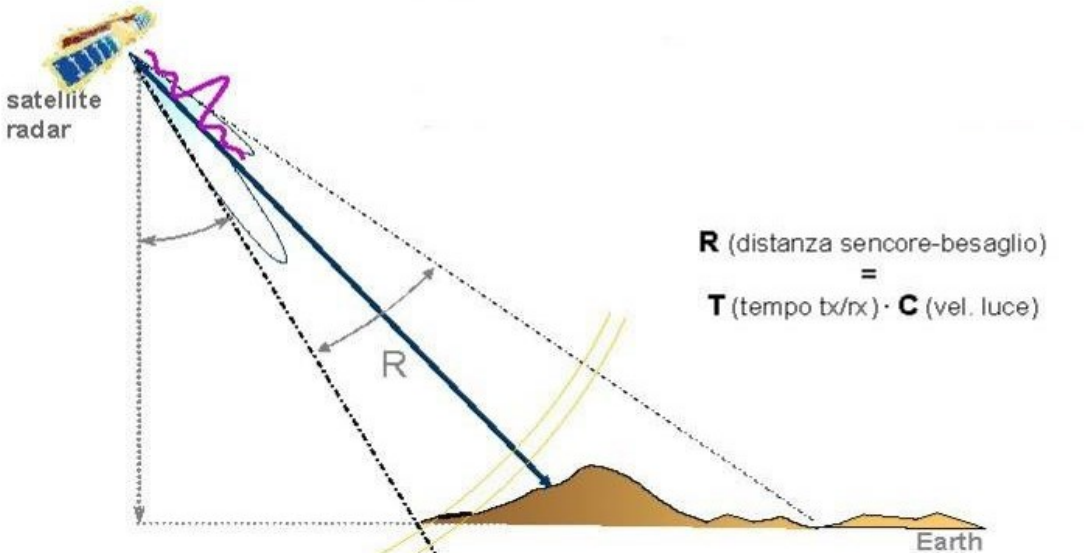

Figure 31. Principle of radar system

To make up for this we thought of constantly combining the data acquired by a small sensor in successive positions, you can synthesize in this way a large dummy antenna, called synthetic aperture, which guarantees high resolution even in the azimuth direction.

3.2.1. Synthetic Aperture Radar (SAR)

To obtain a good spatial resolution while keeping the antenna small, it was decided to use a sequence of acquisitions of a shorter antenna to simulate a larger antenna, thus providing high resolution data. This is the idea behind the SAR technique. A Synthetic aperture radar is an active sensor that first transmits microwave signals and then receives back the signals that are returned, or backscattered, from the Earth's surface.

The resulting images contain two types of information: phase that represent the target sensor distance index and the amplitude of the signal reflected from the ground.

Each pixel of an image contains both quantities. The amplitude identifies the part of the incident electromagnetic field reflected towards the sensor and can be used to assess the change of surfaces over time (identifying the various uses). The phase represents the most important information for the purposes of interferometric applications and is used to derive, through specific algorithms, the displacements of the soil, or rather of points called permanent scatters (PS).

3.2.1.1. Interferometric techniques (PSInSAR)

Radar satellites allow to measure the surface displacements of the ground with millimetre precision thanks to the use of data processing techniques called "interferometric". Satellite interferometry is based on the measurement of phase changes between two satellite acquisitions at the same point (*Figure 31*).

The satellite passes over a point that captures a signal whose phase depends on the sensor-target distance at that moment. In case of ground movement (in this case a tectonic descent) the distance sensor of the target increases and consequently the phase undergoes a measurable change. This type of processing is commonly called differential interferometry (acronym DInSAR).

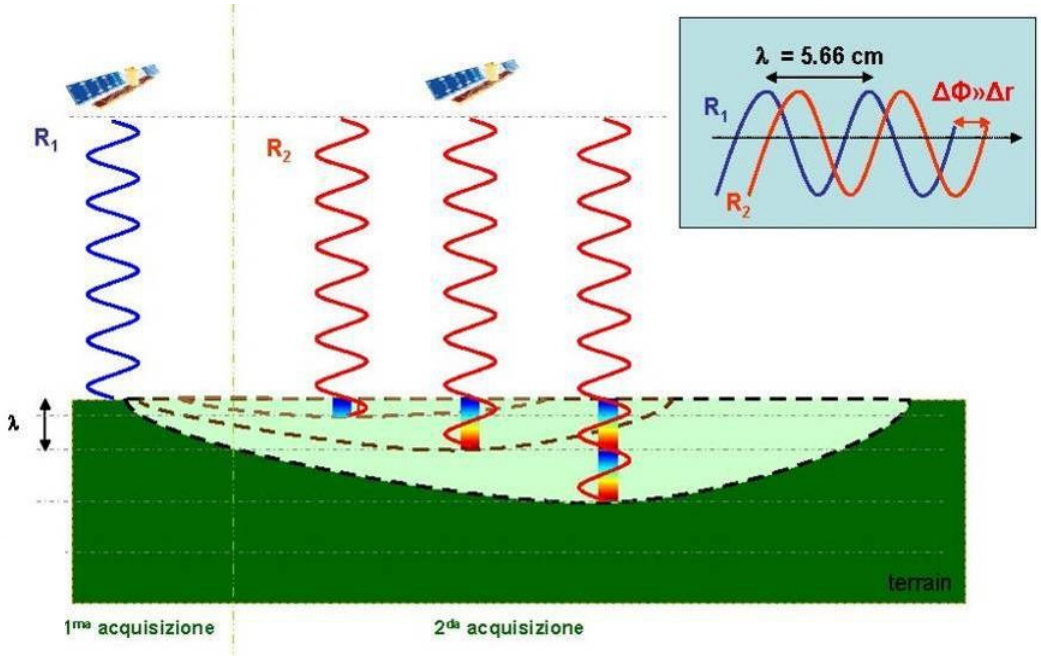

Figure 32. PSInSAR techniques

The objective of the differential interferometric technique is to isolate the actual phase contributions due to target movement and not attributable to atmospheric disturbances or noise and to accurately estimate the phase difference ($\Delta\phi$) the electromagnetic wave transmitted in two successive acquisitions and retransmitted from the target to the ground (*P. Canuti, 2006*).

Several effects reduce the quality of the results obtained with the analysis of DInSAR. First, the phenomena of temporal decorrelation. These are caused by the variability of the electromagnetic properties (reflectivity) of the radar targets between the different data acquisition days, indicated by the basic parameter of time.

Areas covered by vegetation, which are easily influenced by the wind and a different appearance depending on the season, are often a source of decorrelation (*Figure 32*), while urban centres and exposed rocks remain more stable over time (although problems such as snow may occur).

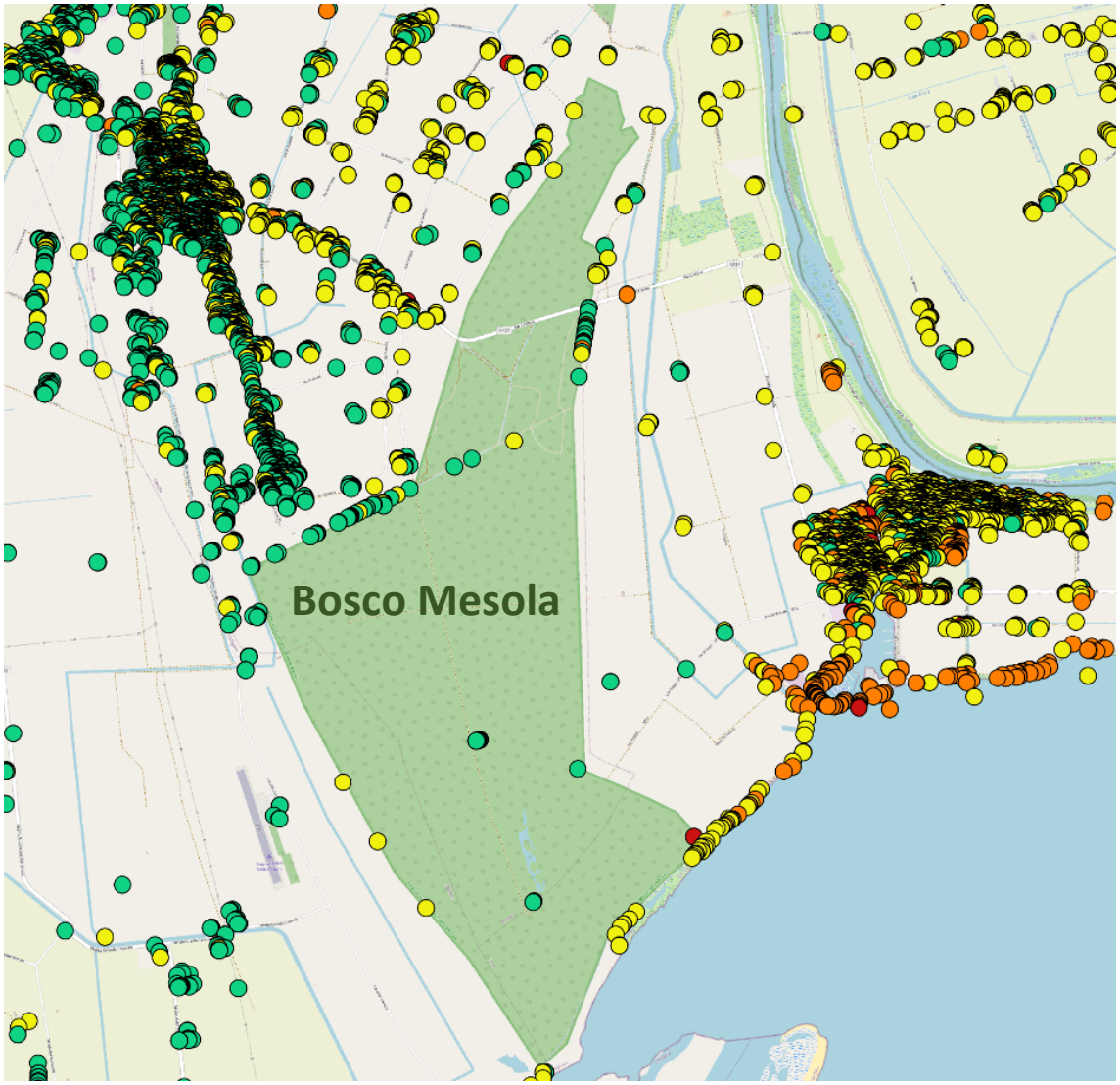

Figure 33. Effects of temporal decorrelation on a forest

The quality of the interferogram also depends on the distance between the two orbits traveled by the sensor during the acquisition of the two images (called normal or geometric baseline). The interpretation of interferometric data can be further complicated by the variation of atmospheric conditions during the two acquisitions that can be translated into a further phase term, difficult to discriminate from the contribution related to movement.

The PSInSAR technique is the progenitor of all the multi-interferogram techniques, that is those techniques that employ a long series of satellite radar images for the identification and measurement of the phenomena of deformation of the Earth's surface. In particular, the technique is based on the observation of a small subset of radar targets, called permanent diffusers (PS), which are virtually immune to the effects of temporal and spatial decorrelation. This means that they maintain the same "electromagnetic signature" in all radar images used, depending on the acquisition geometry and climatic conditions, preserving the phase information over time. The phase signal is precisely the element that contains information about the position on the ground and the distance of the target from the satellite. Since the signals used have centimetre wavelengths (microwaves), displacements of even a few millimetres induce phase displacements between waves that can be detected.

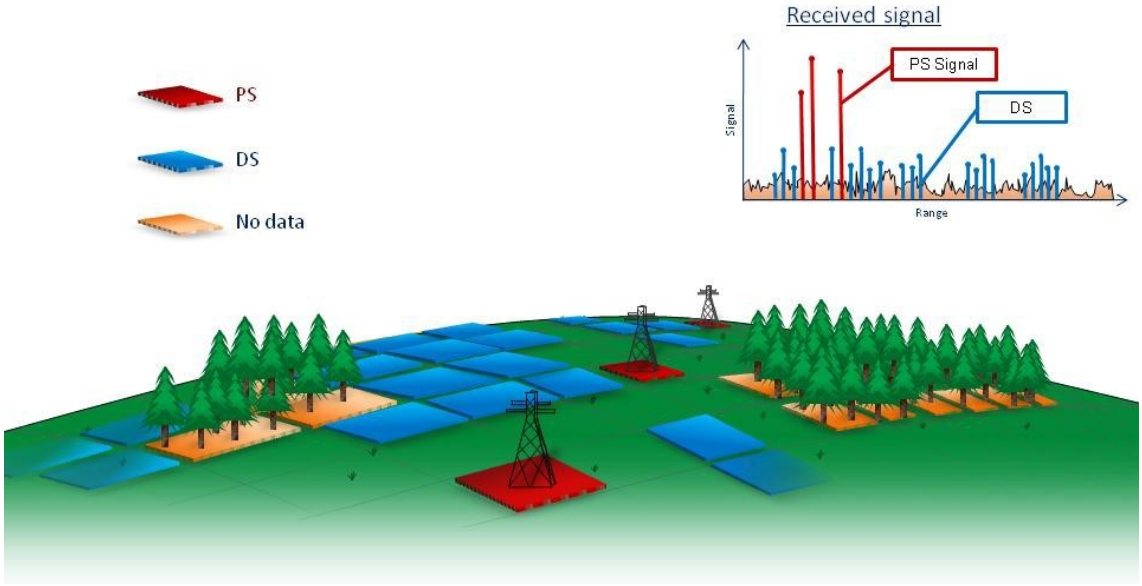

Figure 34. PS data

The PS (*Figure 33*) generally correspond to elements already present on the ground, such as structures of anthropic origin (buildings, monuments, roads, railway lines, antennas, pylons, metal elements, etc.), or natural elements (rocky outcrops, accumulations of debris) or to all those elements already present on the ground, whose electromagnetic characteristics do not vary significantly with the variation of the acquisition geometry and climatic and atmospheric conditions.

On the contrary, the electromagnetic response of vegetation, whose appearance changes continuously, changes even for short periods of time. The spatial density of the PS will therefore be variable depending on the sensor used for analysis (*Figure 34*), land use and soil morphology. In general, the PS reach a very high density in correspondence of the urban centres and the anthropized areas (up to several hundred PS /km2), while they are almost absent in vegetated or snowy areas.

Figure 35. Difference in point density between Sentinel's and Cosmo's sensor

In general, a data set of at least 25-30 radar images is required for successful application of the technique. The higher the number of images available and the homogeneity of their time distribution, the better the results.

For each individual target (PS) the position (its geographical coordinates: latitude, longitude, altitude), the mean deformation trend (calculated in mm/yr as linear interpolation of the displacement measured throughout the monitoring period) and the entire time series of displacements (providing a displacement value for each of the available acquisitions) are obtained (*Figure 35*).

	Field1	E [m]	N [m]	Velocity	Field11	Field12	Field13	Field14	Field15	Field16	Field17
1	264611	755211,450312	4979375,870698	-3,4	10,59700000000	8,84500000000	7,58400000000	7,02100000000	5,23900000000	5,92800000000	6,10700000000
2	264612	755206,392342	4979376,533966	-3,8	9,42200000000	8,88500000000	10,09200000000	8,96800000000	6,44000000000	7,52000000000	7,79800000000
3	264648	755282,874900	4979352,357008	-3,4	7,65200000000	8,40300000000	7,95500000000	6,97900000000	6,28200000000	8,31300000000	8,55200000000
4	264649	755212,312735	4979361,719201	-3,4	9,56900000000	7,67600000000	8,00500000000	6,89300000000	4,34300000000	5,51100000000	6,67700000000
5	264696	755313,849426	4979334,205642	-4,1	17,35200000000	9,82300000000	8,89100000000	7,28800000000	6,00800000000	7,47100000000	8,96100000000
6	264697	755315,333880	4979334,020930	-3,5	4,91600000000	9,70000000000	9,26100000000	8,37000000000	6,85900000000	7,30500000000	8,18800000000
7	264698	755251,315216	4979342,501484	-3,4	8,19800000000	8,91000000000	8,61400000000	7,50400000000	6,08400000000	8,28000000000	7,85100000000
8	264699	755249,060057	4979342,799675	-3,4	7,56000000000	8,73000000000	9,16100000000	8,58600000000	6,66600000000	8,38200000000	8,02200000000

Figure 36. Example of attribute table

All measurements are always calculated along the sensor-target line (sensor line of view, LOS), which is inclined relative to the vertical by an angle (θ) that varies depending on the satellite used. In addition, all measurements are of a differential type, obtained after having determined one or more ground reference points of known and presumably stationary coordinates (on geological bases or indicated as such, for example by means of GPS or optical levelling measurements).

In addition, all movement information provided by the PS is relative and not absolute, it refers to the date of acquisition of the master image, used as a measure "zero". the precision that can be obtained with this technique is millimetre, for example the precision that can be obtained in the case of use of a Sentinel satellite is shown in the table (*Table 2*).

Parameter	*Precision*
North position	± 2 m
East position	± 7 m
Ellisoidic height	± 1.5 m
Mean velocity of displacement	± 2 mm/yr
Single displacement	± 5 mm

Table 2. Precision of Sentinel

The inconsistency between the displacement accuracy (millimetre) and the positioning accuracy (metric) of the points on the ground depends on the fact that the displacement is measured as a fraction of the wavelength, while the positioning accuracy is in fact a function of the pixel size of the image on the ground (a few meters). In addition, it must be considered that in the case of the PS, the radar target corresponds to the dominant element within the pixel and that therefore the actual size of the point monitored on the ground is generally less than the pixel size of the image.

3.2.2. Advantages & Disadvantages of SAR

The advantages of this innovative technique compared to traditional relief is mainly related to the great precision obtainable with this method. In particular, the PSInSAR technique can measure movements of the order of the millimetre, an ideal precision to detect the lowering of the ground in the Delta area. It is also possible to obtain a multitemporal analysis of a certain area being the relief and therefore the lowering obtained on a limited area equal to the spatial accuracy of the satellite (for example with Cosmo-SkyMed the accuracy is 3m) thus deriving the temporal evolution of deformation (*Figure 37*). In addition, through the ESA archives it is possible to have a long time series of radar images from 1992 to the present. Another advantage is the ability to acquire data with regular inferiority per week (for example for Sentinel-1 is equal to six days) without having to send men on the field because the survey takes place completely remotely.

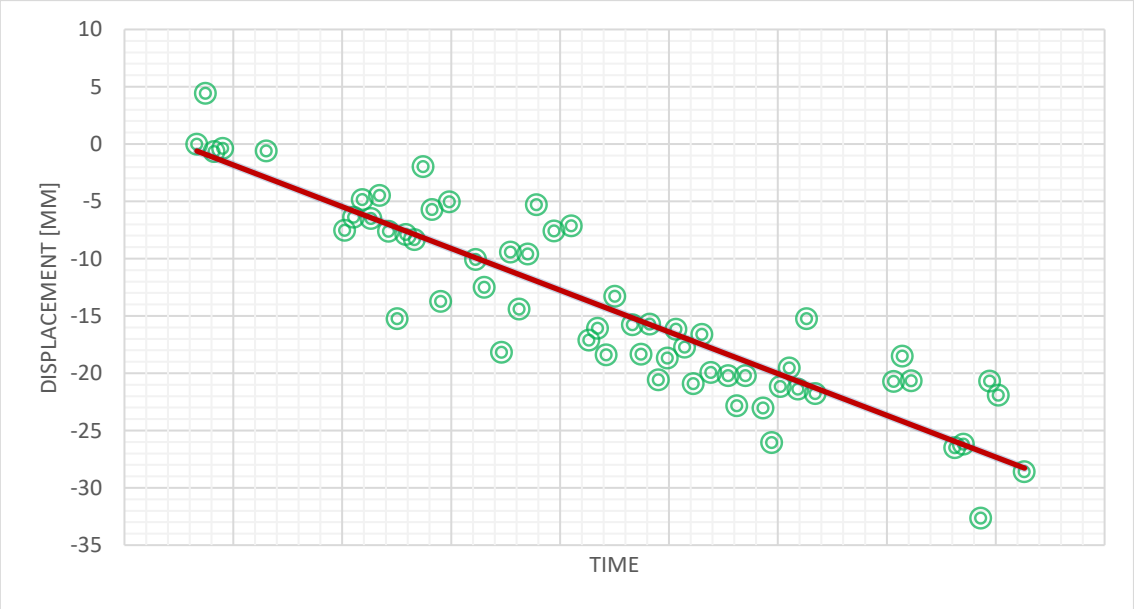

Figure 37. Temporal evolution of deformation

The method unfortunately has several disadvantages and within the area in question the main one concerns the impossibility of acquiring points in rural or lagoon areas due to the absence of sufficiently reflective materials (asphalt is not a sufficiently reflective material). This problem is very large in the Delta area and to limit it may be necessary to insert artificial reflectors. Another interesting problem is the loss of permanent scatters (PS) due to sharp drops between two juicy images. The Po Delta is a territory characterized by a slow but constant lowering, this lowering is not such as to allow the loss of PS, but the cases in which this can manifest are earthmoving works such as excavations, the reconstruction of cliffs or works of defence at sea or any reconstructions that cause the loss of electromagnetic information. the limit of displacement between two successive images is equal to a quart of the wavelength of the incident wave. Other problems are related to the acquisition of points in wooded areas where there is a strong temporal decorrelation. Another problem is the processing of radar images that requires special knowledge.

3.2.3. Applicability of SAR

Considering the accuracy of measurements and spatial and temporal coverage, the primary fields of application of interferometric data are:

- Identification and mapping of land subsidence areas;
- Monitoring of sea defence works;
- Identification and mapping of slow kinematic landslides if artificial reflectors are present inside;
- Large-scale mapping of deformed areas;
- This relief, on the other hand, is not indicated in areas of wooded, agricultural or perennial snow cover because they would have no PS.

  One possible solution is to insert artificial reflectors on the areas under examination.

The PSInSAR technique is not suitable for assessing the structural integrity of buildings but must be applied only to the study of soil.

3.2.4. Sentinel satellites

Sentinel-1 (*Figure 38*) is the first of the five missions that ESA is developing for the Copernicus observation programme.

Figure 38. Sentinel Satellites

Is a System of two satellites launched in 2014 (Sentinel-1A) and in 2016 (Sentinel-1B) by European Space Agency (ESA) and designed to deliver a vast amount of data and imagery for Europe's Copernicus program. The Sentinel-1 is equipped with twin polar orbiting satellites designed to provide a spatial data for environment, security warranting and global economic and business growth.

The satellites can operate day-and-night and perform a synthetic aperture with radar imaging; can capture synthetic radar images band C (5.5 cm), it works by capturing high-resolution images (18m x 18m) and providing the average speed lowering of the PS. Sentinel-1 bands allow to get imagery in all weather conditions and the review time is 6 days with the use of both satellites. It works in a pre-programmed conflict-free operation mode allowing to reach a high reliability of service and create a long-term consistent data archive to be used in the application based on long time series.

There are four exclusive acquisition modes produced using satellite bands: stripmap (into this mode, the instrument provides constant coverage which uses a geometric resolution of 5 x 5 m with a swath width of 80 km), interferometric wide swath

(combines swath width of 250 km with a moderate resolution of 5 m by 20 m, so appears to be the most used over land as helps to spot a target on the ground), extra wide swath mode (this unit only takes photo at a medium resolution up to 20 by 40 m away from the ground. Extra wide swath mode is mostly applicable for maritime and in area where it is necessary to have wide coverage and short revisit time) and wave mode (In this mode the stripmap image is taken by using alternating elevation beams at a fixed on/off duty cycle, to get vignettes 20 by 20 km every 100 kms along the orbit). This last mode is used over ocean, giving a result of long wave mode data-takes per orbit. The applications of Sentinel are monitoring sea ice and icebergs, monitoring of land ice, river and lake ice monitoring, oil spills and ships, marine winds and waves, land-use change, agriculture, deforestation land deformation and support to emergency management such as floods and earthquakes. The data can be downloaded and to give some data at the end of 2020, about 6 million products have been generated and made available for download, culminating a total of 10 Petabytes (*https://www.esa.int/*)
In the future there will be the launches of a new generation of Sentinel-1, there will be Sentinel-1C and Sentinel-1D.

3.2.5. Cosmo-SkyMed satellites

COSMO-SkyMed (COnstellation of small Satellites for Mediterranean basin Observation) is the largest Italian investment in space systems for Earth observation, commissioned and funded by Italian Space Agency (ASI) and Italian Ministry of Defence (MoD), and it is “natively” conceived as a dual-use (Civilian and Defence) end-to-end Earth Observation System aimed to establish a global service supplying provision of data, products and services compliant with well-established international standards and relevant to a wide range of applications, such as risk management, scientific and commercial applications and defence/intelligence applications.
The responsibility for ground infrastructure and management in orbit is civil, entrusted to Telespazio at the “Fucino Space Center”, while the processing and management of satellite signals, being a dual system, is entrusted to the “Centre for Satellite Remote Sensing” in Rome. Then these centres will make available the information from the satellite system to the company e-GEOS that will market and make the products available to commercial users.

The satellite system consists of a constellation of four low Earth orbit (about 619 Km) mid-sized satellites (*Figure 39*), each equipped with a multi-mode high-resolution synthetic aperture radar (SAR) operating at X-band (3.1 cm) by capturing high-resolution images (3m x 3m) and providing the average speed of descent of the PS. The review time is 16 days for satellite and 4 days with the use of the entire constellation.

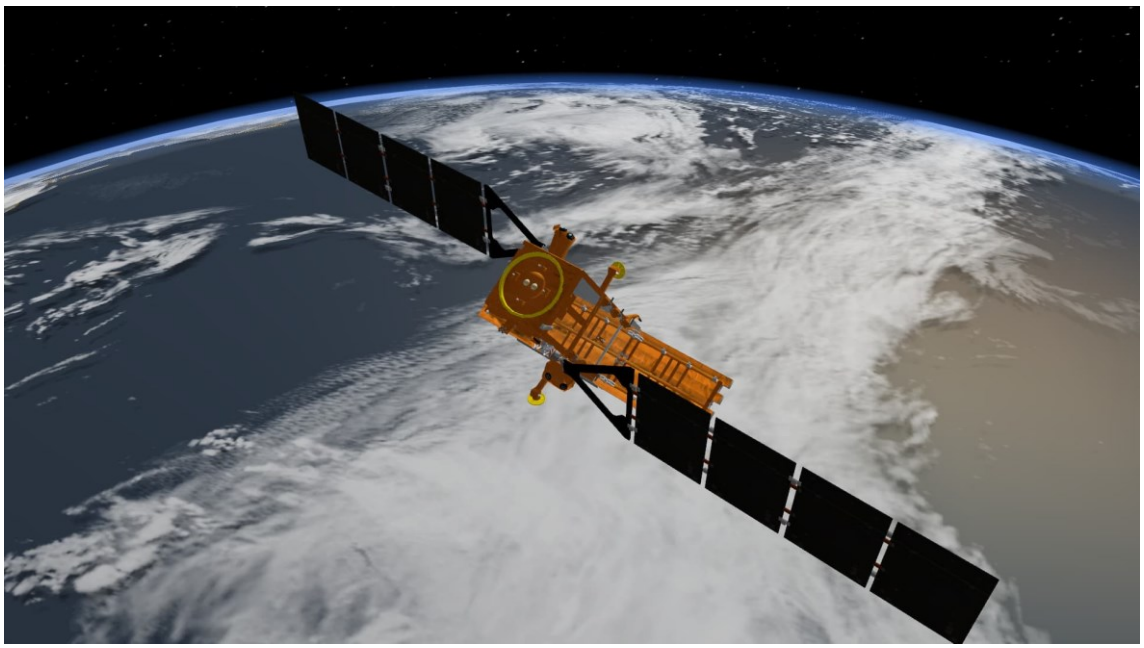

Figure 39. Cosmo satellite

The mission can provide information and services to several activities and applications, such as risk management applications, cartography and planning applications, agriculture, forest, hydrology, geology, marine domain, archaeology etc.

Due to the need of many combinations between image size and spatial resolution the SAR was chosen as a multimode sensor operating in spotlight mode (for metric resolutions over small images), stripmap modes (for metric resolutions over tenth of km images) and ScanSAR (for medium to coarse (100 m) resolution over large swath). The first constellation has been launched from 2007 (Cosmo-SkyMed-1) to 2010 (Cosmo-SkyMed-4). In the 2021 the second generation of satellites has been launched and will replace the previous one. In the future there will be the launches the second generation of Cosmo-SkyMed, the first two satellites have been already launched in 2019 and 2022 from the base of Cape Canaveral in Florida (*https://www.asi.it/*).

3.3. Survey of coastline

To reproduce and exhaustively study of the effects of land subsidence and other phenomena affecting the PRD, it will be necessary to study also what happens along the coast and to do this it will be need to reproduce and monitor the evolution of the wet front over the years. Such monitoring will be possible thanks to surveys performed with different techniques such as LiDAR, GNSS survey, classical topography with total station and photogrammetry with UAV instrument.

3.3.1. Survey with total station

A total station consists of a theodolite with a built-in distance meter (spacer), and thus can measure angles and distances at the same time. Today's total electronic stations all have an opto-electronic distance meter (EDM) and electronic angular scanning. The coded scales of horizontal and vertical circles are scanned electronically, and then the angles and distances are displayed digitally. Horizontal distance, height difference and coordinates are calculated automatically, and all additional measurements and information can be recorded.

3.3.1.1. Total station Leica TCR1201

The Leica TCR1201 Total Station (*Figure 40*) can perform highly accurate angular measurements and precise distance measurements with long range. It supported by excellent automatic positioning and fast and reliable reflector position using an intuitive interface. the data is managed by integrated programs and their visualization becomes easy thanks to the large graphic display that makes the measured data immediately accessible. For measurements, the highly accurate and reliable angular measurement system consists of a static glass circle with coded lines which is read by a linear CCD matrix. A special algorithm determines the exact position of the code lines on the array and instantly determines the precise measurement. A double-axis compensator constantly controls both components of the vertical axis inclination. These components are then used to immediately correct all measured angles. After digitisation and storage of the signal, the distance is determined using modern phase measurement techniques. A modulation frequency of 100 MHz is the time base for high precision. The angle of coaxiality and divergence of the laser beam and the automatic target recognition (ATR), enables fast and accurate three-dimensional dynamic monitoring. The instrument can

perform measurements with different reflectors such as standard prism, prism 360, mini prism 360, mini prism, reflective tape or without the use of the reflector, using a laser point (RL), in this case the EDM Pinpoint R400 without reflector transmits a visible red beam, carefully collimated to the target.

Figure 40. Total Station

3.3.2. Advantages and Disadvantages of total station survey

The main advantage of the relief with total station is the accuracy. precision which unfortunately is superfluous for the actual purpose for which it is used in this thesis. In fact, to detect the shoreline is sufficient a centimetric precision, being the error caused by the subjective choices of the operator in evaluating the wet front of considerable thickness (the theoretical tolerance is in fact equal to the meter). Unfortunately, this method is useful as a check on subsequent tests, but unfortunately it is useless for applications on the Delta being a type of slow, cumbersome detection, in which there must be two operators (except that the total station is not motorized). Furthermore, it is not possible to assess subsidence as the measurements for a point are also in motion.

3.3.2. Survey with LiDAR

LiDAR is a remote sensing technique that is based exclusively on the use of laser technology for measuring both horizontal and vertical distances using the same principle as the electronic distance meter and is currently one of the most used in the creation of cartography for technical use. The reason for this lies essentially in the speed of tracing and acquiring topographical elements (anthropogenic and natural), as well as in the geometric precision obtainable in relation to vast areas of land to be mapped.

In short, the operation is easy to understand: a series of light pulses (more than 100,000 pulses per second) are emitted by the laser scanner; both the start time from the laser scanner and the return time to the instrument after being reflected from the ground are measured. Using the constant speed of light, the delay can be converted to an inclined distance and knowing the position and orientation of the sensor (thanks to the use of GPS and IMU), it is possible to determine the coordinates of each point. The collection of these coordinates is known as the "point cloud".

3.2.1. Advantages and disadvantages of LiDAR

The main advantages of this technology are the simplicity and relative reduction of the use of tools. Although it is a latest technique, as it is based on the source of a beam of light, its use is quite easy.

In addition to simplicity and ease of use, there is to consider the speed in surveying, managing to detect large portions of territory quickly with good precision and with a huge amount of data. This last aspect, however, is often seen as a disadvantage because the computational load of the data is very high.

The major advantages of LiDAR are related to the fact that all data are geo-referenced from the beginning, so an analysis with a GIS software are very simply, then the survey is faster and is need a less laborious delivery times, moreover these techniques may collect data both on steep terrain and shadow areas. Moreover, this techniques can produce DSM and DTM (*Figure 41*). This technique is useful for detecting large portions of land in a short time and this is useful for obtaining the wet front, even if data related to astronomical tides and tides due to weather events will be indispensable. Thanks to DTM in fact it will be possible to vary the wet front to bring it back to zero tide.

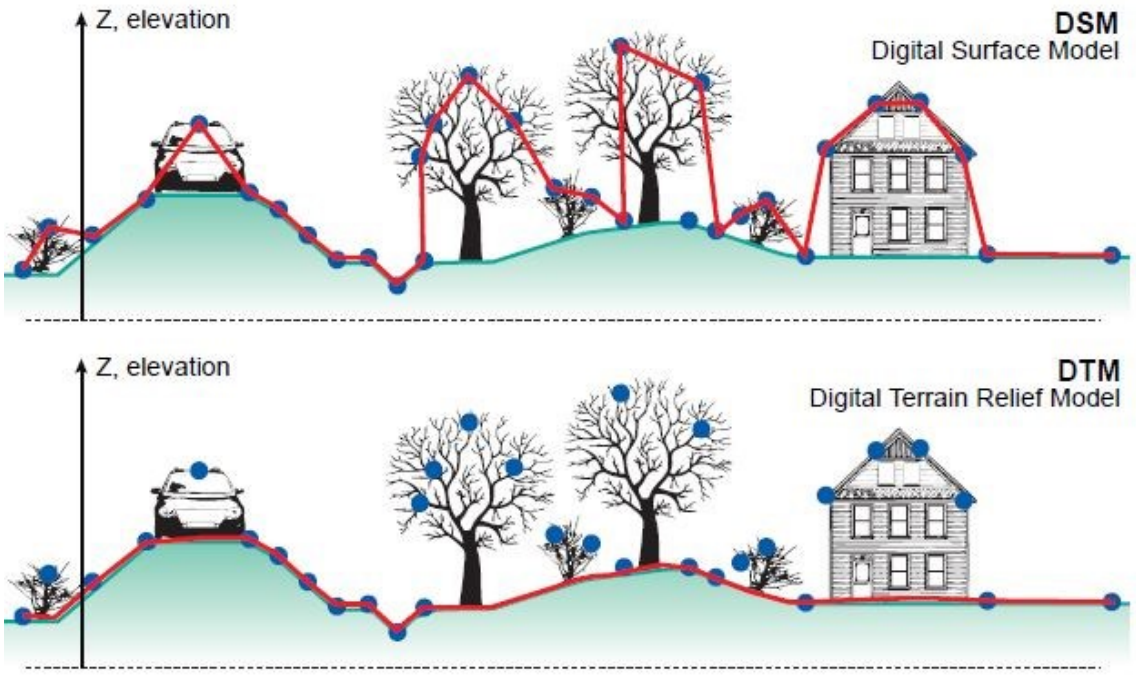

Figure 41. DSM and DTM

The method in the present case can only be used to detect the wet front, since the accuracy of this method is reduced and equal to 30 cm, the lidar is useless in the monitoring of the subsidence being the values of it in the order of the millimetre. Moreover, for the monitoring of the wet front the lidar technique has some disadvantages, it cannot penetrate the dense vegetation (e.g. Bosco Mesola), the computational cost due to the points is high, Moreover, in lagoon areas or with the presence of bodies of water, the lidar pad often has a lot of noise, and these errors will be eliminated in post processing with a high computational cost. Another factor to keep in mind is the cost of $400/square mile in a one meter resolution.

3.5. Survey with UAV instruments

Photogrammetry can be divided into three different classes: aerial photogrammetry, terrestrial photogrammetry and the most innovative photogrammetry with UAV (Unmanned Aerial Vehicle). Several types of aircraft belong to the UAV group (aircraft, helicopters, airships) and now also highly innovative aircraft such as small multi-rotor helicopters that can be defined as automatic or MICRO-UAV. A drone refers to the use of a unmanned aerial vehicle (UAV), to capture aerial data with downward-facing sensors, such as RGB or multispectral cameras or LIDAR device. During drone detection with an RGB camera, the terrain is photographed multiple times from different angles, and each image is marked with coordinates. From this data, a photogrammetry software can create georeferenced ortho-mosaics, elevation models or 3D models of the project area. These maps can also be used to extract information such as very accurate distances or volumetric measurements.

Unlike manned aircraft or satellite imagery, drones can fly at much lower altitudes, making high-resolution and precision data generation much faster, less expensive. In addition, I can insert a different camera (thermal camera or 4K camera) into the drone to improve the survey.

3.5.1. Drone Parrot

Is a particular drone (*Figure 42*) stabilized on 5 axes (2 mechanical axes and 3 electronic axes), the Sony optical sensor integrated in ANAFI allows you to take clear images, despite the vibrations associated with drone flights. The x3 zoom and the 180 p.m. tilt of the camera provide a detailed view of the target observed.

Figure 42. Drone parrot ANAFI

CHAPTER 4. VISUALIZATION OF DATA

Now it is necessary to find a way to view, analyse and manage these data from different sources. Since all data are georeferenced, it is logical to use a GIS software (*Figure 43*) that allows to integrate the processing potential of a CAD software with the databases of a geodatabase, thus combining alphanumeric information with spatial information.

Figure 43. Logo QGIS

4.1. SOFTWARE GIS

GIS are powerful tools for data collection and processing to provide all the information needed to solve a certain problem. This tool consists of a series of software to capture, archive, extract, process and visualize spatial data of the real world. In practice, GIS software combines alphanumeric information with spatial information and this information is superimposed on each other (*Figure 44*).

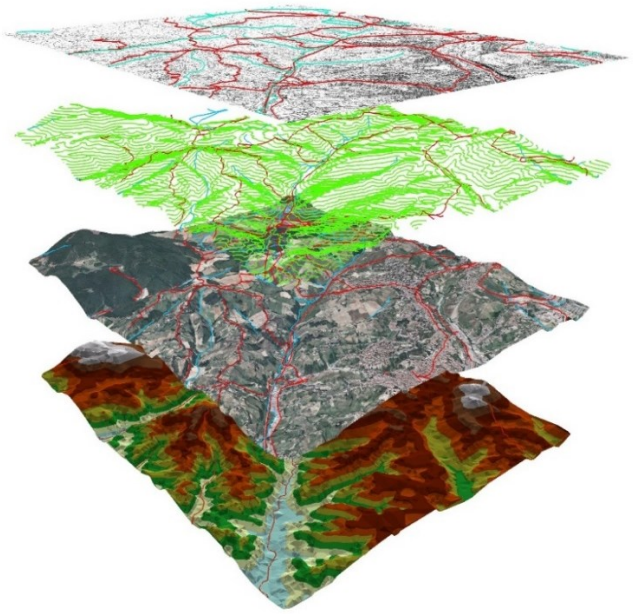

Figure 44. Overlap of layer

GIS consists of a software (commercial such as ESRI Arcgis or freeware such as QGIS), a hardware (PC in which I have the software), a large amount of data from various sources (punctual, vectors, polygons, raster, table, or historical cartography), methods and human resources. This tool is not only a computer program, but a system made of hardware, software and especially people capable of developing territorial analysis both at the scientific level and at the logical-conceptual level.
QGIS can be used for various reasons, such as land use planning, water network management, land use classification, calculation of possible routes.
All data, geographical or otherwise, shall be converted to an appropriate digital format before being used in a GIS (*M. Fabris, 2022*).

Often the data are collected in tables containing the geographical coordinates of the point and its attributes, the points will then be treated to make them compatible with them, achieve the required goals and correctly showing the information on the map using frames, legends, titles. For large GIS projects it is convenient to store geographic information in a database management system (DBMS) that helps to store, organize and manage data. The database appears as a set of tables linked together by common attributes. In addition, a simulation model can be created to represent future events and thus demonstrate the importance of future interventions. The data will then be made available to users via geodatabases or webGIS.

4.1.1. Geodatabase

Geodatabase is an archive of georeferenced data within a DBMS (Database Management System), which, through specific procedures and functions, can be consulted and manipulated to extract information. Within the database, the data are organized according to logical structures specially designed for GIS applications.

Geodatabase collects different types of data according to a precise logical organization. In this way you can at any time enter, consult, modify and delete data. In general, the data are stored in the database according to specific criteria that define the logical organization of the data (how the data relate to each other) and the management method (indicating the complexity of the consultation).

Based on the logical organization of the data, there are three different database models: hierarchical (the data are organized according to an inverted tree scheme, based on the father-son relationship), reticular (here a child node can also be linked to several higher-level elements) and relational in which are used mathematical concept and relationship (*M. Fabris, 2022*). The advantages of geodatabase are versatility and usability, performance optimization, easy data migration, raster data storage, customizable storage configuration and allow you to use data compression.

4.1.2. WebGIS

A WebGIS is an online platform that combines the tools of GIS with the sharing of data in a dissemination perspective. WebGIS applications allow the distribution of geo-spatial data in Internet networks by exploiting the analysis deriving from the GIS software, in particular the shared data will be organized in specific databases that will then be uploaded to the appropriate cloud such as NextCloud or Dropbox.

A WebGIS system is based on normal Client-server functionalities that relate the user interface to the technician's interface. In particular, the technician works thanks to the use of a GIS software (QGIS, ArcGIS), while the user has a server that provides the tools for viewing and querying georeferenced data.

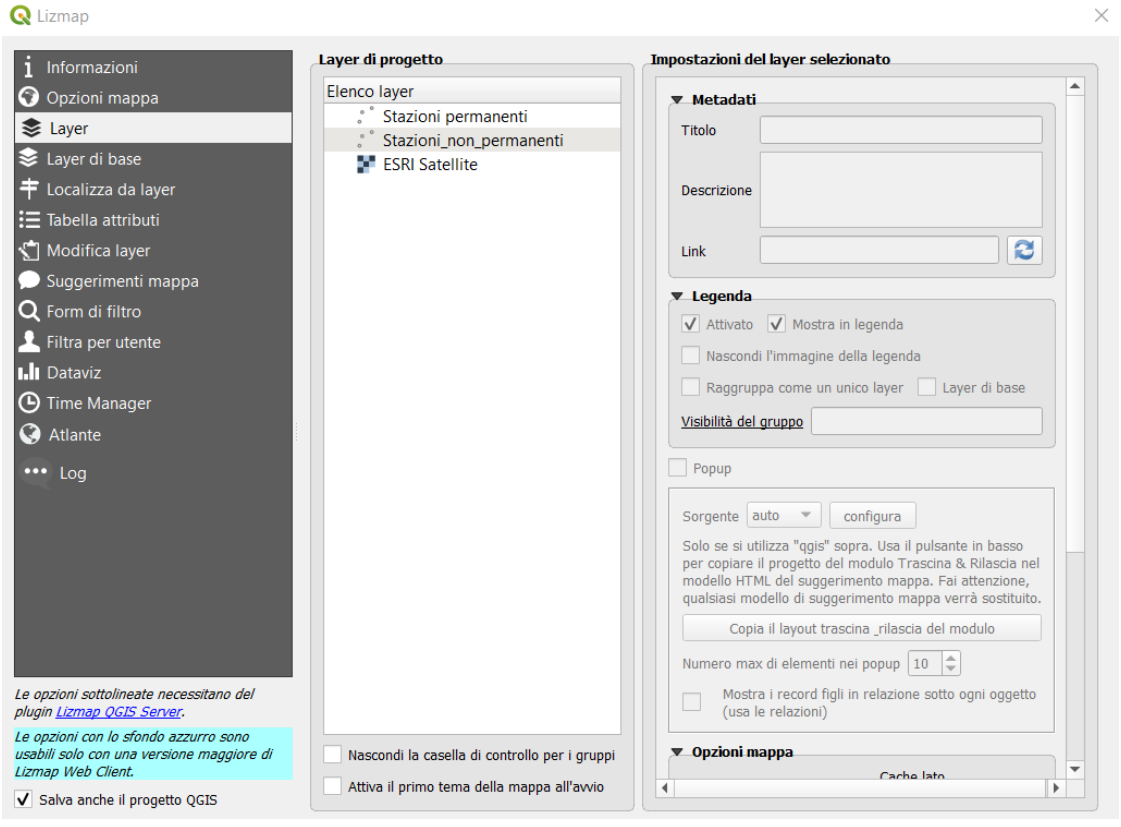

Figure 45. Lizmap interface

The most used servers are QGISservers, map-servers and Arcgis-mapservers. Now it is necessary to relate the data of the analyst with what the customer can see. This step takes place thanks to the graphical interface (the main ones are Lizmap (*Figure 45*), G3W-suite, Qgis-webclient) which allows to load and set the way the data will be displayed going to intervene in scipt in java language and going to limit the display of the most sensitive data, thus going to set the actions that the user can do or not with the data loaded.

A GIS (as in the case presented in this thesis) often has the task of processing data to design future interventions useful to limit or avoid geomorphological problems or natural disasters. Often, however, we do not worry about these events until they do not occur. For this reason, perhaps the main step for a GIS technician is the data sharing phase, in this way it is possible to make public opinion aware of the possible problems in which a certain area may run. In this way it will be possible to increase the awareness of the political bodies to finance projects and thus to make the elaboration that has been made more useful. Below are represented an example of WebGIS (*Figure 46*) in which it is possible to visualize more information such as a short description of data and the goals of the study.

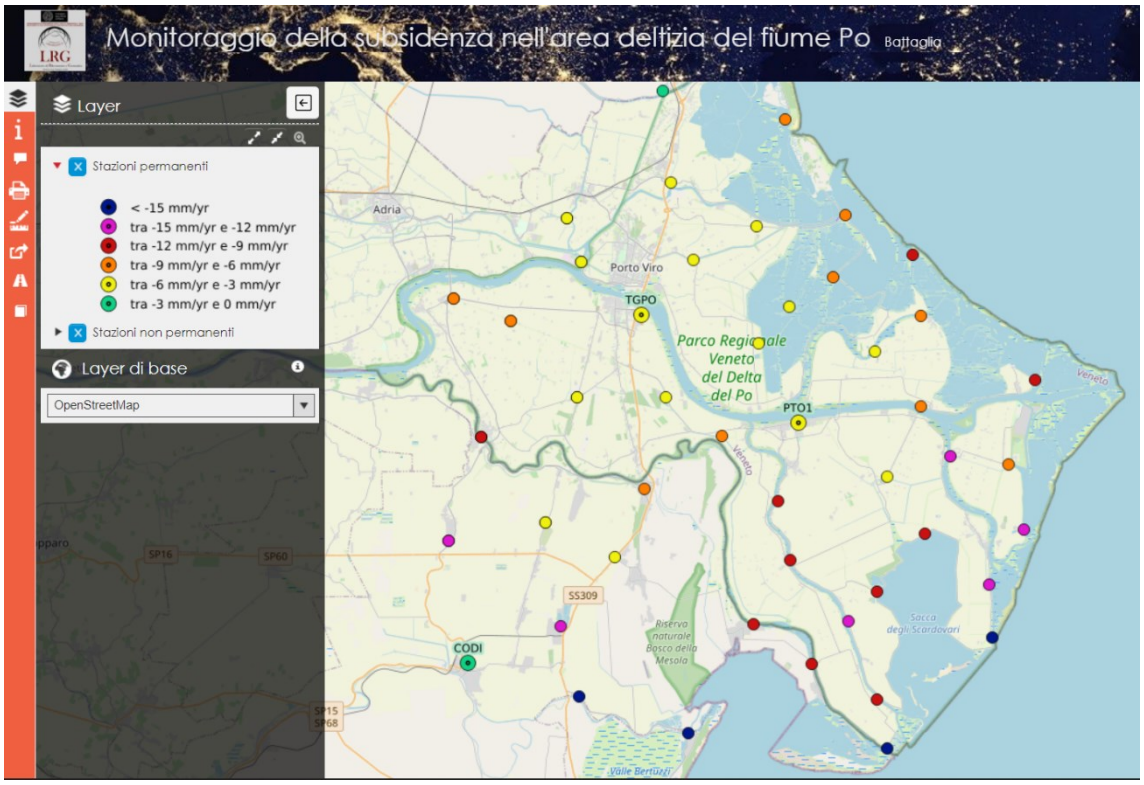

Figure 46. WebGIS interface

CHAPTER 5. ANALYSIS OF DATA

5.1. GNSS data analysis

The GNSS campaign is based on the PODELNET network, a network of 46 rover stations and three permanent stations (TGPO, PT01, CODI) present in the Po Delta. In the choice of area extension and in the choice of permanent stations to be used, a comparison was made on the availability and extent of SAR data (*Figure 47*). In fact, the area under study has been limited spatially and temporally by GNSS data. This avoids giving much weight to inland SAR data that would not be verified by GNSS data. Moreover, studying the points starting from 2016, being the lowering speed strongly dependent on time, it was possible to have a direct evaluation between SAR and GNSS speeds.

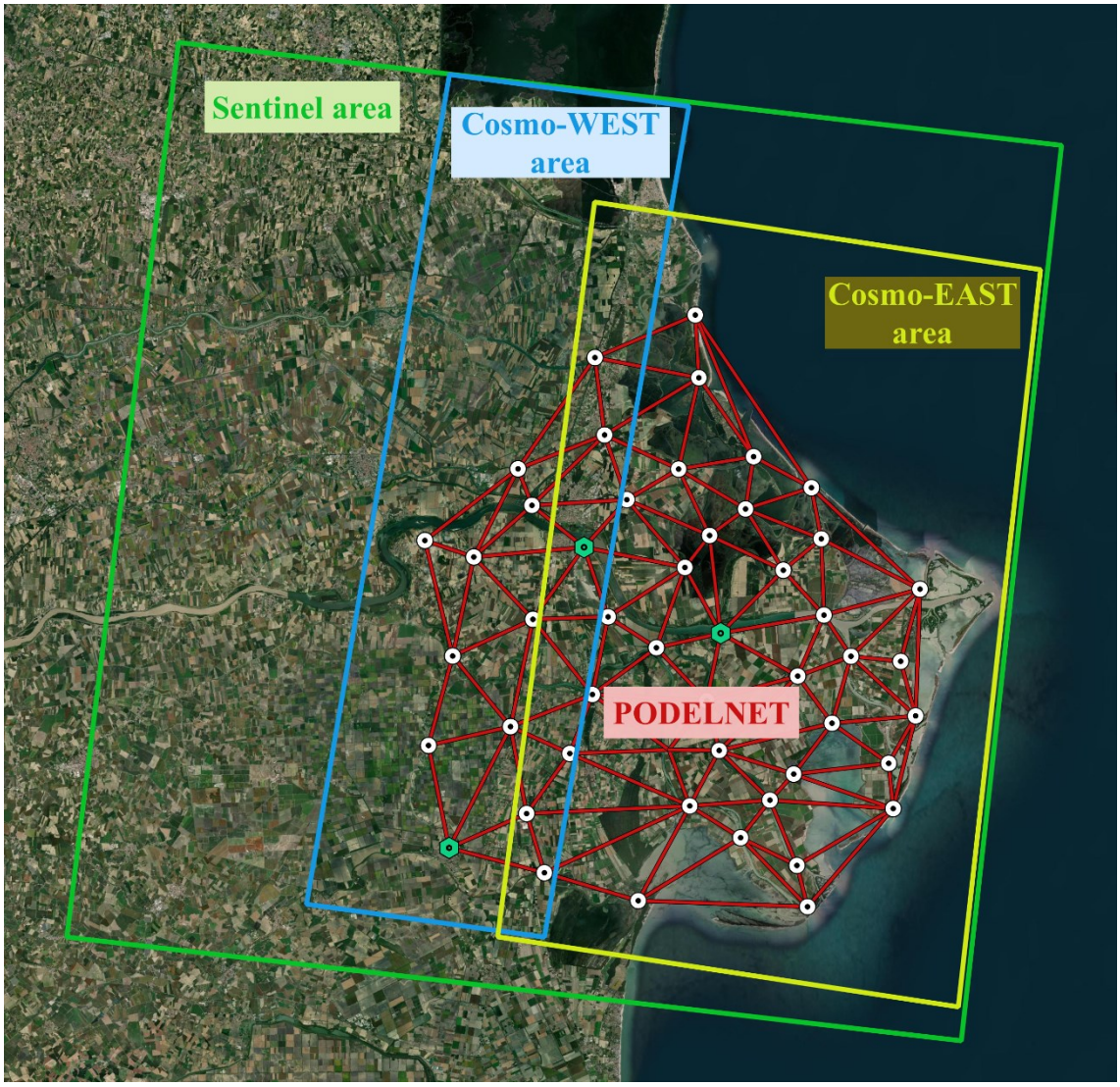

Figure 47. Extension of SAR data and PODELNET

Data from the permanent stations will be collected by the network operators, in particular the CODI station is managed by the "Collegio dei Geometri", the TGPO station is managed by the Veneto Region and the PT01 station is managed by LEICA. The data will then be sent to the University of Padua and then managed through the BERNESE software system, a package of about 100 programs able to process the data in RINEX (Receiver Independent Exchange Format) and obtain in this way the coordinates of the points (*Yibin Ren, 2021*).

On rover stations the detection was carried out with relative positioning in a static way with a minimum of 3 hours, duration that allows an excellent compromise between speed (and consequent lower cost) and accuracy. After taking the measurements, the rover's data processing continued in the office using Gamit software (*GNSS at MIT*), which is a collection of programs to process phase data to estimate the three-dimensional relative positions of ground stations (*http://geoweb.mit.edu/gg/*).

The data used in this software are multiple, the precise ephemeris and Earth orientation parameters are downloadable from IGS (*International GNSS Service*), the antenna calibration information from ARTEX files and the basic network compensation (bases linking the top of the network) with the methodology "Compensation of indirect observations" (*N. Cenni, 2021*). The data will finally be translated using the data of the terrestrial reference system ITRF00 which uses as an input data series the positions of the stations and the terrestrial orientation parameters of the Earth, the result will allow to obtain over the years a rate of lowering of the ground along the vertical direction. While permanent stations offer continuous monitoring, surveying of rover stations is carried out every two years. This decision is made considering the rate of soil lowering which on average in the area considered is higher than 5mm/yr and the maximum precision obtainable with GNSS relief of 1 cm. For this reason, a major campaign every two years represents the minimum time to be able to appreciate a displacement of the soil with this technique. In the elaboration is also made the hypothesis of linearity, in this way we will consider the lowering between two successive linear reliefs over time. This hypothesis is valid because the time factor is very short.

To compare the GNSS data with SAR data it is necessary to project the speeds obtained during the two measurement campaigns along the LOS of the satellites on which the comparison takes place.

To project the measurements, it is sufficient to divide the value along the vertical by the cosine of the off-nadir angle (*Figure 48*).

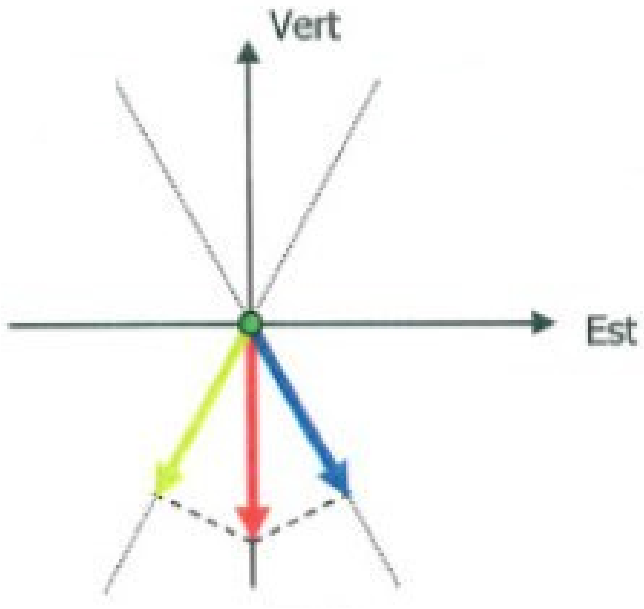

Figure 48. LOS of satellites

In particular, the angle is equal to 39.2° for the Sentinel data, 34.1° for the Cosmo data in the EAST direction and 26.0° for the Cosmo data in the WEST direction. In this way I obtain the results shown in *Table 3*.

ID	E [m]	N [m]	vel_Sentinel [mm/yr]	vel_Cosmo EAST [mm/yr]	vel_Cosmo WEST [mm/yr]
077703	757825.256	4966209.149	-12.6	-13.4	-14.6
077912	750825.087	4971669.295	-9.8	-10.4	-11.3
077704	751940.974	4967960.692	-12.4	-13.2	-14.3
077902	775501.151	4985737.955	-9.2	-9.8	-10.7
065906	768690.503	4992097.303	-8.4	-8.9	-9.7
065704	744443.14	4988787.557	-6.8	-7.2	-7.9
065908	769308.307	4988892.977	-6.4	-6.9	-7.5
077911	771170.294	4981529.522	-11.5	-12.3	-13.3
077710	762125.124	4978742.982	-8.5	-9.1	-9.9
077914	754954.745	4979134.403	-5.5	-5.9	-6.4
065907	764558.913	4990762.553	-6.5	-6.9	-7.5
077714	758966.315	4982066.132	-5.2	-5.6	-6.1
077801	744670.489	4975941.71	-11.4	-12.2	-13.2
065904	761631.296	4998989.19	-6.3	-6.8	-7.3

077708	768445.765	4965830.68	-13.4	-14.3	-15.6
077707	746188.739	4981545.757	-7.8	-8.3	-9.0
CODI	745967.869	4969519.825	-2.2	-2.3	-2.5
TGPO	754427.755	4988361.841	-4.0	-4.2	-4.6
PTO1	762996.544	4982974.015	-4.0	-4.2	-4.6
077909	766925.645	4986922.727	-3.7	-4.0	-4.3
065706	765062.79	4994042.661	-5.3	-5.7	-6.2
077721	766087.388	4972512.072	-10.9	-11.6	-12.6
065903	761407.718	5002922.314	-6.8	-7.2	-7.9
065905	751160.271	4990990.377	-4.2	-4.5	-4.8
077910	751223.757	4983847.229	-3.7	-3.9	-4.2
065901	762304.224	4989103.169	-4.4	-4.7	-5.1
077719	769980.197	4977334.481	-8.1	-8.6	-9.4
077715	762902.394	4975624.273	-7.2	-7.6	-8.3
077917	747512.15	4987754.104	-5.6	-6.0	-6.5
077713	769475.861	4984110.782	-5.6	-6.0	-6.5
065909	760358.32	4993264.166	-3.1	-3.3	-3.6
065705	757109.453	4991346.546	-3.9	-4.2	-4.6
077718	773819.108	4971981.29	-11.6	-12.9	-14.0
077905	774288.277	4981212.813	-6.2	-6.6	-7.1
065715	755717.585	4995403.759	-3.2	-3.4	-3.7
077907	753535.649	4975435.115	-3.6	-3.9	-4.2
077712	755936.765	4984002.507	-3.5	-3.7	-4.1
077915	759756.954	4975668.396	0.0	0.0	0.0
077913	749816.246	4977120.667	-3.4	-3.6	-3.9
077908	761059.962	4972149.939	-8.5	-9.1	-9.9
065707A	750286.76	4993280.113	-3.6	-3.9	-4.2
077904	767831.251	4980289.859	-4.5	-4.8	-5.2
077903	760753.491	4987098.085	-2.7	-2.8	-3.1
065708	755113.675	5000253.036	-2.3	-2.5	-2.7
077716	767579.113	4974146.538	-7.5	-8.0	-8.7
077916	764249.412	4970158.938	-7.9	-8.4	-9.1
077906	775224.129	4977794.295	-9.5	-10.2	-11.0
077717	767781.618	4968418.334	-7.2	-7.7	-8.4
077720	773535.229	4974818.483	-9.2	-10.1	-11.0

Table 3. Velocity along vertical

5.2. SAR data analysis

The analysis of the interferometric data available for the territory of the Po delta has allowed to extend the study of subsidence to areas not covered by geometric levelling or GPS surveys, at the same time providing new measures useful for comparison with the results obtained so far through classical techniques. Data processing is based on the satellite image analysis of the Sentinel and Cosmo-SkyMed systems. The images (*Figure 49*), respectively downloadable from the NASA website and from the ESA website, are processed using SARSCAPE's Interferometry Stacking tool. This tool includes processing techniques of Permanent Scatterers Interferometry (PSI) and SmallBASeline Subset (SBAS). The use of one method or the other depends on the number of SAR images available and soil conditions (*N. Necula, 2021*).

Figure 49. Example of SAR image

The PSI approach generates all interferograms indicated as a common master image, detecting point targets characterized by a stable back-scatter signal over time, and high consistency between different acquisitions. The SBAS algorithm maximizes space-time consistency based on interferograms with small perpendicular base values. The PSI technique is generally applied to analyse deformation affecting urban areas, while SBAS is more adequate in distributed dispersion conditions (M. Floris, 2019).

For the area in question, it was decided to use the SBAS technique. The SBAS algorithm is an advanced DInSAR technique that allows the analysis of the spatio-temporal characteristics of deformation phenomena observed by the generation of maps and time series of surface deformation. It is based on an appropriate combination of interferograms, obtained from data acquired from sufficiently close orbits (small spatial baselines) and possibly with low revision times (small temporal baselines); these characteristics allow to minimize the effects of noise (called spatial and temporal decorrelation), thus increasing the number of points per unit of area on which it is possible to provide a reliable measurement of the observed deformation.

In addition, all surface displacement measurements refer to a single point in space (Master image), chosen in an area deemed stable, and to an instant in time, which typically corresponds to the first available acquisition, and refer to the component of the surface displacements detected, projected along the radar line of sight (LOS).

A crucial aspect of the SBAS approach is also to allow DInSAR analysis of surface deformation at two different spatial scales, defined as regional (low resolution) and local (high resolution) scales. At the regional scale, SAR data generated at medium spatial resolution is exploited (with a pixel spatial resolution ranging from 30 m to 100 m, depending on the type of SAR data used) in order to obtain average speed maps and deformation time series relating to areas extending over several thousand square kilometres. At the local scale, the technique instead exploits the SAR data generated at full spatial resolution (spatial resolution of a few meters) for detailed analysis in sensitive areas, allowing to detect deformative phenomena, even very localized spatially, relating to buildings or individual structures (*M. Manzo, 2012*).

The SBAS technique allows to obtain maps of average speed and historical series of deformation, with an accuracy of about 1-2 mm/year and 5-10 mm for, respectively, measurements of average speed of deformation and individual displacement measurements. The quality of the measurements carried out by this technique is strongly influenced by the type of territory to be analysed. The accuracy and spatial coverage obtained from an elaboration, in fact, are linked to the characteristics of consistency that the targets on the ground have over time: the greater the consistency over time, the better the response, in terms of the quality of the result, given by the processes. The portions of territory that most keep unchanged over time their characteristics of consistency are the urbanized areas (houses, roads, ports, infrastructure...) and the rocky outcrops without coverage; heavily vegetated areas, as woods, meadows and

cultivations of various kinds and the marshy areas, on the other hand, lose this characteristic very quickly and are, therefore, difficult to study through SBAS techniques (*M. Fabris, 2016*).

Although most of the area of the Po delta is unfavourable from this point of view, using, as in this case, a high number of radar images and optimizing the parameters used in the processing, it was possible to achieve good spatial coverage, although the latter is mainly concentrated in residential areas and along the coast.

At the end of the processing for each individual target (PS) you will get the position (its geographical coordinates: latitude, longitude, altitude), the tendency to average deformation (calculated in mm/year as linear interpolation of the displacement measured throughout the monitoring period) and the entire time series of displacements (providing a displacement value for each of the available acquisitions).

About the SAR data, the first step was to eliminate the points that could have disturbances and anomalies within them. The elements present along the electric poles (*Figure 50*) were immediately eliminated, which due to the electric field present, suffer an error.

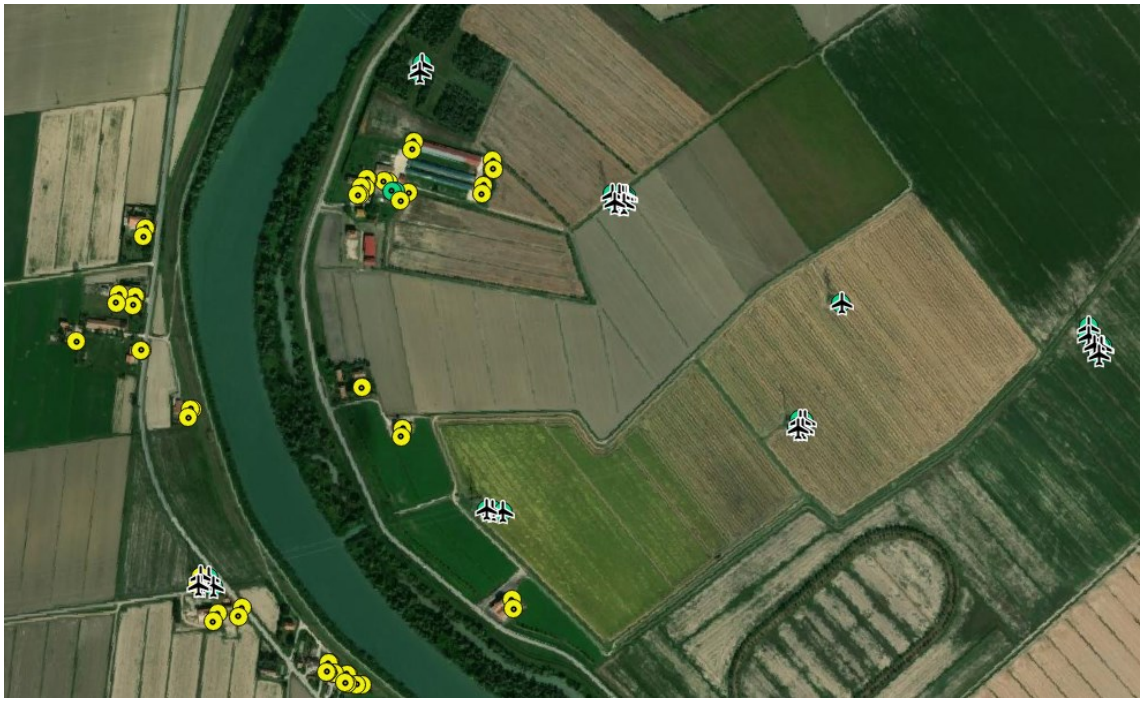

Figure 50. Electric poles

Observations were then made on the possible cause-effects that can influence the SAR data without intervening on the lowering of the ground. By analysing the orthophotos and SAR data, attention was paid to:

- **Power plant**: the Porto Tolle power plant is in disuse, but due to the high weight it still affects the compaction of the soil;
- **Breakwaters**: breakwaters protect the coastal area from the action of the waves, reducing erosion at the base of the cliffs. This protection allows me to have more realistic values on the ballast.
- **Cavane**: the recent construction of the cavane (*Figure 51*) following the 2019 storm carried out in the Sacca of Scardovari only resulted in the loss of many PS due to the creation of a phase ambiguity.

Figure 51. Cavane

- **Dewatering pumps**: through their action, they can bring to the surface areas composed of organic material that in contact with the air begins to degrade, reducing their volume and causing a real lowering.
- **Urban areas and embankments**: urban areas and embankments cause a real lowering of the area due to their own weight.
- **Type of soil**: difficult to assess due to the geological survey carried out in the 90s by the geology department of the University of Padua, of which little information is available on the actual accuracy and methodology used.

It was therefore decided to keep all the points as it is not clear the extent of the different causes and effects.

Before carrying out an in-depth study in the hinterland, the points with high lowering velocity (*Figure 52*) were analysed to verify whether they are reliable measurements (due to wells in operation or particularly yielding areas), or if these points are to be considered out-layer due to errors in the post-processing or points where excavations or demolitions have been carried out and therefore to be eliminated in data processing.

Figure 52. High lowering velocity

From the study carried out, it was verified that most of the points with high sag are due to phenomena not attributable to soil compaction but are due to surface works by private individuals such as the use of a certain area as a warehouse for machinery or the presence of embankments in fishing areas.

However, five points with strange characteristics were found, including a possible well with a speed of -18.9 mm / y, two yielding roof tiles and two areas in which strange "spots" in the soil can be seen, perhaps due to the salinization of the soil (this is not directly via satellite images, Cosmos are not needed, because Cosmos do not take the speed of the point on the ground without PS). A possible use of Cosmo data is to determine roofs at risk of failure because they are made up of heavy tiles, it is known that beyond a certain deflection arrow the roof can yield; therefore, with Cosmo data you can find by when the structure will collapse (*Figure 53*).

Figure 53. Old roof

The Ministry of the Environment, however, invites you to take these observations with caution since the satellite survey was created for the monitoring of the soil and not of individual buildings. It was therefore decided to eliminate the points with high sag.

5.3. Comparison between GNSS data and Sentinel data

First, the basic methodology for the comparison between GNSS points and SAR points has been determined. The first step was to evaluate the size of the radius in which to compare the SAR points with the relevant GNSS station. A high radius allows to acquire many SAR points but reducing the reliability of the data (distant points may have different drops due to variations in the type of soil or external factors). A reduced radius instead allows you to have points having the same characteristics as the PODELNET station, but reducing the number of data, with the possibility of having outlayers that involve large errors.

For this purpose, several attempts have been made starting from the permanent stations (*Table 4*) and obtaining the following results:

		n. points	mean_vel [mm/yr]	Vel_GNSS [mm/yr]	Type of soil
PT01	1 point close	1	-4.5	-4.0	Clay
	2 points close	2	-4.5±0.0		
	3 points close	3	-4.5±0.0		
	50m points close	8	-4.5±0.3		
	100m points close	36	-4.5±0.3		
	150m points close	57	-4.4±0.9		
	200m points close	73	-4.4±0.8		
TGPO	1 point close	1	-4.1	-4.0	Clay
	2 points close	2	-3.9±0.1		
	3 points close	3	-4.0±0.1		
	50m points close	2	-3.9±0.1		
	100m points close	13	-3.9±0.4		
	150m points close	38	-4.0±0.3		
	200m points close	49	-4.2±1.5		

CODI	1 point close	1	-2.7	-2.2	Sand
	2 points close	2	-2.6±0.1		
	3 points close	3	-2.7±0.2		
	50m points close	4	-2.7±0.2		
	100m points close	25	-3.1±0.4		
	150m points close	44	-3.1±0.4		
	200m points close	62	-3.2±0.5		

Table 4. Sentinel-1, permanent stations

In the end, the "moving average" methodology with a buffer of 200m was chosen which allows to obtain a good number of SAR points without the risk of falling back into soils of different geological conformations. The results obtained for the different rover stations (*Table 5*) of the PODELNET network are reported below:

	GNSS station	vel. GNSS [mm/yr]	n. point SAR	vel. SAR [mm/yr]	Diff.Vel [mm/yr]
Buffer 200m	065704	-6,8	3	-3,2±0.1	3,6
	065705	-3,9	5	-3,3±0.1	0,6
	065706	-5,3	49	-4,1±0.9	1,2
	065707A	-3,6	26	-3,8±1.6	0,2
	065708	-2,3	29	-3,3±1.9	1.0
	065715	-3,2	18	-2,7±0.4	0,5
	065901	-4,4	11	-5,3±1.4	0,9
	065903	-6,8	39	-5,6±1.1	1,2
	065904	-6,3	3	-3,2±0.3	3,1
	065905	-4,2	7	-4.6±0.8	0.4
	065906	-8,4	4	-6,1±1.7	2,3
	065907	-6,5	34	-4,2±1.3	2,3
	065908	-6,4	10	-4,8±0.8	1,6
	065909	-3,1	3	-1,3±1.3	1,8
	077703	-12,6	20	-3,9±1.3	8,7
	077704	-12,4	2	-4,7±0.3	7,7

Buffer 200m	077707	-7,8	60	-3,1±0.6	4,7
	077708	-13,4	0	NULL	/
	077710	-8,5	3	-3,9±0.1	4,6
	077712	-3,5	17	-3,3±0.6	0,2
	077713	-5,6	0	NULL	/
	077714	-5,2	11	-3,4±0.2	1,8
	077715	-7,2	0	NULL	/
	077716	-7,5	12	-4,9±1.2	2,6
	077717	-7,2	5	-4,3±0.5	2,9
	077718	-11,6	8	-6,7±2.7	4,9
	077719	-8,1	15	-4,5±0.7	3,6
	077720	-9,2	7	-4,3±1.0	4,9
	077721	-10,9	11	-3,8±0.3	7,1
	077801	-11,4	36	-2,7±1.3	8,7
	077902	-9,2	4	-5,6±2.5	3,6
	077903	-2,7	11	-3,6±1.3	0,9
	077904	-4,5	19	-5,0±2.2	0,5
	077905	-6,2	8	-5.5±1.8	0.7
	077906	-9,5	8	-5,0±0.6	4,5
	077907	-3,6	30	-2,4±0.5	1,2
	077908	-8,5	57	-4.0±1.0	4,5
	077909	-3,7	3	-7,5±4.7	3,8
	077910	-3,7	8	-1,0±4.3	2,7
	077911	-11,5	23	-3,3±1.0	8,2
	077912	-9,8	55	-2,9±1.6	6,9
	077913	-3,4	2	-1,9±0.0	1,5
	077914	-5,5	71	-3,2±0.8	2,3
	077915	NULL	0	NULL	/
	077916	-7,9	0	NULL	/
	077917	-5,6	0	NULL	/

Table 5. Sentinel-1, rover station with buffer 200m

From the table you can see the presence of six points with a difference between the SAR and GNSS speed higher than the tolerance. In the table in red are marked stations with error greater than 5mm/yr, while in green are indicated stations that do not have SAR points in the around 200m. The same symbology is also applied to the following tables. For this reason, it was decided to reduce, for these six points (*Table 6*), the buffer radius (bringing it to 100m) to eliminate due errors to a change in geology.

	GNSS station	vel. GNSS [mm/yr]	n. point SAR	vel. SAR [mm/yr]	diff. Vel [mm/yr]
Buffer 100m	077703	-12,6	4	-4,7±2.0	7,9
	077704	-12,4	2	-4,7±0.3	7,7
	077721	-10,9	11	-3,8±0.3	7,1
	077801	-11,4	11	-2,9±1.6	8,5
	077911	-11,5	1	-3,1±0.0	8,4
	077912	-9,8	4	-1,6±0.9	8,2

Table 6. Sentinel-1, rover station with buffer 100m

As a result of the buffer change, no points fell within the tolerance. These points will be studied to determine the causes of the error.

We now proceed to analyse the stations that do not have SAR points around 200m, to be able to solve the problem it was decided to increase the buffer, reaching 250m, to see further points (*Table 7*), but without risking having points in different geological areas.

	GNSS station	vel. GNSS [mm/yr]	n. point SAR	vel. SAR [mm/yr]	diff. Vel [mm/yr]
Buffer 250m	077708	-13,4	0	NULL	/
	077713	-5,6	0	NULL	/
	077715	-7,2	1	-3,9±0.0	3,3
	077915	NULL	0	NULL	/
	077916	-7,9	3	-4,1±0.2	3,8
	077917	-5,6	4	-3,4±0.1	2,2

Table 7. Sentinel-1, rover station with buffer 250m

It is noted that in this way there are only three stations that do not have points around them of 250m, these GNSS stations are therefore indispensable for the study of the lowering of the areas in question.

5.4. Comparison between GNSS data and Cosmo data

The Cosmo data is the sum of the data collected with two different line of sight and therefore two different incident angles: ϑ = 0.82806 that detects the EAST zone of the delta and ϑ = 0.89879 that detects the WEST zone. This type of modes is called ScanSAR and is capable to operate with single and dual polarization capability (*Agenzia Spaziale Italiana, 2017*).

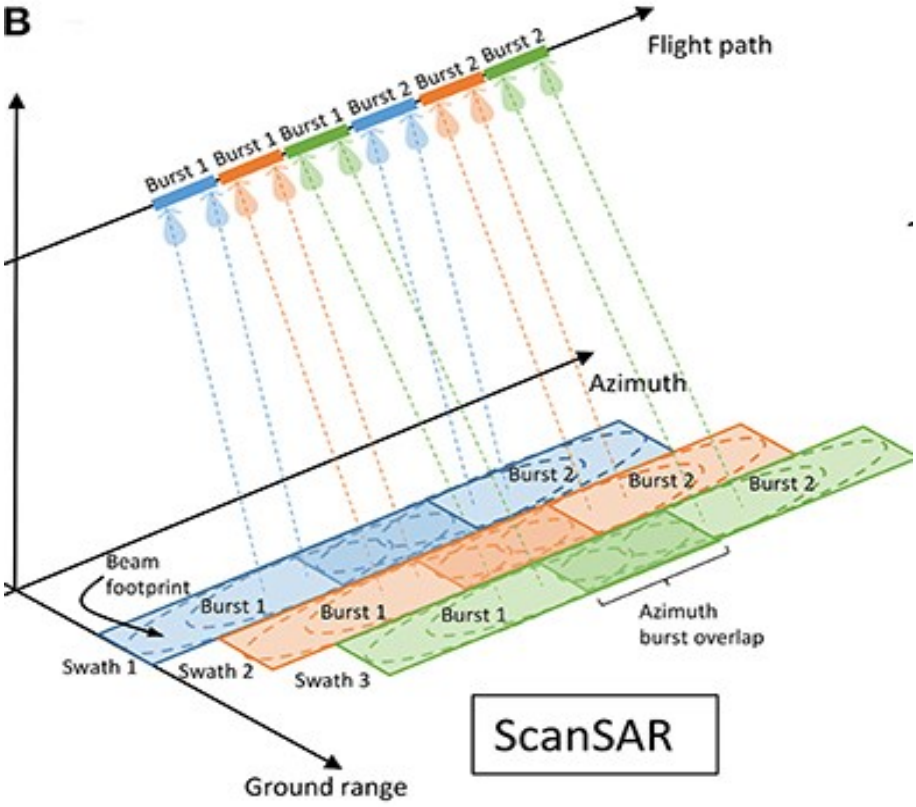

Figure 54. ScanSAR mode

Moreover, for the EST zone, in the attempt to acquire more points, two different thresholds were applied to determine the PS; in this way two files were obtained:

- **threshold 3**: file with higher point density but with poor correlation and consequent accuracy.
- **threshold 35**: file with lower point density but with a correlation and resulting in greater accuracy.

At the end of a check, it was decided to use threshold 35, which provides greater accuracy, even if with fewer data. After a careful evaluation, it was also found that the points obtained with threshold 3 did not guarantee coverage in areas where there is a shortcoming with threshold 35.

First, the basic methodology for comparing SAR and GNSS points was determined. As in the case of Sentinel-1, different tests were performed on the permanent stations (*Table8*) to find the ideal radius within which to process and compare SAR data.

	EAST - soglia35	n. points	mean_Vel [mm/yr]	Vel_GNSS [mm/yr]
PT01	1 point close	1	-2,8	-4,2
	2 points close	2	-3,3±0.6	
	3 points close	3	-3,3±0.5	
	50m points close	31	-2,9±0.4	
	100m points close	171	-3,2±0.5	
	150m points close	315	-3,2±0.5	
	200m points close	461	-3,3±0.8	
	EAST - soglia35	**n. points**	**mean_vel [mm/yr]**	**Vel_GNSS [mm/yr]**
TGPO	1 point close	1	-2,4	-4,2
	2 points close	2	-2,5±0.0	
	3 points close	3	-2,6±0.2	
	50m points close	16	-2,4±0.4	
	100m points close	75	-2,2±0.6	
	150m points close	128	-2,2±0.6	
	200m points close	199	-2,2±0.6	
	WEST	**n. points**	**mean_vel [mm/yr]**	**Vel_GNSS [mm/yr]**
CD01	1 point close	1	-1.0	-2,5
	2 points close	2	-0.7±0.3	
	3 points close	3	-0.7±0.2	
	50m points close	6	-0.4±1.1	
	100m points close	44	-0.5±0.5	
	150m points close	92	-0.6±0.7	
	200m points close	147	-0.7±0.7	

Table 8. Cosmo-SkyMed, permanent stations

In this analysis it is possible to notice a high error between Cosmo-SkyMed and GNSS data, with a value close to the tolerance of 2 mm/yr in the case of TGPO and CODI. This error may be since when SAR data is processed, the deformations are calculated with respect to the position of a reference point on the ground of known coordinates, which is supposed to be stationary or expressly indicated by GNSS measurements. In the present case the reference point is taken randomly, and the actual lowering of the point is not known, this results in a high error being that the point is in an area with high dynamics. To solve the problem, it is therefore necessary to apply a translation to all the SAR points, to simulate the lowering of the master point. To derive the translation to be applied, several tests were performed using a 200m buffer (ideal for Sentinel data).

Initial data				Processed data			
ID	**Vel_GNSS [mm/yr]**	**Vel_SAR [mm/yr]**	**Err.**	**ID**	**Vel_GNSS [mm/yr]**	**Vel_SAR [mm/yr]**	**Err.**
PT01	-4,2	-3,3	0,9	**PT01**	-4,2	-5,3	1,1
TGPO	-4,2	-2,2	2,0	**TGPO**	-4,2	-4,2	0,0
077720	-10,1	-3,8	6,3	**077720**	-10,1	-5,8	4,3
065909	-3,3	-1,5	1,8	**065909**	-3,3	-3,5	0,2
077912	-10,4	0,1	10,5	**077912**	-10,4	-1,9	8,5
077710	-9,1	-2,8	6,3	**077710**	-9,1	-4,8	4,3
065706	-5,7	-3,5	2,2	**065706**	-5,7	-5,5	0,2
077909	-4	-3,0	1,0	**077909**	-4	-5,0	1,0
065708	-2,5	-1,2	1,3	**065708**	-2,5	-3,2	0,7
065715	-3,4	-1,2	2,2	**065715**	-3,4	-3,2	0,2
077721	-11,6	-2,6	9,0	**077721**	-11,6	-4,6	7,0
077719	-8,6	-3,7	4,9	**077719**	-8,6	-5,7	2,9
065903	-7,2	-3,7	3,5	**065903**	-7,2	-5,7	1,5
065705	-4,2	-1,5	2,7	**065705**	-4,2	-3,5	0,7
077911	-12,2	-2,8	9,4	**077712**	-12,2	-4,8	7,4
077712	-3,7	-1,3	2,4	**077712**	-3,7	-3,3	0,4
077906	-10,2	-3,2	7,0	**077906**	-10,2	-5,2	5
065908	-6,9	-2,9	4,0	**065908**	-6,9	-4,9	2

077914	-5,9	-2,5	3,4	**077914**	-5,9	-4,5	1,4
077718	-12,9	-4,7	8,2	**077718**	-12,9	-6,7	6,2
065901	-4,7	-2,8	1,9	**065901**	-4,7	-4,8	0,1
077717	-7,7	-3,1	4,6	**077717**	-7,7	-5,1	2,6
065904	-6,8	-1,3	5,5	**065904**	-6,8	-3,3	3,5
077907	-3,9	-0,6	3,3	**077907**	-3,9	-2,6	1,3
077903	-2,8	-1,4	1,4	**077903**	-2,8	-3,4	0,6
077902	-9,8	-6,4	3,4	**077902**	-9,8	-8,4	1,4
077904	-4,8	-2,6	2,2	**077904**	-4,8	-4,6	0,2
077716	-8	-3,1	4,9	**077716**	-8	-5,1	2,9
077905	-6,6	-4,2	2,4	**077905**	-6,6	-6,2	0,4
077714	-5,6	-2,2	3,4	**077714**	-5,6	-4,2	1,4
077908	-9,1	-2,1	7,0	**077908**	-9,1	-4,1	5
065907	-6,9	-3,3	3,6	**065907**	-6,9	-5,3	1,6
077916	-8,4	-4,9	3,5	**077916**	-8,4	-6,9	1,5
077703	-13,4	-1,8	11,6	**077703**	-13,4	-3,8	9,6
		Mean error: 4.3			*Mean error:*	*2.6*	

Table 9. Research of translation

Following the study, it was decided to shift all SAR points to a speed of -2 mm/yr, in this way it is possible to minimize the error between the PODELNET network stations and the SAR points. Moreover, by applying this translation, we can see that the error between the SAR points and the permanent TGPO station has been reset to zero, which is why we can deduce that the master point is near it.

Now that the translation of -2 mm/yr has been applied, it is possible to estimate the best methodology to compare Cosmo-SkyMed data with GNSS data. The methodology applied for the evaluation of the buffer within which analysing the SAR points remains the same as previously performed.

In this case, however, attention should be paid to the correct use of Cosmo-SkyMed data referring to the EAST or WEST zones.

EAST – threshold.35		n. points	mean_vel [mm/yr]	Vel_GNSS [mm/yr]	Soil
PT01	1 point close	1	-4,8	-4,2	Clay
	2 points close	2	-5,3±0.6		
	3 points close	3	-5,3±0.5		
	50m points close	31	-4,9±0.4		
	100m points close	171	-5,2±0.5		
	150m points close	315	-5,2±0.5		
	200m points close	461	-5,3±0.8		

EAST – threshold.35		**n. points**	**mean_vel [mm/yr]**	**Vel_GNSS [mm/yr]**	**Soil**
TGPO	1 point close	1	-4,4	-4,2	Clay
	2 points close	2	-4,5±0.0		
	3 points close	3	-4,6±0.2		
	50m points close	16	-4,4±0.4		
	100m points close	75	-4,2±0.6		
	150m points close	128	-4,2±0.6		
	200m points close	199	-4,2±0.6		

	WEST	n. points	mean_vel [mm/yr]	Vel_GNSS [mm/yr]	Soil
CD01	1 point close	1	-3.0	-2,5	Sand
	2 points close	2	-2.7±0.3		
	3 points close	3	-2.7±0.2		
	50m points close	6	-2.4±1.1		
	100m points close	44	-2.5±0.5		
	150m points close	92	-2.6±0.7		
	200m points close	147	-2.7±0.7		

Table 10. Cosmo-SkyMed, permanent stations

After the analysis carried out on the buffer size, we chose the "moving average" methodology with a buffer of 200m that allows to obtain a good number of SAR points without risking falling into soils of different geological conformation. Below (*Table 11*) are shown the results obtained for the different top rover of the PODELNET network, paying attention to the correct use of speeds along the EAST and WEST area.

	GNSS station	vel. GNSS [mm/yr]	n. point SAR	vel. SAR [mm/yr]	diff. Vel [mm/yr]
Buffer 200m	065704	-7,2	NO DATA EAST	NULL	/
	065705	-4,2	6	-3,5±0.5	0,7
	065706	-5,7	139	-5,5±1.6	0,2
	065707A	-3,9	NO DATA EAST	NULL	/
	065708	-2,5	166	-3,2±1.0	0,7
	065715	-3,4	22	-3,2±0.6	0,2
	065901	-4,7	19	-4,8±1.1	0,1
	065903	-7,2	172	-5,7±1.0	1,5
	065904	-6,8	8	-3,3±0.2	3,5
	065905	-4,5	NO DATA EAST	NULL	/
	065906	-8,9	0	NULL	/
	065907	-6,9	65	-5,3±0.8	1,6
	065908	-6,9	17	-4,9±1.4	2,0

Buffer 200m	065909	-3,3	59	-3,5±0.5	0,2
	077703	-13,4	161	-3,8±0.7	9,6
	077704	-13,2	0	NULL	/
	077707	-8,3	NO DATA EAST	NULL	/
	077708	-14,3	0	NULL	/
	077710	-9,1	8	-4,8±0.3	4,3
	077712	-3,7	72	-3,3±0.9	0,4
	077713	-6,0	0	NULL	/
	077714	-5,6	39	-4,2±0.4	1,4
	077715	-7,6	0	NULL	/
	077716	-8,0	27	-5,1±1.6	2,9
	077717	-7,7	8	-5,1±0.7	2,6
	077718	-12,9	1	-6,7±0.0	6,2
	077719	-8,6	33	-5,7±0.7	2,9
	077720	-10,1	24	-5,8±0.7	4,3
	077721	-11,6	21	-4,6±0.4	7,0
	077801	-12,2	NO DATA EAST	NULL	/
	077902	-9,8	2	-8,4±0.8	1,4
	077903	-2,8	24	-3,4±0.6	0,6
	077904	-4,8	61	-4,6±0.6	0,2
	077905	-6,6	45	-6,2±1.9	0,4
	077906	-10,2	9	-5,2±0.8	5,0
	077907	-3,9	133	-2,6±0.5	1,3
	077908	-9,1	378	-4,1±0.7	5,0
	077909	-4,0	9	-5,0±1.3	1,0
	077910	-3,9	NO DATA EAST	NULL	/
	077911	-12,3	142	-4,8±0.8	7,5
	077912	-10,4	188	-1,9±0.7	8,5
	077913	-3,6	NO DATA EAST	NULL	/
	077914	-5,9	319	-4,5±0.7	1,4
	077915	NULL	7	-3,6±0.5	3,6
	077916	-8,4	4	-6,9±0.6	1,5
	077917	-6,0	NO DATA EAST	NULL	/

Table 11. Cosmo-SkyMed, rover station with buffer 200m

The table shows the presence of five points with a difference between SAR and GNSS speeds exceeding the tolerance of 5 mm/yr, for this reason it was decided to reduce the inclusion radius for these six points (bringing it to 100m) to eliminate errors due to a change in geology or external actions.

	GNSS station	vel. GNSS [mm/yr]	n. points SAR	vel. SAR [mm/yr]	diff. Vel [mm/yr]
Buffer 100m	077703	-13,4	42	-3,4±0.7	10
	077718	-12,9	1	-6,7±0.0	6,2
	077721	-11,6	21	-4,6±0.4	7
	077911	-12,3	60	-5,0±0.8	7,3
	077912	-10,4	69	-1,9±0.6	8,5

Table 12. Cosmo-SkyMed, rover station with buffer 100m

As a result (*Table 12*) of the buffer change, no point is within the 5 mm/yr tolerance. These points will be studied later to determine the possible causes of error.

The stations which do not have SAR points in the region of 200m are now analysed. To solve the problem, it was decided to increase the buffer (reaching 250m) to find additional SAR points but taking care not to fall back into different geological areas.

	GNSS station	vel. GNSS [mm/yr]	n. point SAR	vel.SAR [mm/yr]	diff. Vel [mm/yr]
Buffer 250m	065906	-8,9	0	NULL	/
	077704	-13,2	0	NULL	/
	077708	-14,3	0	NULL	/
	077713	-6,0	0	NULL	/
	077715	-7,6	1	-5.9±0.0	1.7
	077718	-12,9	1	-6,7±0.0	6,2
	077902	-9,8	4	-8.0±0.7	1,8
	077916	-8,4	14	-5,3±1.2	3,1

Table 13. Cosmo-SkyMed, rover station with buffer 250m

From the analysis conducted (*Table 13*), there are four vertices that do not have SAR points in their vicinity of 250m, so a final verification is carried out based on Cosmo-SkyMed data processed with threshold 3 to try to get points to compare.

	GNSS station	vel. GNSS [mm/yr]	n. point SAR	vel. SAR [mm/yr]	diff. Vel [mm/yr]
Buffer 250m	065906	-8,9	1	+4.6±0.0	13.5
	077704	-13,2	0	NULL	/
	077708	-14,3	0	NULL	/
	077713	-6,0	0	NULL	/
	077718	-12,9	14	-4.3±1.4	8.6
	077902	-9,8	7	-6,6±1.7	3.2

Table 14. Cosmo-SkyMed, threshold.3, rover station with buffer 200m

Using a SAR data processing with a threshold 3 (*Table 14*) the rover vertices that do not have SAR points in the vicinity of 250m are three, these GNSS stations will therefore be fundamental for the study of the lowering of the area, being probably present in rural areas where there is no type of reflective material and therefore it is free from the presence of houses or metal structures.

It is now necessary to verify and compare SAR data for PODELNET stations present in the area covered by Cosmo-SkyMed images in the WEST area (*Table 15*) to assess the presence of errors or stations on which to pay special attention.

Cosmo_WEST					
	GNSS station	**vel. GNSS [mm/yr]**	**n. point SAR**	**vel. SAR [mm/yr]**	**diff. vel [mm/yr]**
Buffer 200m	065704	-7,9	3	-3,1±0.4	4,8
	065707A	-4,2	28	-3,2±1.6	1,0
	065905	-4,8	19	-7,6±4.8	2,8
	077703	-14,6	36	-7,9±0.8	6,7
	077707	-9,0	125	-2,6±0.6	6,4
	077801	-13,2	93	-2,6±0.9	10,6
	077910	-4,2	7	-2,1±1.9	2,1
	077912	-11,3	90	-3,5±0.8	7,8
	077913	-3,9	11	-4.0±3.1	0,1
	077917	-6,5	0	NULL	/

Table 15. Cosmo-SkyMed, WEST zone, rover station with buffer 200m

The study shows the presence of four rover stations with a high error of more than 5 mm/yr and a rover station (077917) that does not have SAR points in the vicinity of 200m, however, increasing the buffer, a SAR point was obtained at 253m with a speed of -3,2 mm/y, a speed that when compared with the GNSS data respects the tolerance, even if the presence of a single point has a great uncertainty.

In addition, points with a high error between GNSS and SAR will be studied later to determine the possible causes that led to such a high-speed difference.

CHAPTER 6. ANALYSIS OF RESULTS

6.1. Analyses of points with high errors

From previous comparisons, two types of vertices were found to be analysed. The first category concerns the study of rover vertices having an error between the lowering speed SAR and PODELNET exceeding 5 mm/yr. In the analysis of these vertices, the number of considered SAR points will be checked, if the number of these points is relevant, the SAR data can be considered reliable and the study will pass to the PODELNET summit, if instead the number of SAR points is limited, it will be evaluated if the error source is due to the SAR or GNSS data.

The second category concerns the study of the rover vertices that do not have SAR points in the around 200m, on these stations will not occur any source of error, but on the contrary, these rover stations will be of great importance in determining the rate of subsidence of the soil in isolated areas.

- **Point 077801** *(mean error = 9.7 mm/yr)*

Vel_GNSS_Sentinel: -11.4 mm/yr *Vel_Sentinel (buffer 200m): -2.7 mm/yr (36 points)*
Vel_GNSS_Cosmo: -13.2 mm/yr *Vel_Cosmo (buffer 200m): -2.6 mm/yr (93 points)*

Description: Point located on a pillar located a short distance from the water and close to an iron pedestrian bridge. High presence of SAR points, the problem could be due to the GNSS station influenced by the slow lowering of the ground level caused by the subsidence of the road surface, the collapse of the embankment and the flood states of the channel.

Figure 55. Point 077801

- **Point 077704** *(mean error =7.7 mm/yr)*

Vel_GNSS_Sentinel: -12.4 mm/yr *Vel_Sentinel (buffer 200m): -4.7 mm/yr (2 points)*
Vel_GNSS_Cosmo: -13.2 mm/yr *Vel_Cosmo (buffer 200m): NULL*

Description: Point located near the shoulder of a disused bridge. Here there is a reduced number of SAR points, but the speed of them represents a typical trend of the area. The high error is therefore to be traced back to the GNSS summit which is probably influenced by the slow natural lowering of the ground level due to the collapse of the road surface, the collapse of the embankment and the flood states of the canal.

Figure 56. Point 077704

- **Point 077703** *(mean error = 9.2 mm/yr)*

Vel_GNSS_Sentinel: -12.6 mm/yr *Vel_Sentinel (buffer 200m): -3.9 mm/yr (20 points)*
Vel_GNSS_Cosmo: -13.4 mm/yr *Vel_Cosmo (buffer 200m): -3.8 mm/yr (161 points)*

Description: Point located on a wall of stable CLS near a hydro-work plant. Here there is a high presence of SAR points, the error is therefore attributable to the GNSS summit. Being the stable point, the error can be due to the lowering of the ground caused by the weight of the wall in CLS, or to an atmospheric interference problem. It is recommended a stationing greater than 3h.

Figure 57. Point 077703

- **Point 077721** *(mean error = 7.1 mm/yr)*

Vel_GNSS_Sentinel: -10.9 mm/yr *Vel_Sentinel (buffer 200m): -3.8 mm/yr (11 points)*
Vel_GNSS_Cosmo: -11.6 mm/yr *Vel_Cosmo (buffer 200m): -4.6 mm/yr (21 points)*

Description: Point located on a saggy plate with little foundation. Here I have a high presence of SAR points. The mistake is probably due to the GNSS summit and to the instability of its foundation.

Figure 58. Point 077721

- **Point 077911** *(mean error = 7.9 mm/yr)*

Vel_GNSS_Sentinel: -11.5 mm/yr *Vel_Sentinel (buffer 200m): -3.3 mm/yr (23 points)*
Vel_GNSS_Cosmo: -12.3 mm/yr *Vel_Cosmo (buffer 200m): -4.8 mm/yr (142 points)*

Description: Point located on an unstable pillar near the shoulder of a practicable bridge. Here I have a high presence of SAR points, the error is therefore attributable to the GNSS station and the failure of the foundation on which it is inserted. In this specific case, a new position for the new summit has already been studied.

Figure 59. Point 077911

- **Point 077707** *(mean error = 5.6 mm/yr)*

Vel_GNSS_Sentinel: -7.8 mm/yr *Vel_Sentinel (buffer 200m): -3.1 mm/yr (60 points)*

Vel_GNSS_Cosmo: -9.0 mm/yr *Vel_Cosmo (buffer 200m): -2.6mm/yr (125 points)*

Description: Point located near the bus stop of Ariano, on a marble staircase. Here I have a high presence of SAR points, the problem is therefore attributable to the GNSS station the most plausible cause is the presence of interference and disturbances in the GNSS signal. It is recommended a stationing greater than 3h.

Figure 60. Point 077707

- **Point 077912** *(mean error = 7.7 mm/yr)*

Vel_GNSS_Sentinel: -9.8 mm/yr *Vel_Sentinel (buffer 200m): -2.9 mm/yr (55 points)*

Vel_GNSS_Cosmo: -10.4 mm/yr *Vel_Cosmo (buffer 200m): -1.9 mm/yr (188 points)*

Description: Point located near an underground channel. I have a high presence of SAR points; the error is traceable to the GNSS station. The causes may be due to the presence of a saggy foundation plate, but the point is to be monitored.

Figure 61. Point 077912

- **Point 077718** *(mean error = 5.6 mm/yr)*

Vel_GNSS_Sentinel: -11.6 mm/yr *Vel_Sentinel (buffer 200m): -6.7mm/yr (8 points)*

Vel_GNSS_Cosmo: -12.9 mm/yr *Vel_Cosmo (buffer 200m): -6.7 mm/yr (1 point)*

Description: Point present on the port of Barricata in a position considered stable. Here I have a limited presence of SAR points, the error is limited so no evaluation will be made on this point, although in the future it will need to be monitored carefully.

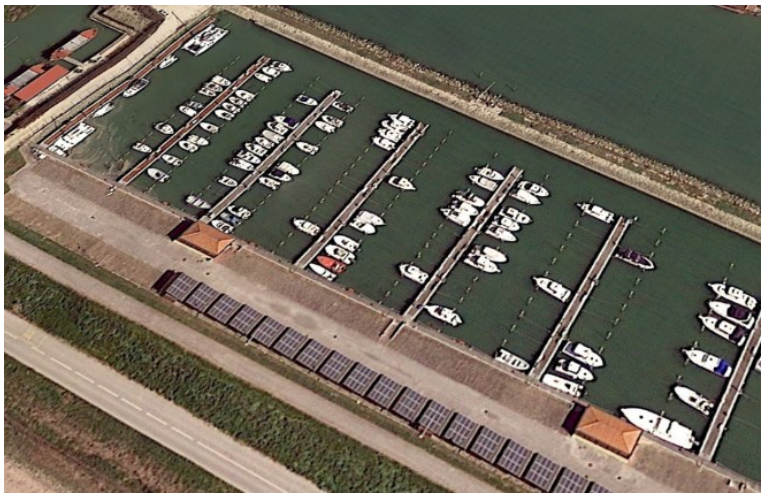

Figure 62. Point 077718

- **Point 077717** *(mean error = 2.8 mm/yr)*

Vel_GNSS_Sentinel: -7.2mm/yr *Vel_Sentinel (buffer 200m): -4.3mm/yr (5 points)*

Vel_GNSS_Cosmo: -7.7 mm/yr *Vel_Cosmo (buffer 200m): -5.1 mm/yr (8 points)*

Description: The area in this case has a smaller error than the tolerance, but the area is of particular interest due to a problem due to water infiltration of a nearby pipe. The area will be monitored and the GNSS and SAR data is of considerable interest.

Figure 63. Point 077717

- **Point 077708**

Vel_GNSS_Sentinel: -13.4mm/yr *Vel_Sentinel & Cosmo (buffer 200m): NULL*

Description: Point located along the chest of an embankment, here is recorded a sharp lowering probably due to substantial changes in the landscape. In recent years, in fact, the formation of a beach has been noted due to a replenishment or an accumulation of natural debris.

Figure 64. Point 077708

- **Point 077713**

Vel_GNSS_Sentinel: -5.6 mm/yr *Vel_Sentinel & Cosmo (buffer 250m): NULL*

Description: Point located in an agricultural area without PS nearby, the GNSS analysis shows a slow decrease that follows the trend of points in the area. Here the presence of a GNSS station is essential.

Figure 65. Point 077713

- **Point 077915**

Vel_GNSS: NO DATA *Vel_Sentinel (buffer 200m): NULL*

Vel_GNSS: NO DATA *Vel_Cosmo (buffer 200m): -3.6 mm/yr (7 points)*

Description: The point was located near the shoulder of a bridge, but recently the point was destroyed due to work on mowing the grass. A new point in the vicinity has already been reconstructed. In the meantime, the SAR points are of fundamental importance.

Figure 66. Point 077915

- **Point 077917** *(mean error = 2.2 mm/yr)*

Vel_GNSS_Sentinel: -5.6 mm/yr *Vel_Sentinel (buffer 250m): -3.4 mm/yr (4 points)*

Vel_GNSS_Cosmo: -6.5 mm/yr *Vel_Cosmo (buffer 250m): NULL*

Description: Point located in an agricultural area without PS nearby, the GNSS analysis shows a slow decrease that follows the trend of points in the area. Here the presence of a GNSS station is essential.

Figure 67. Point 077917

6.1.1. Uses of artificial reflectors

After the analysis, three PODELNET vertices were found to have no SAR points in the vicinity. In fact, especially in a rural and lagoon area such as the Delta, the presence of areas that do not have PS inside them are many and often these areas have a role of considerable importance in safeguarding and security of the territory. Monitoring them is therefore essential.

However, since the creation of large quantities of GNSS points is not feasible due to their considerable cost of management and detection (for each point it is necessary to be stationed at least 3h), the use of artificial reflectors could be more practical (*Figure 68*).

Figure 68. Example of an artificial reflectors

Artificial reflectors are reflective metal structures well anchored to the ground with a deep foundation that allow the detection and acquisition of a point by SAR technology, thus following a first expense for the installation of the structure, monitoring of it does not involve additional costs. Such a system will have to be strongly considered in the future, especially for the monitoring of embankments.

6.2. Analysis of area with high lowering velocity

After having studied and identified the points with a greater difference between GNSS and SAR speeds, we wanted to verify this data going to consider not an area circumscribed to a point but going to consider a greater surface.
First of all, we proceeded to examine the embankment, considered the areas most at risk and in any case fundamental for the protection of the Delta being the only barrier between the sea and a territory located several meters below the surface of the sea.

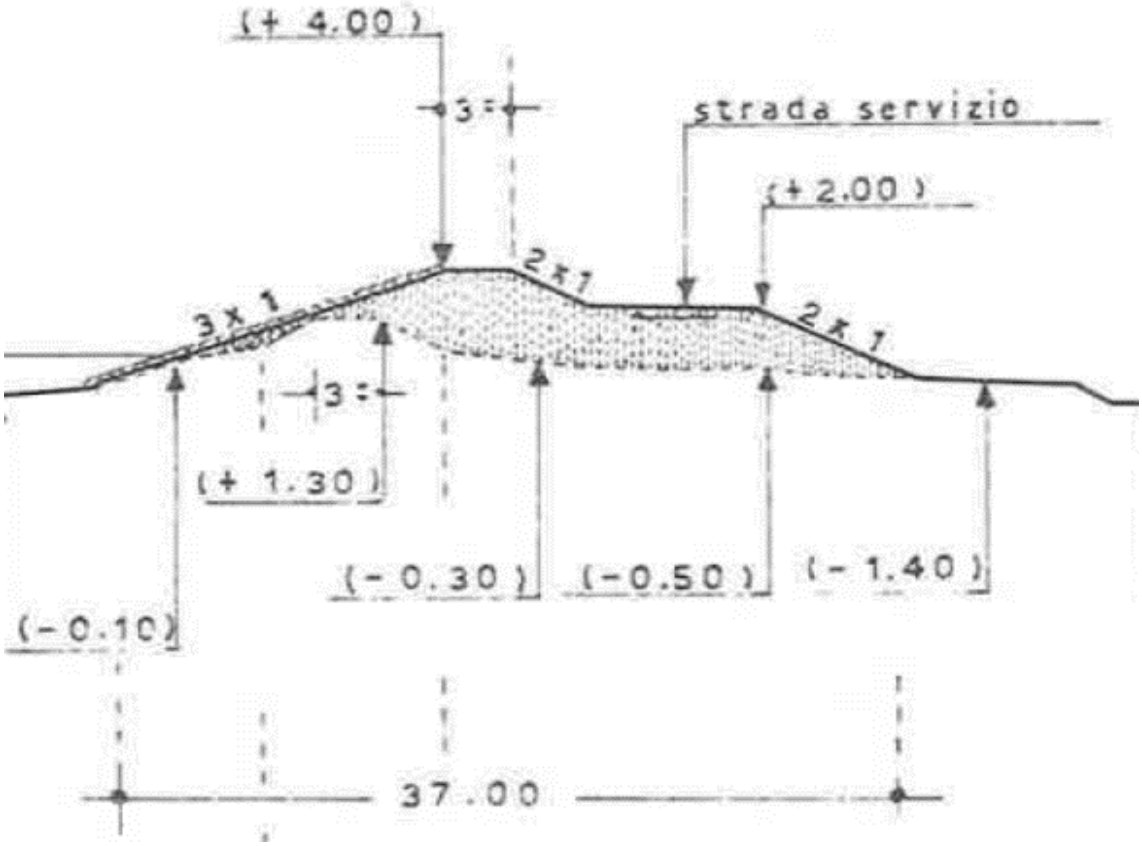

Figure 69. Section of the sea coastal defence embankment

It was decided to consider the SAR points present in a circle equal to 18.5 m from the axis of the top of the embankment, this because considering the sections available in the literature, the average width of the embankments on the waterfront is estimated to be 37 meters from the available sections (*Figure 69*).

Thanks to the good reflectivity of the embankments and in particular to the ballasts covering the latter, it has been possible to obtain many PSs, however these areas are often affected by phenomena of rock sinking and rotation and erosion, factors that then influence SAR measurements (*Figure 70*).

To assess the reliability of the points on the embankment, a purge of the points was previously carried out, where the points near the wet front or directly at sea were eliminated (*Figure 71*). They were then evaluated the average speeds of the banks with and without the points just eliminated finding a good correspondence between the two different cases, which is why it was decided to consider the case cleared from the points that leads to greater accuracy and reliability.

Figure 70. Original points

Figure 71. Points cleared

The importance of the embankments on the protection of the entire Po Delta has led to carry out further checks to increase the reliability of the data and bring to the political bodies responsible for certain evidence regarding the fragility of this system of fundamental protection.

This verification of the SAR data was carried out by evaluating the lowering of the PODELNET network stations and the lowering rate of the nearby urban centers; these centers in fact thanks to the characteristics of the materials from which they are composed (roofing, metal objects, ..) are able to provide a high number of SAR points making the estimate of the lowering reliable and free of gross errors due to excavations or works in general that are common and a major source of error in rural areas.
Obviously, such data will have to be taken with caution and for demonstrative purpose only, being the weight induced from the buildings advanced to the same weight of the land that composes the bank, provoking in this way a greater lowering. These data are available in *Table 16*.

ID	Vel_Cosmo [mm/yr]	ID	Vel_Sentinel [mm/yr]
Gorino	-5.3 ± 0.8	**Gorino**	-4.7 ± 1.0
Tolle	-5.2 ± 0.7	**Tolle**	-4.5 ± 1.8
Scardovari	-5.2 ± 0.8	**Scardovari**	-4.1 ± 1.5
Polesine Camerini	-5.2 ± 0.7	**Polesine Camerini**	-4.4 ± 1.2
Santa Giulia	-5.0 ± 0.8	**Santa Giulia**	-4.5 ± 1.6
Ca' Tiepolo	-5.0 ± 0.7	**Ca' Tiepolo**	-4.3 ± 0.9
Donzella	-5.0 ± 0.7	**Donzella**	-4.3 ± 0.9
Mesola	-4.4 ± 0.7	**Mesola**	-3.5 ± 1.3
Bosco Mesola	-3.0 ± 0.6	**Bosco Mesola**	-3.0 ± 1.1
Bonelli	-5.3 ± 0.8	**Bonelli**	-4.4 ± 1.3
Oca marina	-5.3 ± 0.8	**Oca marina**	-4.3 ± 1.2
Goro	-4.2 ± 0.9	**Goro**	-4.1 ± 1.1
Taglio di Po	-3.4 ± 0.8	**Taglio di Po**	-3.6 ± 1.3
Piano	-2.8 ± 0.6	**Piano**	-2.9 ± 1.2
Pila	-5.9 ± 0.9	**Pila**	-5.4 ± 1.1
Ca' Zuliani	-4.9 ± 0.6	**Ca' Zuliani**	-4.8 ± 1.8
Ca' Venier	-5.0 ± 0.7	**Ca' Venier**	-4.3 ± 0.7
Porto Viro	-3.2 ± 0.8	**Porto Viro**	-3.2 ± 1.1
Boccasette	-4.4 ± 0.5	**Boccasette**	-4.3 ± 0.9
Porto Levante	-4.8 ± 1.3	**Porto Levante**	-3.8 ± 0.8

Rosolina	-3.2 ± 0.7	**Rosolina**	-2.7 ± 1.3
Rosolina mare	-5.0 ± 0.9	**Rosolina mare**	-4.5 ± 1.0
Albarella	-4.8 ± 0.8	**Albarella**	-4.3 ± 1.0

Table 16. Velocity of Sentinel-1 and Cosmo-SkyMed of urban centres

This was done by dividing the banks according to their average lowering speed, dividing each bank into different sections with lengths that cover a large area and thus going to check initially the consistency with the lowering of the neighboring areas and then to a thorough study that led to a classification based on the speed of lowering and therefore to the vulnerability of each embankment.

In addition to the study of the arginal bodies, particular attention has also been paid to the entire territory of the site, the lowering of which has a direct impact on the vulnerability of the area under investigation, so that a greater lowering of the territory in general causes problems both of rising the salt wedge, problems with man-made elements such as buildings, roads, water or sewerage services, etc.; but also with natural factors such as an increase in the rise of the salt wedge, a greater bank vulnerability due to the dangerousness of the line of imbibition; as well as a sense of greater insecurity on the part of citizens especially during the onset of strong storms (*Figure 72*).

Figure 72. Effects of flood events during 1951 in Polesine

.

6.2.1. Analysis of critical levees detected with Sentinel-1

- ***Area NORTH of Boccasette beach***

Vel_GNSS: -8.4mm/yr *Vel_SAR (whole area): -6.6mm/yr*

***Description*:** In the area under consideration there is a significant decrease in the soil detected by both GNSS and SAR data. The lowering, however, is much greater than the average lowering of the surrounding area. The reason is due to an external contribution due to the construction of a roadbed between 2013 and 2015 that benefited in terms of securing the embankment and the hinterland but produced a sharp increase in subsidence due to the new weight to which the soil will have to adapt. A further influence may derive from the greater exposure of the NORTH area to the dynamics of the sea compared to the SOUTH area. To the SOUTH, in fact, the beach is quite extensive and can thus act as a barrier to the erosive action of the sea, keeping stable also the banks to protect the hinterland.

Figure 73. SAR points in north area of Boccasette

- **Area of power plant of Porto Tolle**

Vel_GNSS: -6.2mm/yr *Vel_SAR (whole area): -6.4mm/yr*

Description: In the area under consideration there is a significant decrease in the soil detected by both GNSS and SAR data. The lowering is consistent with the lowering of the areas adjacent to the Porto Tolle plant, an index that makes us understand how the compaction due to the weight of the plant itself (built between 1980 and 1984) is still high. In addition, the weight of the structure induces a lowering of the surrounding areas, observation that should be a reason for analysis in future studies, in particular to understand the extent of the affected area. Between 2010 and 2020, no safety works were carried out in the area in question, so the lowering is due only to the presence of the plant.

Figure 74. SAR points in central oil of Porto Tolle

- ***Area SOUTH of Boccasette***

Vel_GNSS: NULL *Vel_SAR (whole area): -14mm/yr*

Description: In the area under consideration there is a significant lowering of the soil detected by SAR data. The lowering is higher than the speed of the surrounding area, which is why we will have to identify the possible causes. A probable external contribution is due to the construction of a roadbed on the SOUTH side between 2013 and 2015, to the reconstruction of the opposite embankment in 2015 (with soil probably dredged by the canal itself and therefore producing strong subsidence of the adjacent embankment), construction of an additional cliff on the EAST side between 2016 and 2017 (most affected area) and construction of quarry on the SOUTH side between 2018 and 2020. These works benefited from the safety of the embankment and the hinterland and allowed to obtain an area with additional services to the population, but the effects have been a strong increase of the subsidence because of the new weight to which the soil will have to adapt and to an instability due to the dredging of the channel.

Figure 75. SAR points in south area of Boccasette

Figure 76. SAR points in south area of Boccasette

6.2.2. Analysis of critical levees detected with Cosmo

- ***Area of Goro and Gorino***

Point GNSS: 077908 → -9.1 mm/yr 077916 → -8.4 mm/yr

Description: The lowering of the banks is consistent with the lowering of the urban centers of Goro and Gorino, which is why the area will be kept under control for the high lowering that is suffering. GNSS speeds appear to be higher, but within the tolerance limits of 5mm /year. As a result of this study, several considerations will be made to explain the causes of such a movement and to intervene in the future with works that can protect the urban centers in question.

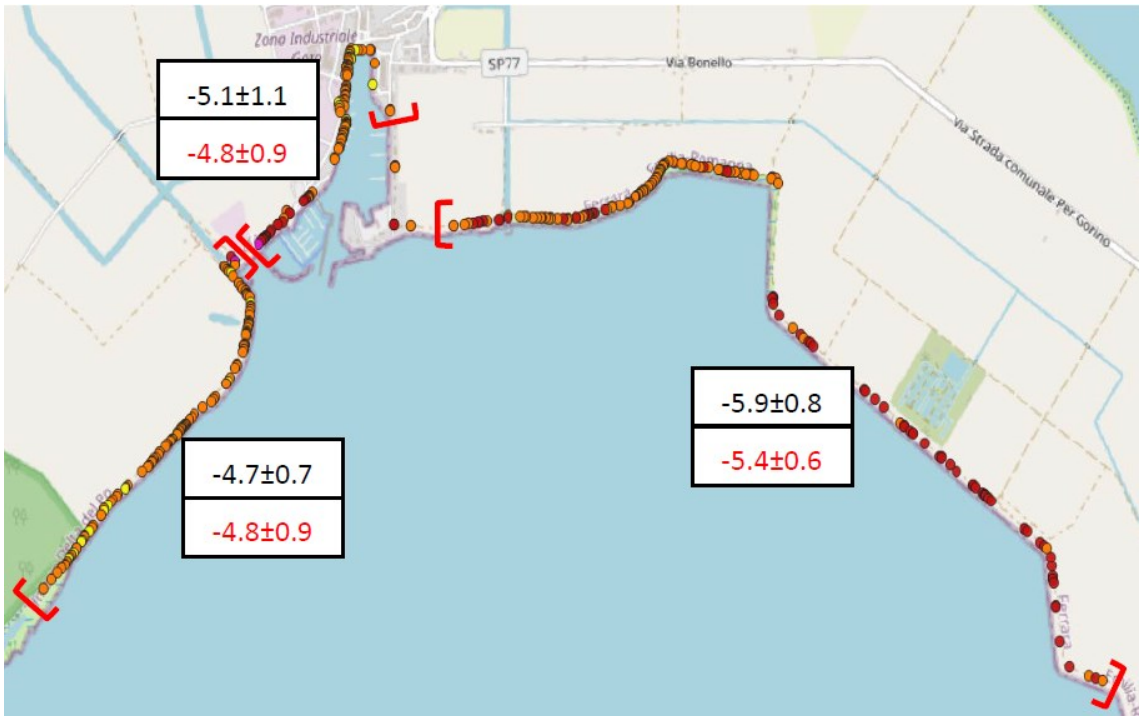

Figure 77. SAR points in area of Goro and Gorino

- ***Area of Sacca Scardovari***

Point GNSS: 077717 → -7.7 mm/y 077721 → -11.6 077716 → -8.0 077719 → -8.6

Description: In the area in question, the largest falls concern the NORTH and NORTH-WEST of the Sacca degli Scardovari. The lowering of the banks is consistent with the lowering of the Urban Centres of Santa Giulia and Scardovari and also the speed of the

GNSS stations is in line with the lowering of the banks, why the area will need to be studied to explain the causes that induce such a movement. Particular attention will be paid to the EAST zone of the Sacca degli Scardovari which does not have a sufficient number of Cosmo-SkyMed SAR points to carry out a detailed study. It will then be necessary to verify the area with data Cosmo-SkyMed soglia3 or Sentinel to make sure that the area is safe or if the lowering is high as in the rest of the Sacca, to implement a campaign to protect the banks.

The area has no SAR points probably due to the construction of the cavane that have not allowed the recognition of the PS from satellites. In the future, there will be a large number of PSs that will enable a reliable assessment to be made.

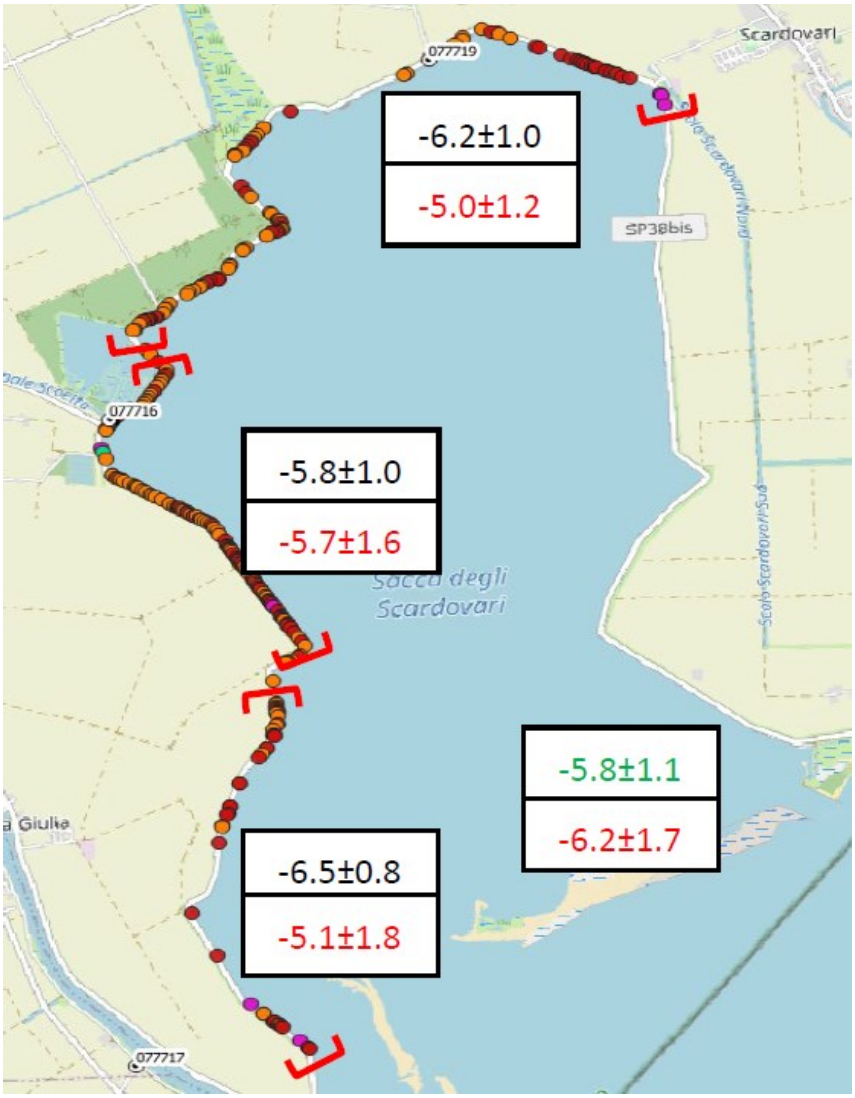

Figure 78. SAR points in "Sacca degli Scardovari"

- ***Area of Bonelli***

Point GNSS: 077718 → -12.9 mm/y *077720 →-10.1 mm/y*

Description: The area in question is located along the residential road of Bonelli located above the dock of the embankment of protection at sea. The lowering of the banks is consistent with the lowering of the urban centre of Bonelli, the GNSS speeds are higher but within the limits of the tolerance of 5mm/yr. The area will be studied to understand the causes of such speed and to plan in the future useful works to protect the urban centre.

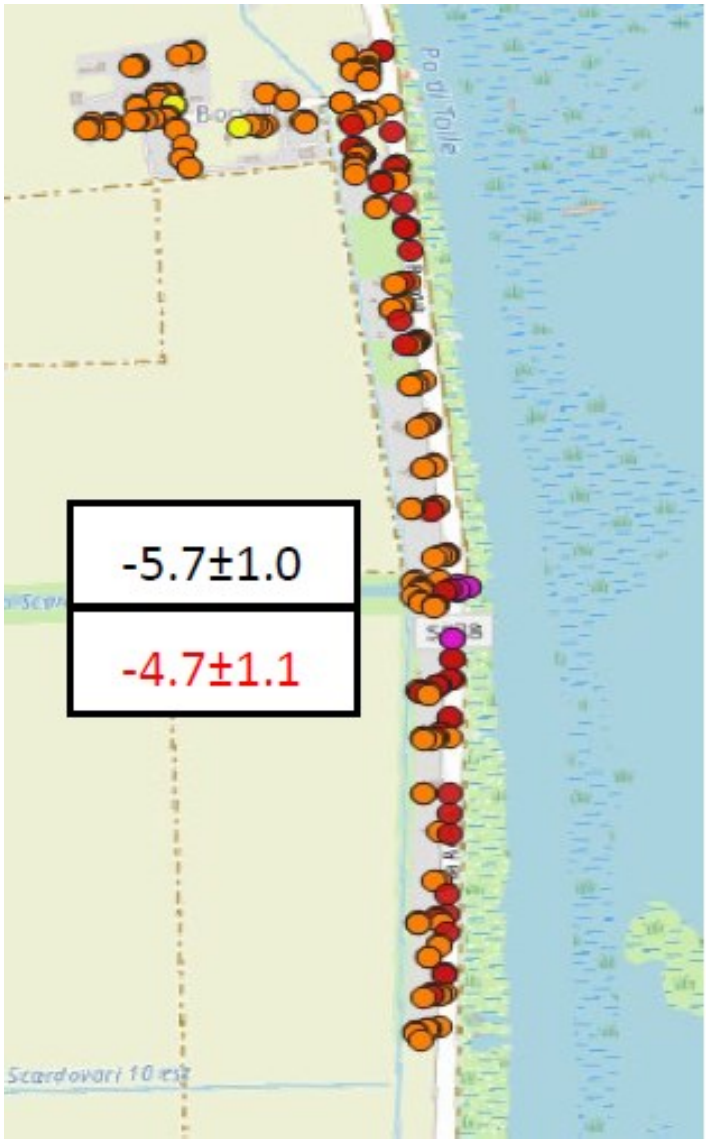

Figure 79. SAR points in area of Bonelli

- ***Area of Polesine Camerini***

Point GNSS: 077906 → -10.2 mm/y *077905 → -6.6 mm/y*

Description: In the Polesine-Camerini area, the area of the Porto Tolle power plant has not been considered because it is affected by a decrease due to the weight of the plant itself, which is why the area will be studied separately.

The area SOUTH of the plant has a lowering of the banks consistent with the lowering of the urban centres of Polesine-Camerini and Scardovari, also the speeds of the banks are consistent with the speeds of GNSS stations.

From the work you can see an area with a high bending of -8 mm / y, this is probably due to the reconstruction of a roadbed in 2009 and the weight of the work still affects the subsidence of the ground.

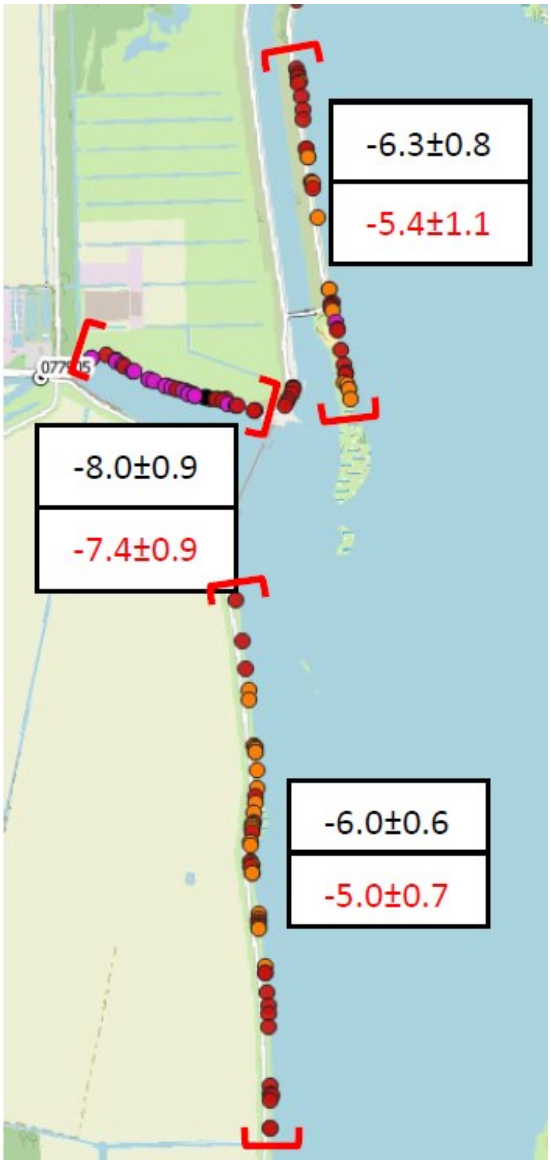

Figure 80. SAR points in area of Polesine Camerini

- ***Area of power plant of Porto Tolle***

Point GNSS: 077902 → -9.8 mm/y

Description: The study area is characterized by the presence of the Porto Tolle power plant, which has such a weight that it has repercussions also on the surrounding areas, producing a strong lowering for the nearby banks, but especially for the urban centre of Pila and GNSS data confirm this trend to decrease.

The plant also has many points with a high lowering speed due to the dismantling that the plant is undergoing in recent years.

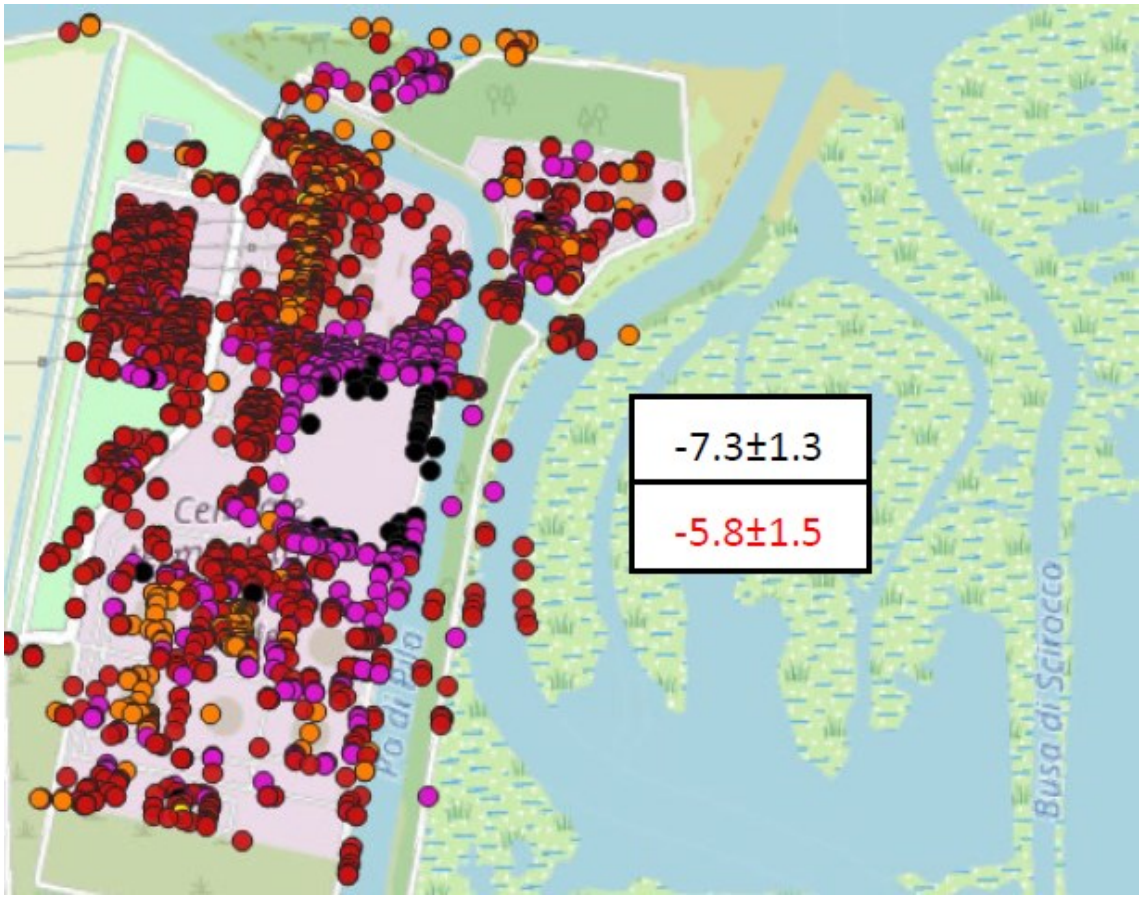

Figure 81. SAR points in central oil of Porto Tolle

- ***Area NORTH of Pila***

Point GNSS: 077902 → -9.8 mm/y

Description: In the study area, the lowering of the banks is consistent with the lowering of the neighboring urban centres, in fact Pila has a speed of -5.9 mm/ yr. Note that the area located to the south have a greater lowering probably due to the weight of the plant, this hypothesis will have to be studied in order to verify its veracity. The lowering of the embankments is also consistent with the GNSS station, information that certifies the quality of the data.

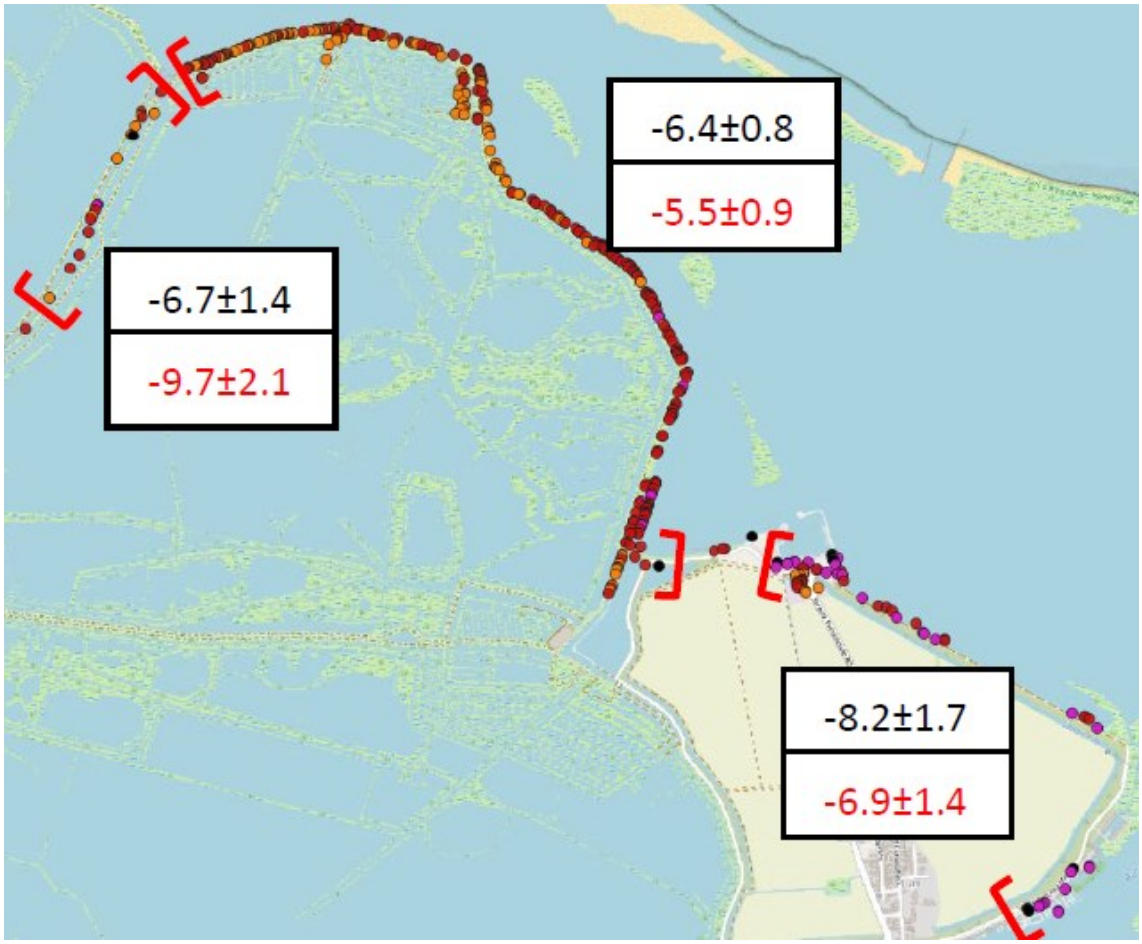

Figure 82. SAR points in north area of Pila

- ***Area of Boccasette***

Point GNSS: 065908 → -6.9 mm/y *065906 → -8.9 mm/y*

Description: The area in question has a criticality in the area north of Boccasette that has a strong lowering. This value is in contrast with the adjacent lowering values, for this reason the reduction obtained is due to the weight increase due to the recent construction of a roadbed that is settling and that, due to its weight, is increasing the lowering speed. This lowering is confirmed by station 065906 which is probably affected by the work carried out on the embankments. The banks to south of the zone instead have values in line with the lowering speed of the centre of Boccasette (-4,4 mm/yr) and of the GNSS station.

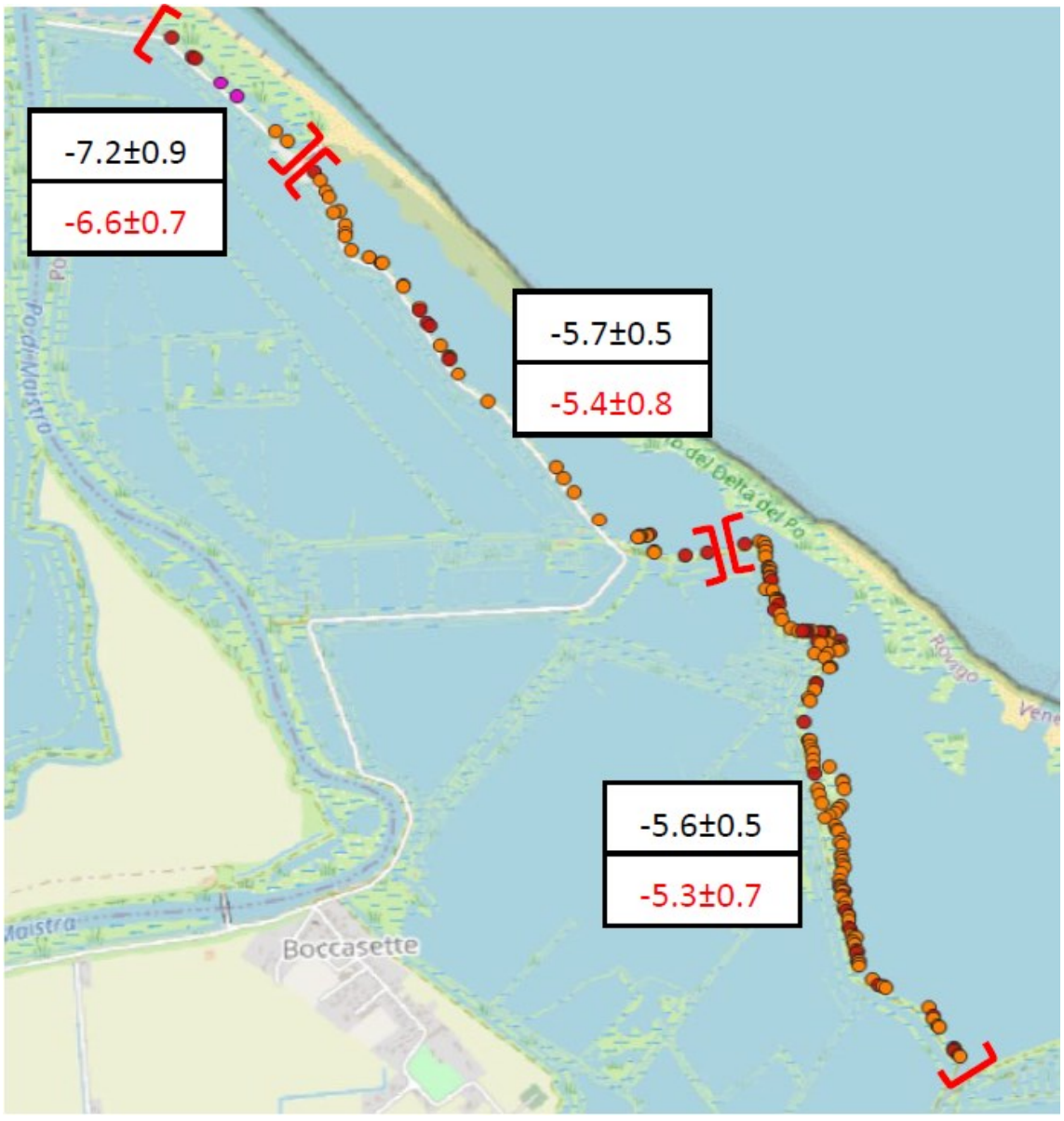

Figure 83. SAR points in Boccasette area

- ***Area NORTH of Boccasette***

Point GNSS: 065908 → -6.9 mm/y

Description: The area is affected by a low density of points, which is why it is difficult to estimate the veracity of the criticality, even with a threshold Cosmo-SkyMed equal to 3 you cannot get a good density of points. The reason for this deficiency is due to the dense vegetation present on the banks that drastically reduces reflectance as well as resulting in a high temporary decorrelation. The decreases are in any case consistent with the nearby GNSS station and the town of Boccasette; therefore, the points present are consistent with the lowering of the area.

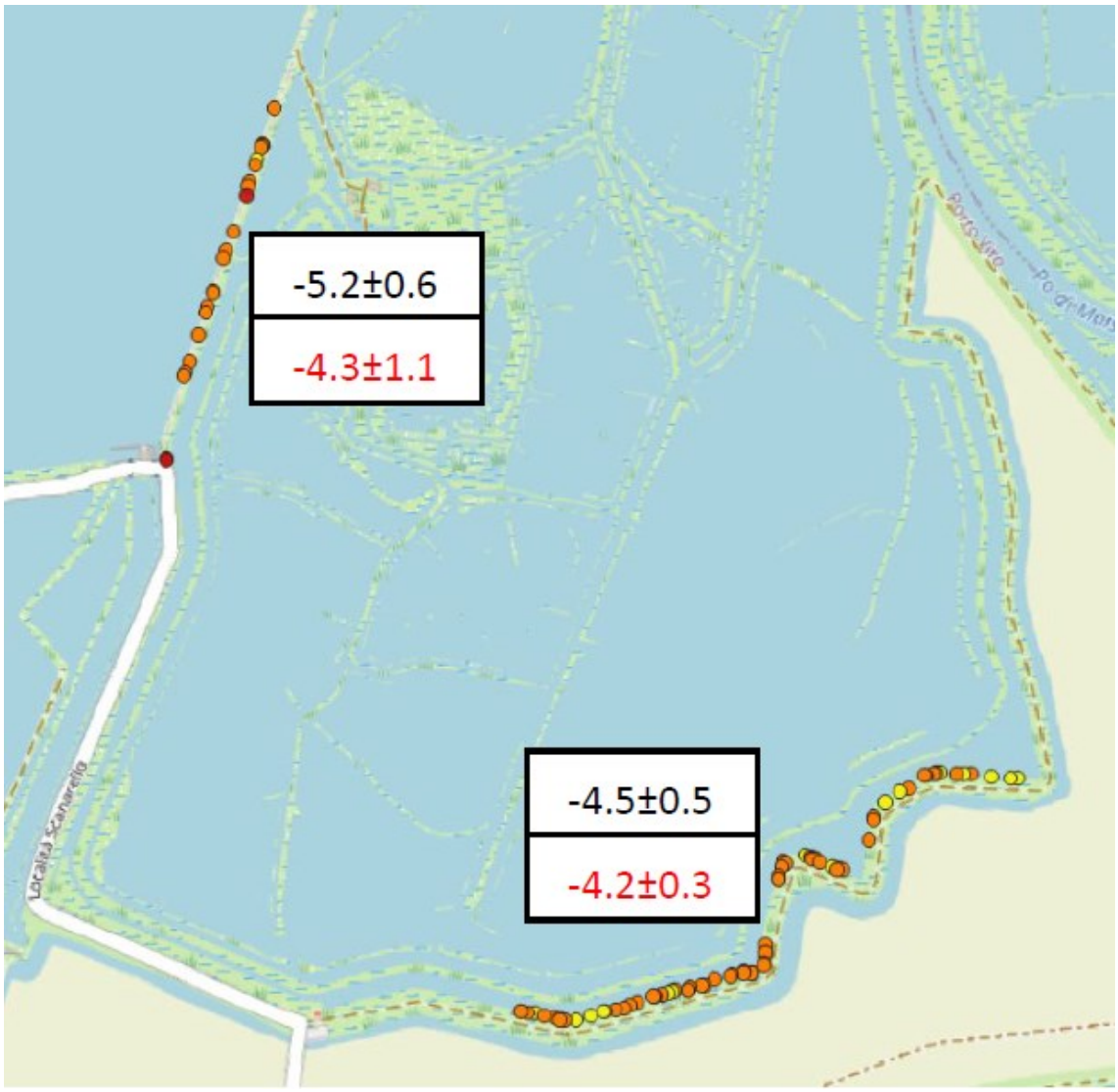

Figure 84. SAR points in north area of Boccasette

- ***Area of Porto Levante***

Point GNSS: 065907 → -6.9 mm/y *065706 → -5.7 mm/y*

Description: The study area is very large, but at the same time it is described by a good density of SAR points having good consistency with the lowering of GNSS points and with the urban centres of Porto Levante. This density of points is due to the lack of vegetation on the ballast and the abundance of reflective surfaces. Particular attention is turned to the optimal job offered from the data SAR in the monitoring of the intense activities of defence in sea and the inlet of Porto Levante.

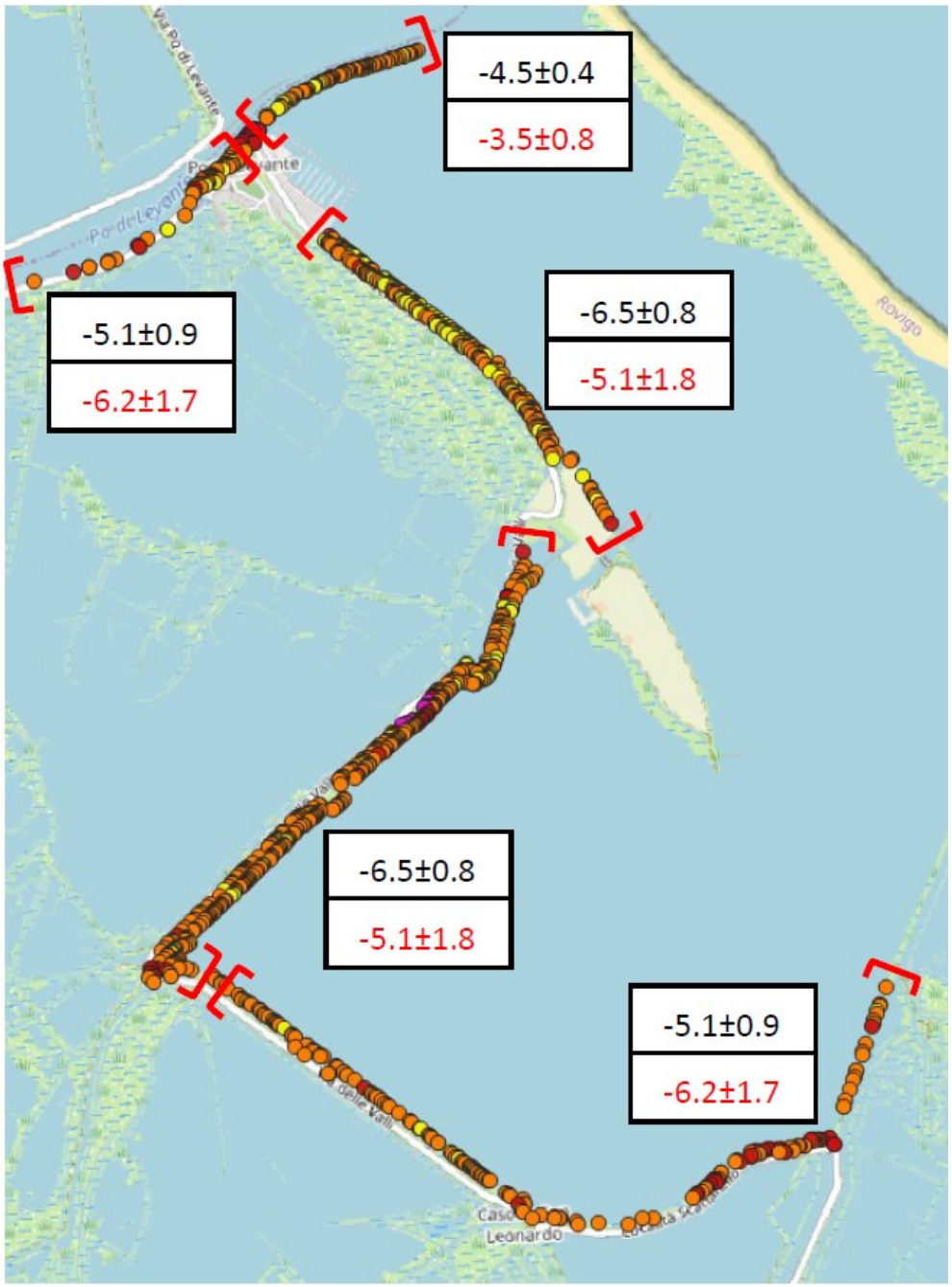

Figure 85. SAR points in porto Levante area

- ***Area of Albarella***

Punti GNSS: 065706 → -5.7 mm/y *065904 → -6.8 mm/y*

Description: Area of particular interest for the presence of the island of Albarella which is characterized by a large urban centre of high tourist importance. The entire area of Albarella has an average drop of -4.8 mm / yr, particular attention should be paid to the defence works of Marina di Albarella that show a high drop probably due to the weight of the defence works at sea.

The decreases evaluated with SAR are however consistent with decreases in GNSS and decreases in urban centres, which shows that the measures are consistent for the area.

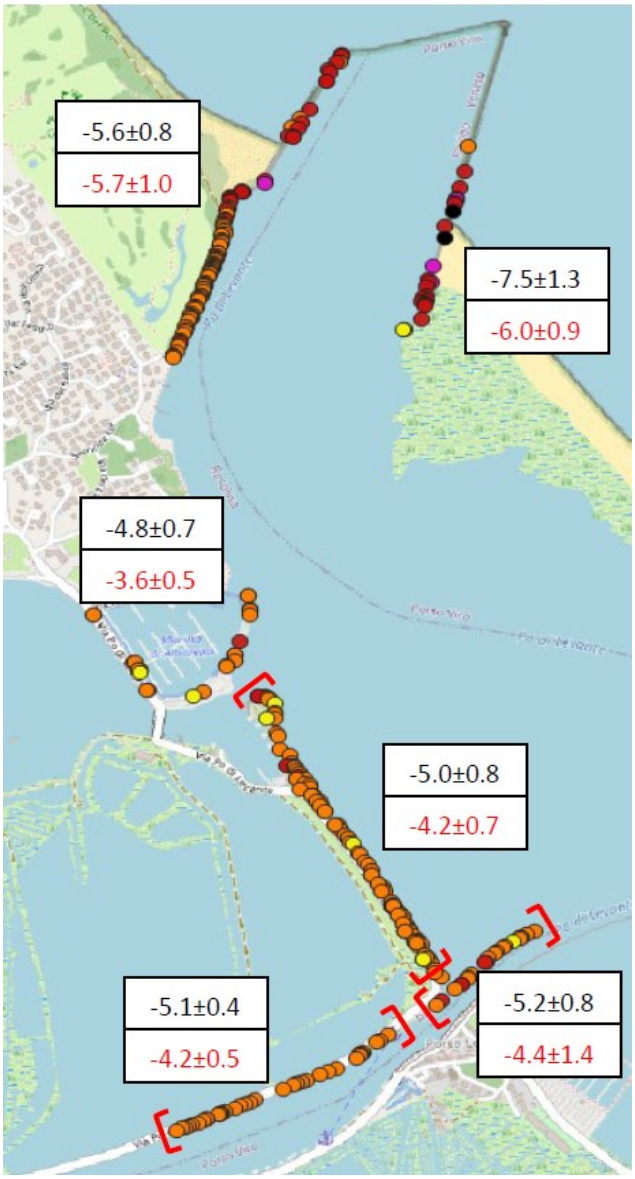

Figure 86. SAR points in Albarella area

- ***CASE STUDY: Construction of a cliff in the SOUTH of Boccasette***

GNSS points: NULL

Description: In this case, particular attention should be paid to the standard deviation value, the fact of having such a high value certifies the uncertainty of measurements, measures largely influenced by the reconstruction of the cliffs and cavane between 2013 and 2020 and that do not allow me a real assessment of the lowering of the area. The measures carried out after 2020 will be interesting and thanks to the new roadbed will allow me to obtain many PS.

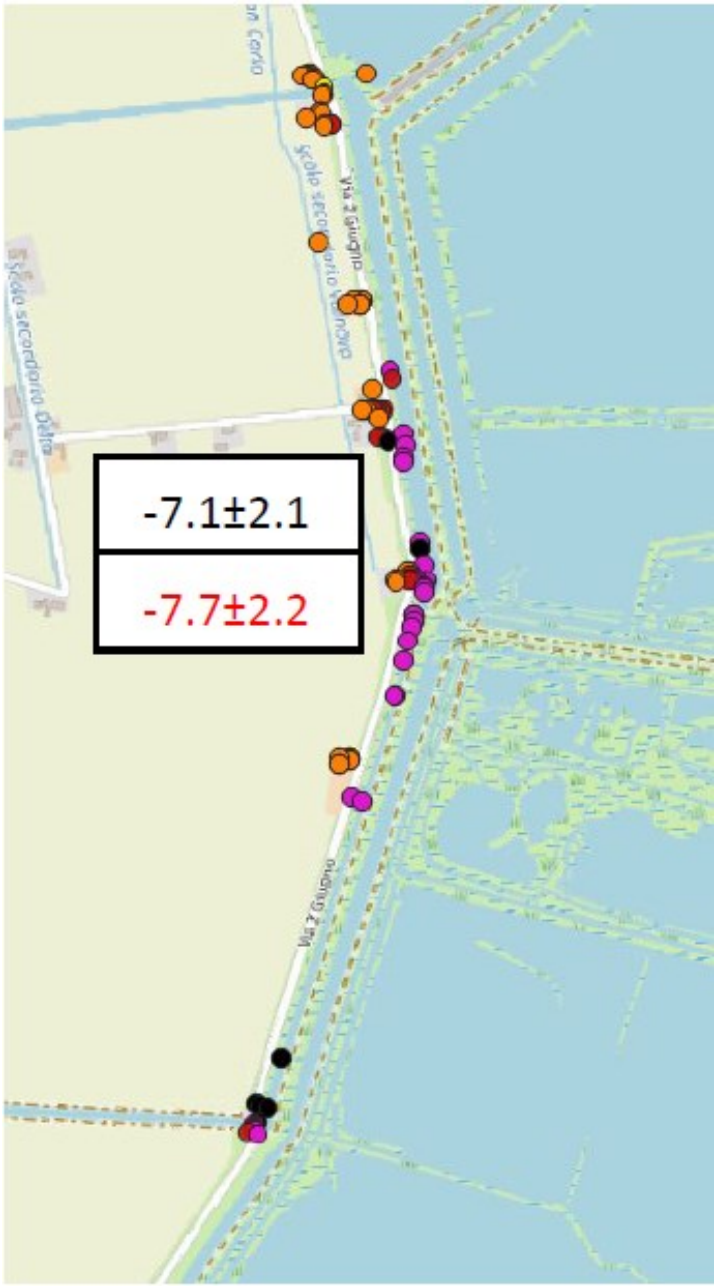

Figure 87. SAR points in south area of Boccasette

6.2.3. Analysis of critical inlet area detected with Cosmo

To assess the presence of areas with high lowering or critical banks, the categorization of the Cosmo points was changed, placing the points with speed between -9 and -7 in red, the points between -7 and -5 in orange and in yellow the “relatively stable” points between -5 and -3. Furthermore, the points belonging to the urban centers (already studied previously) and the points present on the embankments have been eliminated from the map to simplify the visualization.

To make the study easier, the area was divided into two parts, the area south of the Po of Venice (*Figure 88*) and the area north of the Po di Venezia.

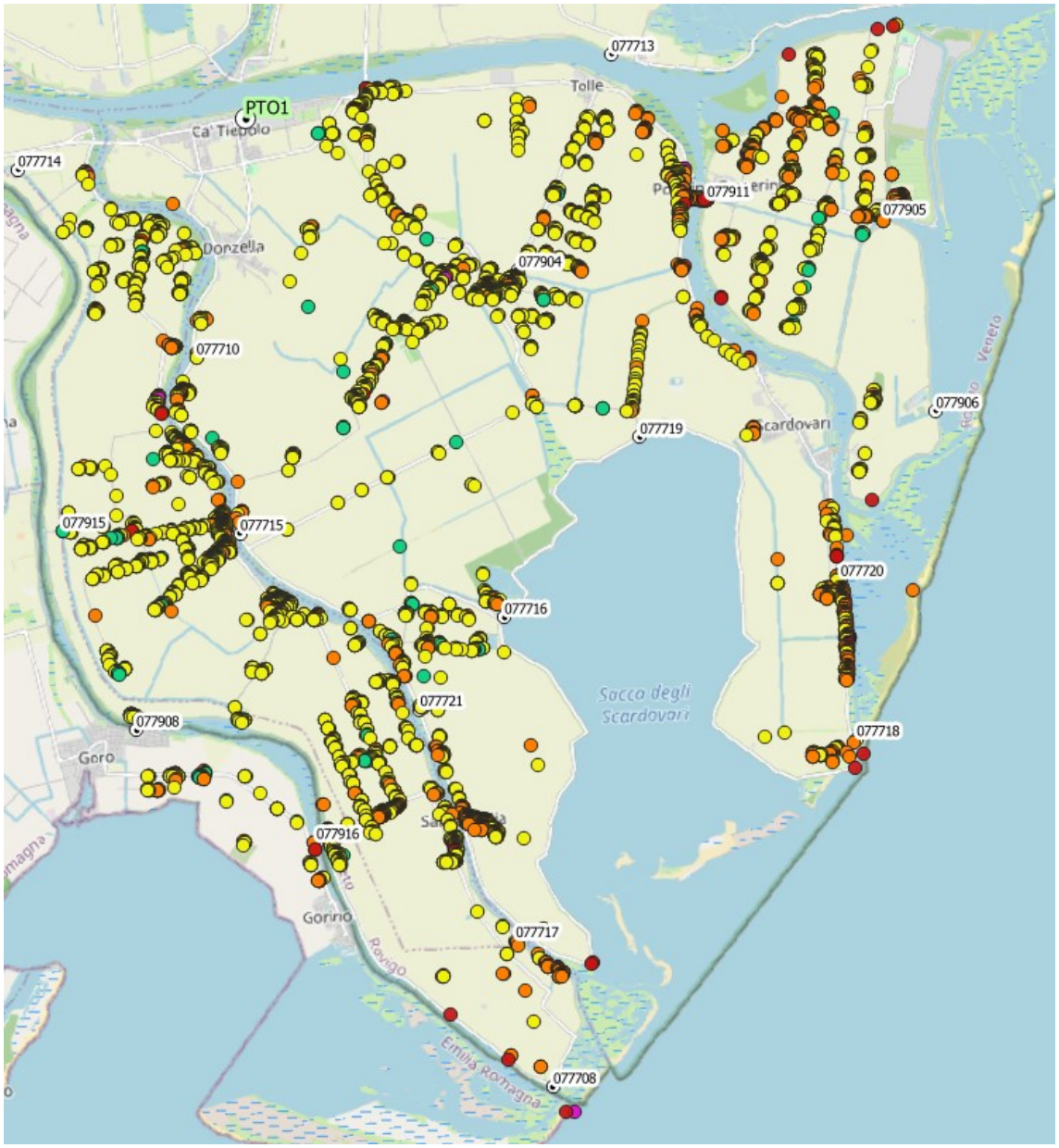

Figure 88. SAR points in the area south of the Po di Venezia

Given these premises, it is noted that the delta area in south area of Po di Venezia does not present any criticalities in the hinterland, except for some higher drops in the area of the Porto Tolle power plant (due to the weight of the structure or to the area which, being recently formed, is still affected by the weight of the surface soil).
Now I do some consideration in North area (*Figure 89*).

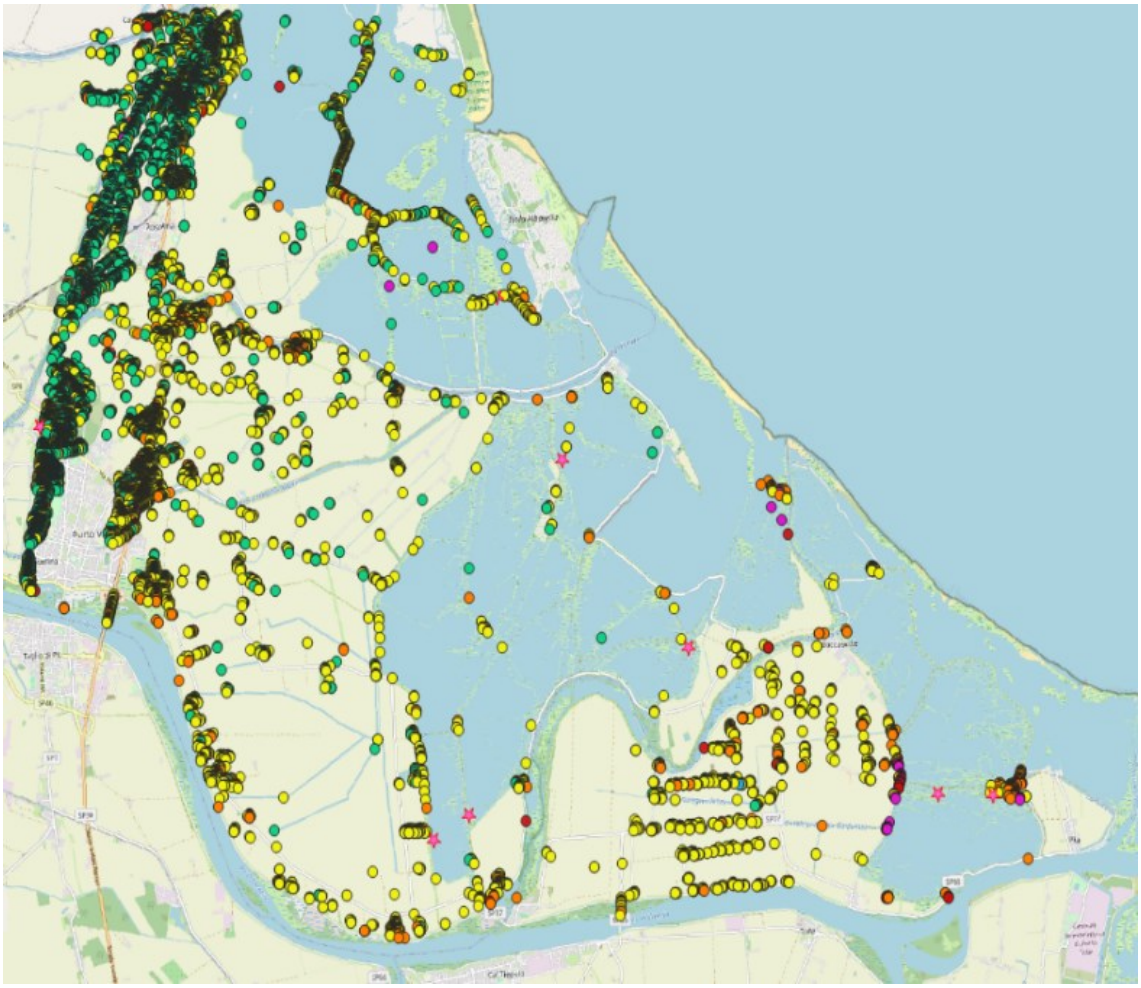

Figure 89. SAR points in the area north of the Po di Venezia

Given these premises, it is noted that the delta area does not present only two critical issues in the hinterland, the first in the south of Boccasette due to the reconstruction of the banks and construction of the cavane, while the second area is located in the north of Pila and the lowering could be influenced by the weight of the Porto Tolle power plant, but also by the works carried out by the "Ca Zuliani" farm which extends over the affected area.

CHAPTER 7. FINAL CONSIDERATIONS

The study in question was carried out to determine the criticalities affecting the Po Delta area due to the phenomenon of subsidence. From the study conducted it is possible to derive numerous localized criticalities along the banks of defence at sea. Often the observed decreases are due to anthropic interventions such as the reconstruction of the embankment with a consequent increase in the weight of the structure and a subsequent greater compaction of the soil or the dredging of the riverbed with subsequent lowering of the embankments. But what interests the study under consideration are not the decreases due to anthropic causes that often are represented by sudden decreases, but of short duration in the time (the effects are manifested for about ten years) but what is particularly interesting are the long-term phenomena represented by natural phenomena. It will be these phenomena that will manifest themselves in the decades to follow and to produce in this way a threat considering the rise of the sea level. In this regard, the forecasts for 2100 forecast increases of:

- IPCC 8-5 min (increase of mean sea level of +594 mm)
- IPCC 8-5 max (increase of mean sea level of +999 mm)
- Rahmstorf (increase of mean sea level of +1395 mm)

In view of these forecasts, it will be necessary to find the causes that manifest themselves as natural subsidence, to study the extent and possibly techniques that allow the risk of future floods to be mitigated. In the following paragraphs we will evaluate two different aspects: the geological aspect and the evolution of the Delta over the years.

7.1. Geological aspect of Po River Delta

A first consideration to interpret and explain the reductions obtained can be given by the geological conformation of the territory. In particular, the geological analysis (Figure 90) was carried out in 1999 by the Department of Geosciences of the University of Padua, the problem with this investigation is that the operational methods, the depth of sampling and the precisions are not known; For this reason, the data collected should be taken very carefully.

However, going to study the old maps of the Province of Rovigo, they confirm the presence of a tongue of sand and being that the geological map of Emilia-Romagna used for the construction still uses this geological relief, I can use the data from this analysis with a good peace of mind.

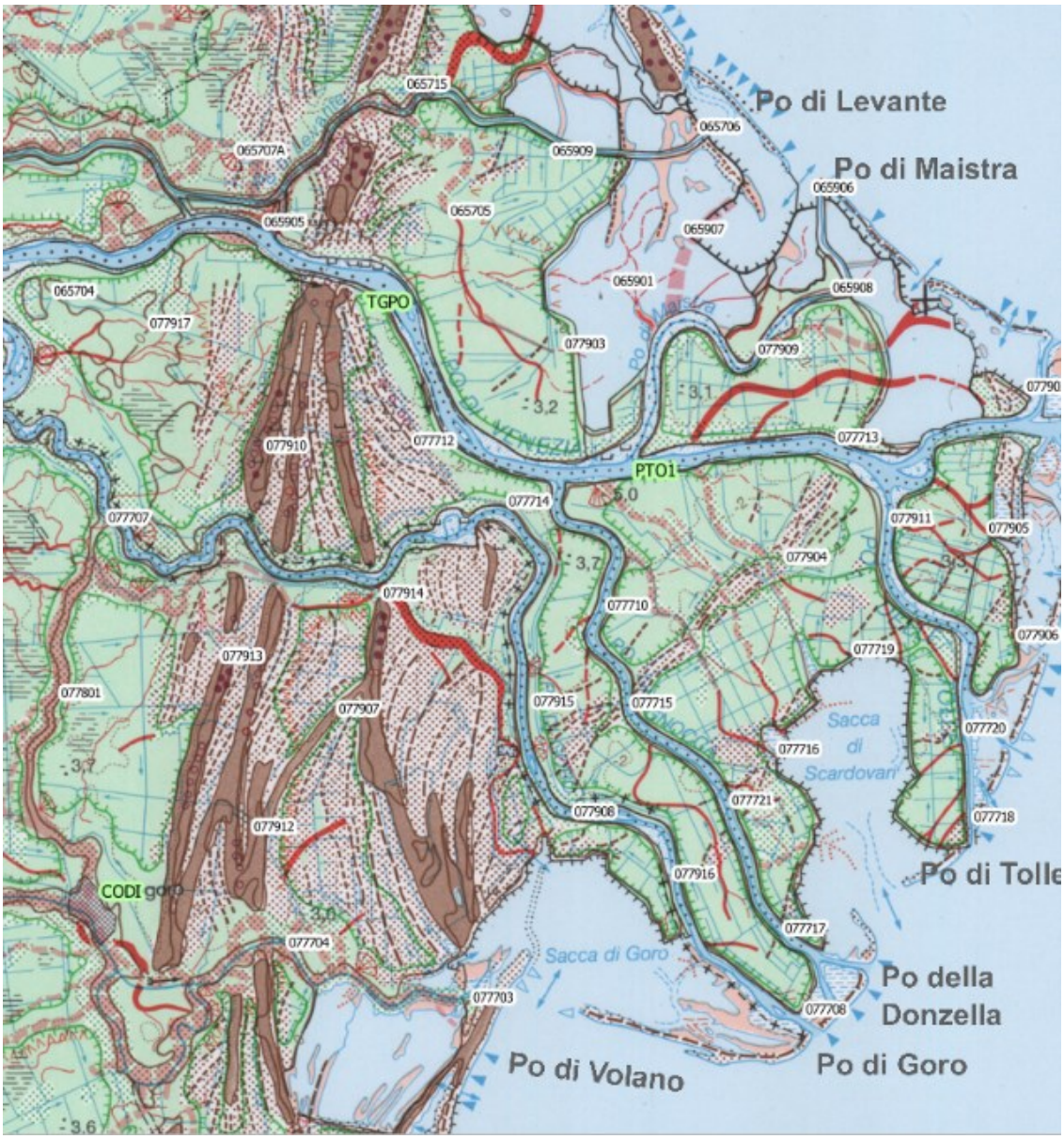

Figure 90. Geological survey of Po River Delta

The subsidence in the whole area was then evaluated, dividing the lowering of the clay soil from the lowering of the soil present in the sandy belt. From the study we expect a lowering velocity of clay and silty soil lower than the sandy soil. This depends on physical characteristics (particle size, shape, etc.) and chemical characteristics (related to electrical charges on particle surfaces). Precisely because of these chemical and mechanical interactions the clay soil will be much more compressible and will therefore be unsuitable for the construction of infrastructure such as roads and bridges as well as civil works such as urban centres.

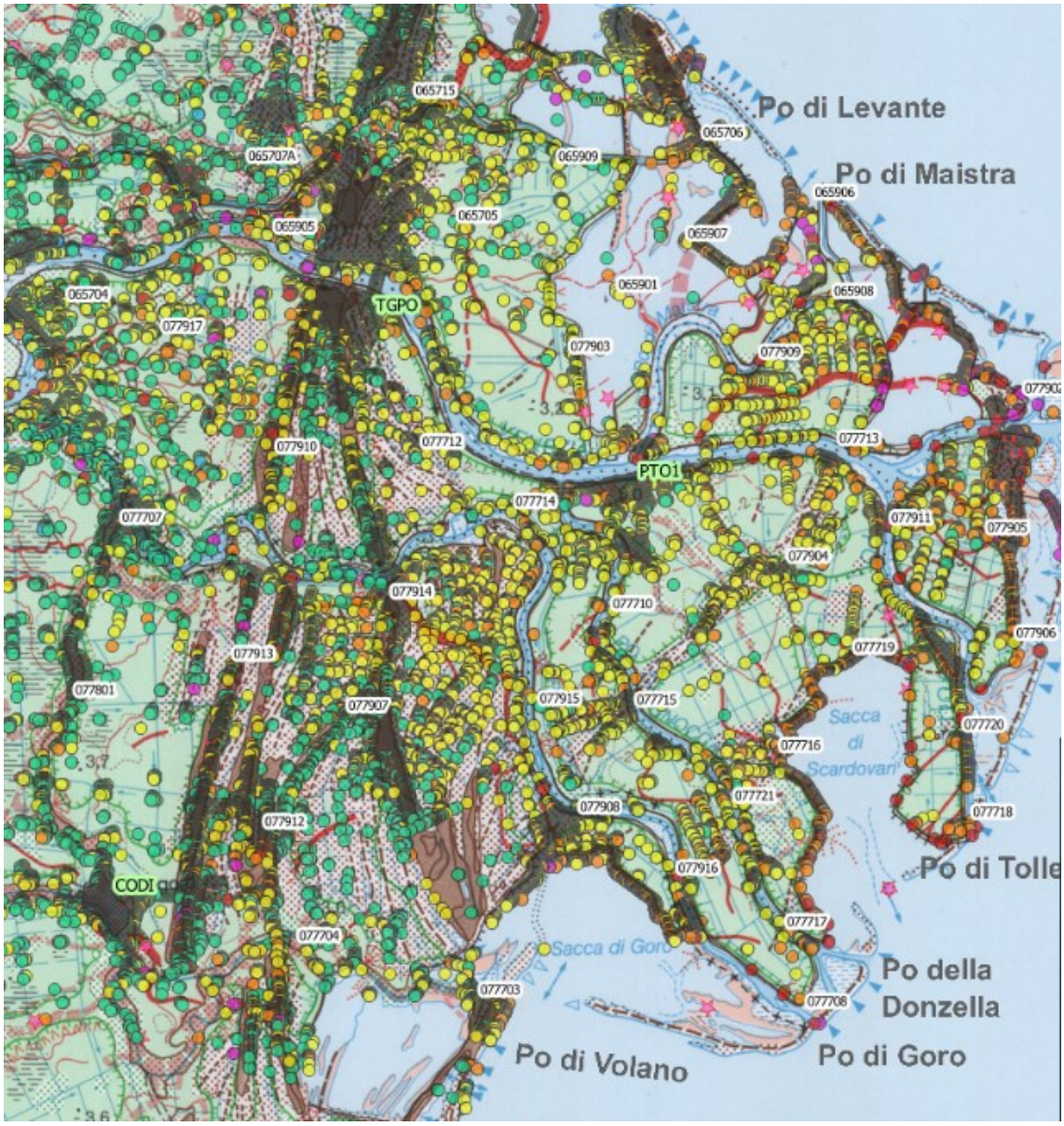

Figure 91. SAR data in PRD over the Geological survey

For this reason, given its stability, the sandy area currently has the highest density of urban areas in fact this belt has 96% of stable points (between -2mm/yr and +2mm/yr) detected by SAR technology (*Figure 91*) on the entire study area. The results obtained by comparing the GNSS data and the SAR data of the Cosmo-SkyMed satellites provide a speed of -3,2 ± 1,3 mm/year for the sandy belt, while for the clay soil the lowering speed is very variable depending on the location where you are (whether inland or along the coast).

The results obtained are in line with theoretical expectations, this makes it possible to understand how the phenomenon of subsidence is greatly influenced by natural aspects that turn out to be uncontrollable and on which the action of man is indispensable not so much to stem the problem, but to limit the effects caused by these phenomena of lowering. From these observations, however, we are able to understand the areas most at risk and on which studies and interventions will focus.

7.2. Expansion of Po River Delta

The delta area is a territory in continuous evolution thanks to the continuous contribution of solid materials by the river for 2000 years (at that time, in fact, the beach line extended along the ridges of sand dunes still visible on the line Chioggia-Ravenna) and by hydrodynamic dynamics that intervene along the coast (*Zambon, 2000*).

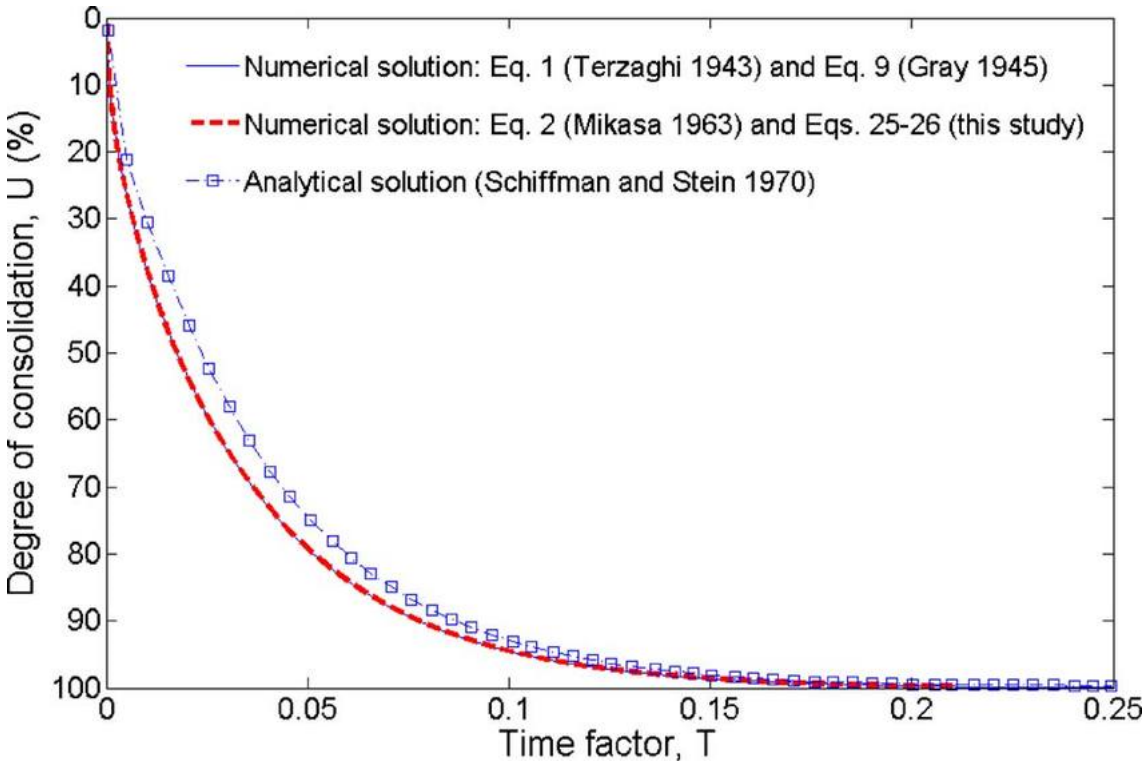

Figure 92. Degree of Consolidation over time

In particular, the expansion of the area of the delta over the centuries has manifested itself with direct consequences on the consolidation of the soil as the very weight of the sediments has created an over-consolidation of the soil acting thus on the lower layers, freeing them from fluids and thus compacting them. In this way in the following study, one will expect a lower decrease for land deposited for longer time being the process of exponential consolidation over time (*Figure 92*) while the lowering will be greater for newly deposited soils that are still rich in water between their particles.

During the study of SAR points (see *Figure 91*) different soil bands with similar characteristics were identified.

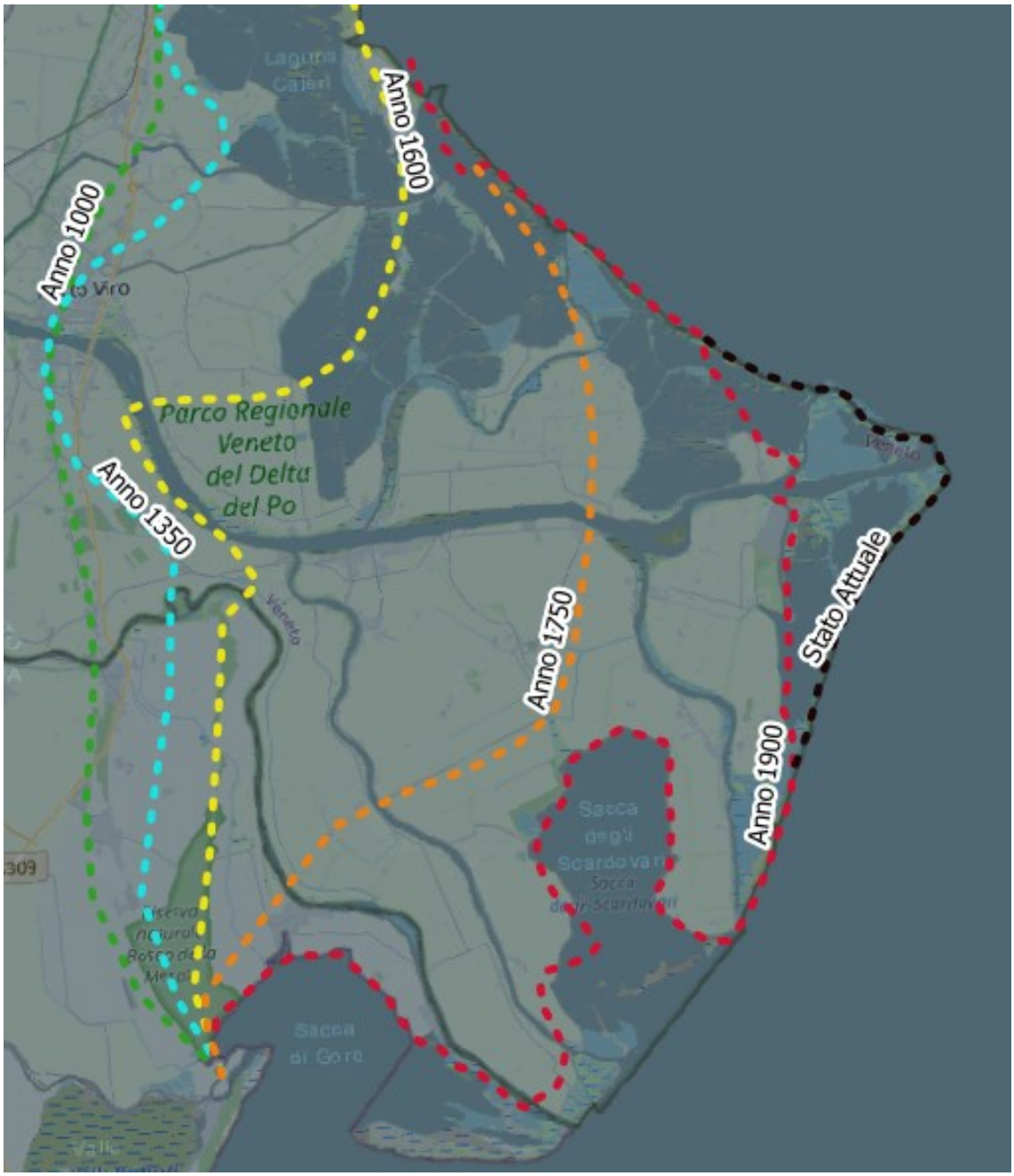

Figure 93. Expansion of the PRD over the centuries

As explained above, an important role is due to the type of soil present, but this is particularly valid if you evaluate a sandy soil with a clay soil. Studying the different velocities of the points, different speeds have been identified also in soils having the same characteristics, for this reason we thought about the phenomenon of consolidation and to verify this it was decided to superimpose on the geographical maps and SAR points the evolution of the Po Delta over the years. The expansion of the delta area has been studied over the centuries, particularly in the years 1000, 1350, 1600, 1750, 1900 and the current situation (*Figure 93*). The data related to the expansion of the Delta are taken from the ancient maps elaborated by the IGM.

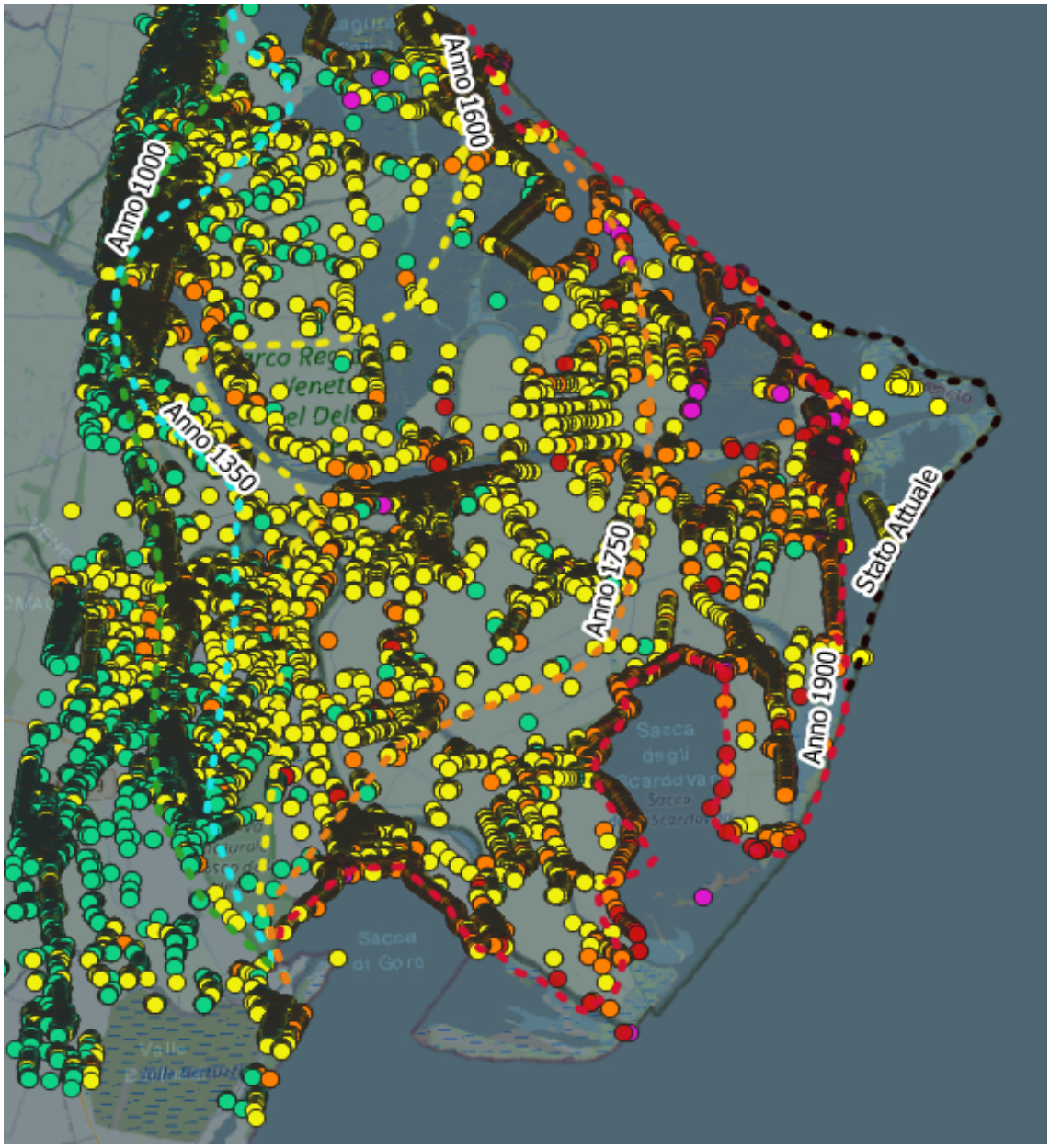

Figure 94.SAR data over expansion of the PRD

To evaluate the decreases in the different bands, the SAR data were filtered (*Figure 94*), and the average speeds were reported in *Table 17*.

	Era	Vel_SAR
Expansion	until 1000	-2,8±0.9
	from 1000 to 1350	-3,4±0.8
	from 1350 to 1600	-3,7±1.0
	from 1600 to 1750	-4,8±0.9
	from 1750 to 1900	-5,2±1.4
	from 1900 to today	-7,1±1.4

Table 17. Analyses of lowering Velocity according to the age of the soil

From the data obtained the weight of the surface sediments no longer affects the subsoil developed in 1600, producing now a negligible compaction, although light due to the presence of sand in the subsoil. This means that the phenomenon of consolidation no longer has a large effect on the velocity of lowering the ground.
A careful analysis will be performed instead in the band generated between 1600 and 1750. Here the subsoil is composed mainly of clay that is more subject to strong drops due to consolidation and the problem of salt intrusion with a variation in chemical characteristics as explained in previous chapters. In this area, therefore, you can still see the effects of the weight of the surface on the subsoil, producing a decrease of about -4.8 mm / y. This area currently has strong decreases, but we know that in the future such consolidation will diminish its effects and such observation will have to be held in consideration before planning works suitable to protect the inner areas in function of the provision's future on the rise of the sea.
Between 1750 and 1900 there is a strong extension of the Po di Goro, Po di Pila, Po della Donzella, Po di Tolle and the formation of the Sacca degli Scardovari. Here we notice a lowering speed equal to -5,2 mm / y that still shows a great uncertainty perhaps due to the presence of points on the banks (which often have artificial works due to the construction of ballast) or the fact that the area, Due to the great expansion, it should be divided into further years to go to check the real influence of the expansion of the deltizia zone. The lowering is, however, due to the weight of the surface material that still affects the subsoil and that will still manifest itself for centuries with strong lowering.
The soil is also composed of clay that in addition to the strong compressibility may be affected by the problem of salt intrusion with a variation in chemical characteristics.
The assessment between 1900 and today is difficult because the area is mainly affected by embankments which, as has often been said, have an abnormal lowering due to the higher weight of the embankment body that is manifested on the ground inducing a greater consolidation and is strongly influenced by work on securing the territory such as the construction of ballast.

In Figure *95*, thanks to the GNSS data (LOS along the vertical), it is possible to see the trend of the lowering speed of the deltizia area that in the north area shows an excellent correspondence with the evaluations previously made. The area to the south-west, on the other hand, shows anomalous values probably due to disturbances in the evaluation of the GNSS points, while the area to the south-east the Goro area has excellent correspondences with the SAR data when compared with the expansion of the Po Delta over the years.

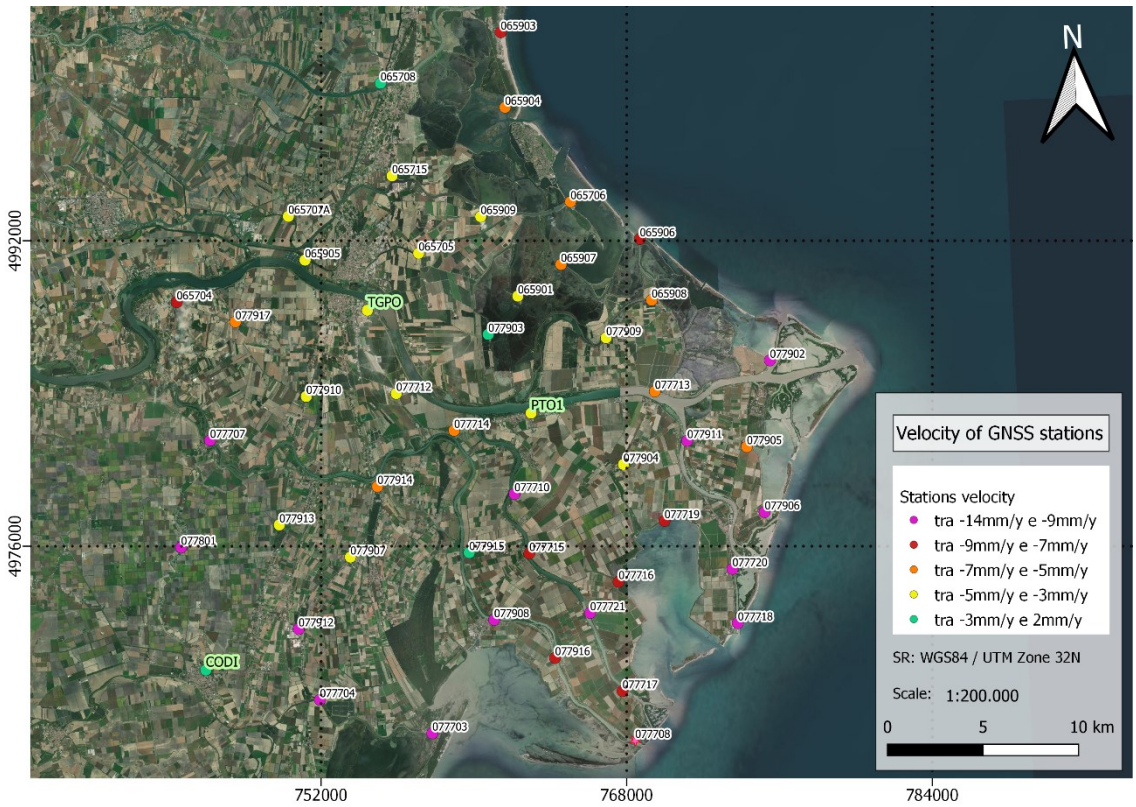

Figure 95. Lowering velocity of the soil measured with GNSS data

CHAPTER 8. CONCLUSION

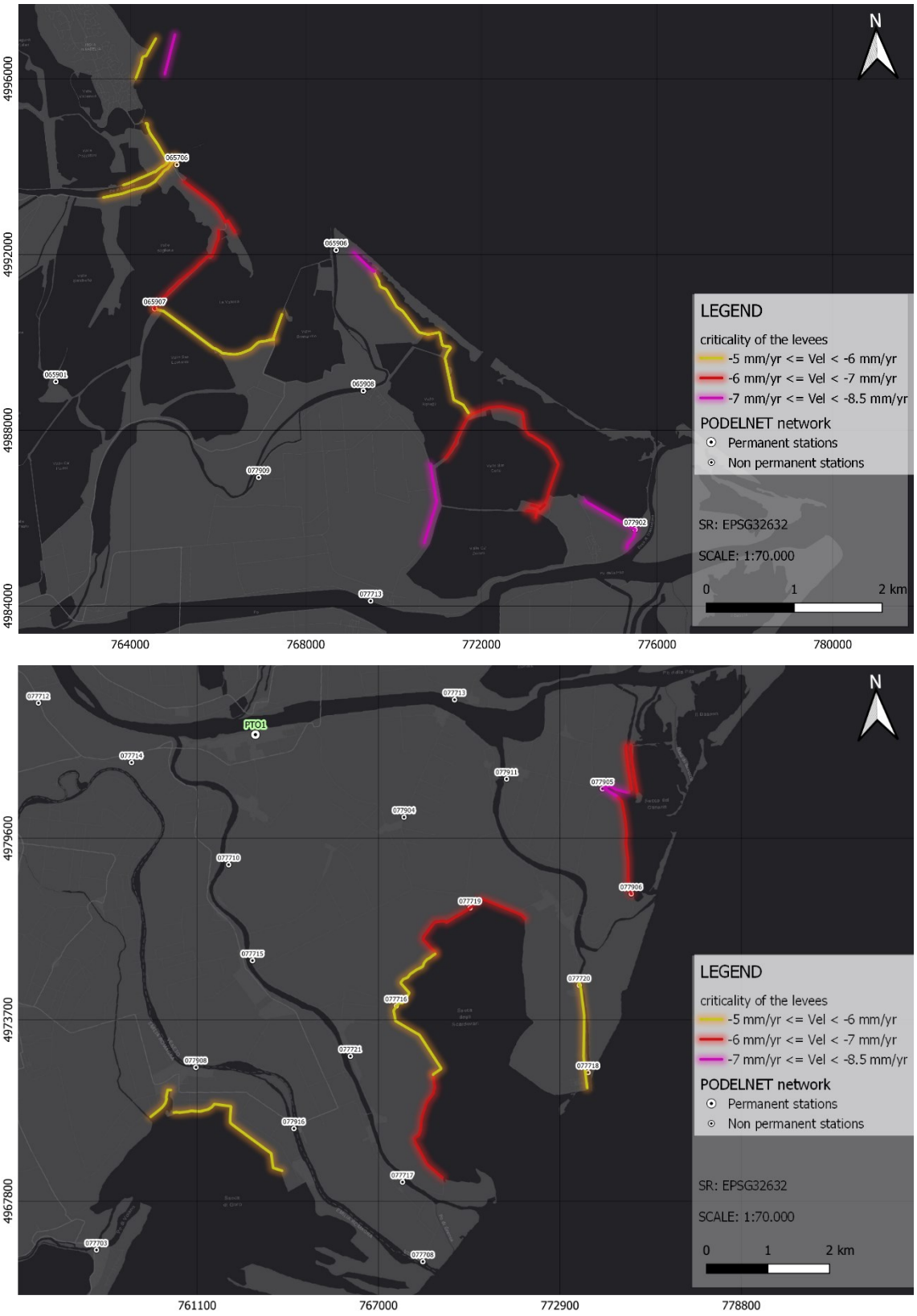

Figure 96. Lowering velocity of the critical embankments

All assessments of land degradation in inland areas are of relative importance compared to the lowering of coastal areas subject to storms. In fact it is true that a strong lowering of the soil in the hinterland can certainly produce destructive effects localized on civil works such as effects on infrastructure or foundations of housing often involving the presence of cracks and a consequent disruption of the structure, but perhaps the greatest danger will be the fact that the greater will be the lowering of these areas and the greater will be the part of territory below sea level, with a consequent catastrophic effect in the event of collapse of the banks.

Precisely these disasters are the most dangerous and given the extent of the area and the unpredictability of nature are the most complicated to predict and limit. For this reason, a thorough study of the causes and effects of the phenomenon of subsidence, of natural phenomena such as the extension of floods and rising sea levels and an increase in monitoring of the area is essential to better plan the defence of this area important from a naturalistic and productive point of view.

As for the defence of the embankments, there are many considerations to be made. First, the embankments were divided into zones according to their lowering speed, in particular the banks were studied with speeds between -6 and -6, between -6 and -7 and finally between -7 and -8,5. The subdivision of the embankments can be shown in *Figure 96*.

At this point the dangerousness of the banks will be evaluated based on the safety franc, or the difference in altitude between the crown of the bank (represented by the top of it) and the height of the sea in case of flood. The flood profile "SIMPO '82" was used to describe the maximum flood level based on the floods of 1951 and 1994. This profile was created in the framework of a project called "Study and general design of the hydraulic arrangements of the main shaft of the Po, from the springs to the mouth, aimed at the defence and conservation of the soil and the use of water resources" drawn up in 1982 by the Magistrate for the Po.

Based on these measures, a GNSS measurement campaign was carried out in 2015 to map the shares of the crowns of the banks, evaluating in this way the franc and dividing the banks into four different classes:

- absent or not present: ex 1,00 m
- low: ex between 0,70 m and 1 m
- average: Franc between 0,30 m and 0,70 m
- high: 0,30 m franc

Following this investigation, the final considerations and benefits of the SAR survey described in this thesis are easily understood. In fact, the study carried out by AIPO using GNSS instruments has obvious limitations such as the fact that it must use many technicians and tools in the field or the fact that given the huge extension of the Po River it would be impossible to have measurement campaigns spaced briefly in time. The SAR investigation instead allows to have a constant monitoring of the quota of the banks, with a consequent evaluation of the decreases in the time correlated to the subsidence. A negative note of the SAR survey is the fact that the points would hardly represent the share of the top of the embankment but considering the lowering speed coming from the SAR data and an initial measure obtained with GNSS instrumentation it will be possible to have in real time the necessary quota to plan defence works from floods and storms.

Having ascertained from the GNSS data that the SAR data approximate very well the lowering of the ground with millimetre accuracy, we understand how in the future such remote sensing methodology can be used for an increasing number of applications. The next step will be to go and perform a study where knowing the crown height of the embankments by GNSS measurements, knowing the state of flood of the sea and knowing the lowering of the ground it will be possible to measure with certainty the year in which the minimum hydraulic franc will no longer be present to ensure the safety of the area. In this way it will be possible to divide the works of the slub of the banks according to their real danger. In this procedure, of course, all the relevant observations will have to be considered, as seen in this study, the work carried out on an embankment will protect the area, but they will load the structure with a greater weight inducing a greater lowering.

In conclusion the objective of the study is to go and monitor the phenomenon of subsidence in the deltizia zone of the river Po going to pay particular attention to the defence banks at sea that turn out to be the only barrage against possible storms. The aim of the study is to study the phenomena that cause a lowering of the ground and to provide the competent authorities with relevant monitoring methods that can provide data accurately, quickly and economically to designers.

Obviously, the work to be carried out on the banks will have huge costs that will require continuous public funding. For this reason, in the study has been considered a Web-GIS able to provide in a simple and free of charge an overview of the criticalities of the Delta to anyone who accesses the page. In this way, sensitizing the population on the catastrophic effects of subsidence in the present it is hoped to attract more and more attention from the political class and consequently increase the funds for the safeguard of this very important territory: the Po Delta Area (*Figure 97*).

Figure 97. Po River Delta

BIBLIOGRAPHY

Characterisation of bed sediments and suspension of the river Po (Italy) during normal and high flow conditions, Vignati D. et Al., 2003

Studio delle deformazioni del suolo mediante analisi satellitare e modellazione geofisica avanzata, M. Manzo et Al., 2010

Correlation between shoreline variations and subsidence in the Po River Delta, Italy, L. Carbognin

Sui fenomeni di anormale abbassamento del suolo con particolare riguardo al Delta Padano, P. Caloi, 1967

Influence of glacial cycles and tectonics on natural subsidence in the Po Plain (Northern Italy): Insights from 14C ages, E. Carminati et Al., 2003

Subsidence Zonation Through Satellite Interferometry in Coastal Plain Environments of NE Italy: A Possible Tool for Geological and Geomorphological Mapping in Urban Areas, M. Floris et Al., 2019

Assessing Urban Landslide Dynamics through Multi-Temporal InSAR Techniques and Slope Numerical Modeling, N. Necula et Al., 2021

Stima della subsidenza recente nell'area del delta del Po da dati GPS e Sentinel-1 A, M. Fabris et Al., 2016

Monitoring of Land Subsidence in the Po River Delta (Northern Italy) Using Geodetic Networks, N. Cenni et Al., 2021

Analysis of the Periodic Component of Vertical Land Motion in the Po Delta (Northern Italy) by GNSS and Hydrological Data, E. Vitagliano et Al., 2022

Editorial for Special Issues "Monitoring Land Subsidence Using Remote Sensing", M. Fabris et Al., 2021

Procedure di elaborazione dati GNSS con software Bernese, B. Brescacin, 2019

La strumentazione UAV nel rilievo e nella modellazione tridimensionale di un sito archeologico, P. Piani, 2015

Linee guida per l'utilizzo dei dati interferometrici del geoportale Regione Toscana, N. Casagli, et Al., 2018

The Sentinel-1 Mission: New Opportunities for Ice Sheet Observations, T. Nagler, 2015

Assessing Forest/Non-Forest Separability Using Sentinel-1 C-Band Synthetic Aperture Radar, J. Hansen, 2020

Linee guida per l'analisi di dati interferometrici satellitari in aree soggetti a dissesti idrogeologici, MATTM, 2009

Quaderni Ca' Vandremin, M. Coppola, 2009

Piano generale di bonifica e di tutela del territorio, G. Mantovani et Al., 2009

Land Subsidence in the Venetian area: known and recent aspects, L. Carbognin et Al., 2005

Numerical Analysis of One-Dimensional Consolidation in Layered Clay Using Interface Boundary Relations in Terms of Infinitesimal Strain, H. Kim et Al., 2010

Indagine sperimentale e verifiche stabilità su un'arginatura del fiume Po, E. Pennisi, 2010

COSMO-SkyMed Seconda Generazione: System and Products Description, ASI, 2021

Sistemi informativi geografici: Analysis of the Periodic Component of Vertical Land Motion in the Po Delta (Northern Italy) by GNSS and Hydrological Data, E. Caiaffa, 2006

Hydrodynamic versus GIS modelling for coastal flood vulnerability assessment: Which is better for guiding coastal management?, A. Seenath, 2015

Analisi di fattibilità tecnico ed economica per il miglioramento delle condizioni di sicurezza rispetto al sormonto degli argini maestri del fiume Po, AIPo, 2017

SITOGRAPHY

https://www.ipcc.ch/

https://sentinel.esa.int/web/sentinel/missions/sentinel-1

https://www.telespazio.com/it/programmes/cosmo-skymed

https://www.asi.it/scienze-della-terra/cosmo-skymed/

https://cdn1.regione.veneto.it/alfstreaming-servlet/streamer/resourceId/84e2d7c9-0933-4ca8-a323-9ab4b59e1609/Piano_Po_cap2.pdf

https://www.epa.ie/publications/

https://ambiente.regione.emilia-romagna.it/it/geologia/geologia/geologia-emilia-romagna/la-pianura-padana-1

https://www.venezia.isprambiente.it/bollettino#Previsioni%20di%20marea%20astronomica%20a%20Venezia

https://www.researchgate.net/publication/284564090_Un_Bacile_di_nome_Delta

https://geochange.er.usgs.gov/sw/changes/anthropogenic/subside/

https://bandiasi.almaviva.it/sites/default/files/attach/scheda-progetto/csk-system-description-users-guide.pdf

https://ieeexplore.ieee.org/abstract/document/9380715

GRATITUDE

La terza legge di Newton enuncia la ormai famosa frase “ad ogni azione corrisponde un’azione uguale e contraria”. Oltre al bel noto significato fisico, secondo me questo enunciato può avere molteplici significati, ma quello che più si avvicina maggiormente al mio pensiero è il seguente: ogni nostra azione e ogni nostra scelta cambia irrimediabilmente il nostro futuro.

Andando a ritroso nel tempo e soffermandomi al mio ultimo anno, comprendo come ogni mia decisione, come la volontà di collaborare con il dipartimento di Geomatica dell’Università degli studi di Padova, l’intenzione di passare giorno e notte a lavorare su articoli accademici insieme a l’Ing. Massimo Fabris fino all’intenzione di farmi trovare sempre a disposizione per qualunque lavoro e opportunità, mi abbiano portato ad ottenere la possibilità di lavorare nell’ambito di cui sono innamorato: la Topografia.

Voglio quindi ringraziare le persone che mi hanno dato la possibilità di prendere certe scelte, partendo ovviamente dalla mia famiglia che mi ha sempre lasciato scegliere in maniera indipendente e a Greta che mi ha sempre supportato nonostante alcuni periodi di “instabilità mentale” dovuti alla moltitudine di cose da fare. Un ringraziamento è dovuto anche alla mia compagnia di una vita (Marco, Debora, Gianluca, Matteo, Gregorio, Andrea, Stefano) con i quali ho condiviso ogni serata e ogni momento bello o brutto che fosse e ovviamente ai miei compagni di Università con i quali ogni sessione di esami regalava sia sfaccettature tragiche che a tratti divertenti. Inoltre, un ringraziamento sincero va ai miei professori che sia durante l’istituto tecnico per Geometri che durante l’Università mi hanno fatto innamorare delle materie tecniche. Un grazie particolare va al prof. Andrea Menin e soprattutto al prof. Massimo Fabris che ha sempre creduto nelle mie capacità e che mi ha avviato passo dopo passo in questo fantastico mondo della topografia, spronandomi a fare sempre meglio.

Per ultimo, ma solo seguendo l’ordine cronologico vorrei ringraziare Giandomenico che in questi mesi mi sta seguendo, aiutandomi ad approfondire il lato pratico e teorico della topografia e che mi sta infondendo i valori di un’azienda leader del settore come la Trimble. Un ringraziamento ovviamente va a tutti i miei colleghi e in particolare al gruppo Nordest che mi sta aiutando a muovere “i primi passi” in questo mondo che al contrario di quanto si possa pensare è caratterizzato da un’evoluzione continua.